



UNIVERSITY OF
BIRMINGHAM



EngD Thesis

On Improving the Cost-Effective
Dispersion of Calcium Carbonate in
Polypropylene for Impact Resistance

Paul Jones

EPSRC

Engineering and Physical Sciences
Research Council

UNIVERSITY OF
BIRMINGHAM

University of Birmingham Research Archive

e-theses repository

This unpublished thesis/dissertation is copyright of the author and/or third parties. The intellectual property rights of the author or third parties in respect of this work are as defined by The Copyright Designs and Patents Act 1988 or as modified by any successor legislation.

Any use made of information contained in this thesis/dissertation must be in accordance with that legislation and must be properly acknowledged. Further distribution or reproduction in any format is prohibited without the permission of the copyright holder.

ACKNOWLEDGEMENTS

Before I get to the specifics, I would like to include the following words to express my gratitude for those who have helped, encouraged and prodded me over the last four years. Only by channelling their efforts have I been able to produce the document that you see before you.

Firstly I would like to mention my academic supervisor, Dr. Neil Rowson for his guidance and fine abilities in facilitation that ensured my working experiences maintained a high collaborative standard. He was also the person who first introduced me to this opportunity and to him I owe great thanks. Dr. Richard Greenwood made certain that my deadlines were reached on time, that the work was to a consistent standard and that the EngD experience was a highly enjoyable and rewarding one. His efforts are also received with deepest gratitude.

I give great thanks also for the industrial supervision I received at Imerys Minerals. The innovation and drive of Dr. David Skuse has enabled a number of doctoral students such as me to gain a plethora of unforgettable industrial and professional experiences. Long may his vision continue. The help of Drs. David Gittins and Jonathan Phipps were also highly appreciated. The patience of Messrs John Slater, Mike Bird, Mark Windebank, Andy Riley, Kelvin Thomas, Clayton Mutton and Dr. Mohammed Abubakar was likely to have been taxed, but each of their calm and informative responses to my practical endeavours is to their utmost credit. I must also highly regard Mrs Eileen Spittle, whose library's overdue policy I believe I took to new levels, Mrs Elaine Crowle who added her professional touch to many of my course documents and to Mrs. Debbie Hancock for all her countless efforts during our time at Imerys.

Dr. Yingdan Zhu, with whom I enjoyed several highly memorable projects in Cornwall and Bristol, deserves warm thanks for her ability to motivate those around her and her indefatigably positive disposition. I would finally like to thank my other fellow students, each of them playing their own role in the story of my EngD experience.

CONTENTS

ABSTRACT	5
DEFINITION OF SIGNIFICANT TERMS	6
1 THESIS INTRODUCTION	8
1.1 A BACKGROUND TO THE PROJECT	8
1.2 THE ORIGINS OF POLYMERS AND THEIR COMPOSITES	11
1.3 BUSINESS CASE	15
1.4 CLOSING WORDS	18
1.5 REFERENCES	19
2 MODERN CHALLENGES IN THE PRODUCTION OF IMPACT-RESISTANT POLYMER MATERIALS	22
2.1 AIMS OF THIS CHAPTER	22
2.2 INTERPRETING THE BEHAVIOUR OF POLYMERS AND THEIR COMPOSITES	22
2.2.1 <i>General Case – Most Polymers</i>	23
2.2.2 <i>Specific Cases – Polymers with Additional Phases</i>	28
2.2.3 <i>Concluding Remarks</i>	36
2.3 CONSIDERATIONS FOR IMPLEMENTING THE CHOSEN MATERIALS	36
2.3.1 <i>Particle Preparation</i>	36
2.3.2 <i>The Mixing of Particles and Polymers to Form Composites</i>	37
2.4 EFFECTIVE MEASUREMENTS	39
2.4.1 <i>Particle Properties</i>	39
2.4.2 <i>Composite Microstructure and Flow</i>	40
2.4.3 <i>Impact Properties</i>	41
2.4.4 <i>Concluding Remarks about Measurements</i>	42
2.5 CONCLUSIONS	42
2.6 REFERENCES	43
3 MATERIALS AND METHODS	49
3.1 AIMS OF THIS CHAPTER	49
3.2 OVERVIEW	49
3.2.1 <i>Materials</i>	49
3.2.2 <i>Methods</i>	51
3.3 FURTHER DETAILS	52
3.4 REFERENCES	78
4 THE APPLICATION OF COST-EFFECTIVE TECHNOLOGY TO RESEARCH THE PROPERTIES OF GCC AND ITS PP COMPOSITES MADE BY TWIN-SCREW EXTRUSION	81
4.1 INTRODUCTION	81
4.2 AIMS OF THIS CHAPTER	82
4.3 HYPOTHESIS	83

4.4	RESULTS	83
4.2.1	<i>Measurement of an Uncoated GCC Grade</i>	84
4.2.2	<i>Identifying Key Indicators of Application Performance</i>	97
4.2.3	<i>Quantifying the Scope for Improvement through Formulation</i>	100
4.5	SUMMARY	104
5	<u>THE APPLICATION OF COST-EFFECTIVE TECHNOLOGY TO IMPROVE THE IMPACT RESISTANCE OF PP/GCC COMPOSITES USING AN ALTERNATIVE MIXING PROCESS</u>	109
5.1	INTRODUCTION	109
5.2	AIMS OF THIS CHAPTER	113
5.3	HYPOTHESIS	113
5.4	RESULTS	113
5.4.1	<i>Research</i>	113
5.4.2	<i>Development</i>	123
5.5	SUMMARY	132
5.6	REFERENCES	133
6	<u>AN AUTOMATABLE VISUAL ANALYSIS TECHNIQUE FOR PARTICULATE CHARACTERISTICS IN SITU OF THIN POLYMER FILMS</u>	136
6.1	INTRODUCTION	136
6.1.1	<i>Material Requirements</i>	138
6.1.2	<i>Types of Visual Analysis</i>	139
6.2	AIMS OF THIS CHAPTER	139
6.3	HYPOTHESIS	139
6.4	SAMPLE PREPARATION	140
6.5	METHOD DEVELOPMENT AND RESULTS	140
6.5.1	<i>Image Capture</i>	140
6.5.2	<i>Image and Data Processing</i>	141
6.6	SUMMARY	154
6.7	REFERENCES	156
7	<u>THE PREPARATION AND TESTING OF FINER FILLER</u>	159
7.1	INTRODUCTION	159
7.2	AIMS OF THIS CHAPTER	161
7.3	HYPOTHESIS	162
7.4	RESULTS	162
7.4.1	<i>Preparation</i>	162
7.4.2	<i>Testing</i>	165
7.5	SUMMARY	174
7.6	REFERENCES	176
8	<u>DISCUSSION</u>	178
9	<u>CONCLUSIONS</u>	184

ABSTRACT

The potential to improve the performance of polymer composites cost-effectively has been researched across various aspects of development and manufacture. Each endeavour fell broadly into one of three categories; the principal ingredients and their required properties, the methods with which they were transformed into products and the means by which they were observed. It was determined that the ingredients with the highest potential as defined, each shared simplicity and abundance as material traits. The use of bespoke functionalised ingredients proved costly to implement, providing only modest property benefits compared to a standard formulation comprising polypropylene, 10 – 30 % w/w of 2 µm calcium carbonate with 0.5 – 1.0 % w/w stearic acid surface treatment. It was found that an apparent deterioration in impact resistance that was encountered on reducing the filler particle size was in each case observed, attributable to a coarsening of these fine particles that resulted from the mixing process. Finer particles could not be implemented more cost-effectively than standard formulations; an effect which was attributed to the tendency of the finest particles to form aggregates that could not be decomposed by mixing under high shear. However, the favourability of particle dispersion in standard formulations was used to implement a production method of polymer composites that required significantly less energy across the entire production stage and held other significant advantages. Concentrates comprising minerals in wax were produced and made to successfully re-disperse from loadings approaching those allowed by their theoretical packing maxima, in some cases up to 90 % w/w. Furthermore, a single injection moulding cycle with minimal back-mixing was used to combine concentrates and neat polymers to make commercially-competitive composite specimens, at final concentrations as low as 10 % w/w. A principal method to obtain *in situ* visual particle data from thin composite films was developed along with several derivative analyses. The techniques allowed rapid and representative data collection for high particle proportions at resolutions of 6 – 8 µm, accounting for particles most relevant to impact-resistance in standard formulations. As a whole, significant and realistic saving opportunities were identified in the expenditure of unnecessary resources, such as; processing energy, capital investment, transportation, labour and time. These findings were supported by experimental data.

DEFINITION OF SIGNIFICANT TERMS

Composite	<i>A material comprising a continuous phase and one or more disperse phases</i>
Continuous Phase	<i>Also known as matrix; material in which filler is suspended in a composite</i>
Dispersed Phase	<i>Also known as filler or reinforcement; particles that are suspended in a continuous phase in a composite</i>
Dispersed Entity	<i>Any material which is not that of the bulk suspending material. Such as filler itself, its surface treatment and other additives</i>
Aggregate	<i>A collection of particles which are held together by van der Waals forces or true chemical bonds</i>
Aggregation Factor	<i>The diameter of an aggregate, relative to that of its component particles</i>
Brittle Fracture	<i>Failure of a material during which little or no energy becomes absorbed</i>
Ductile Fracture	<i>Failure of a material during which energy becomes perceptibly absorbed</i>
Extrinsic Property	<i>A characteristic that is only true of a material when certain conditions are stipulated and maintained, such as dynamic viscosity</i>
Intrinsic Property	<i>A characteristic inseparable from a given material under any conditions, such as phase transition conditions of a pure material</i>
GCC	<i>Ground calcium carbonate; a mineral grade generated by comminution</i>
PCC	<i>Precipitated calcium carbonate; a mineral grade generated by crystallisation</i>
% w/w	<i>The weight-based proportion of filler in a whole composite, as a percentage</i>
Loading	<i>The concentration, typically in % w/w, of filler particles within a matrix</i>
PE	<i>Polyethylene</i>
PP	<i>Polypropylene; the polymer described mostly in this Thesis</i>
Masterbatch	<i>A concentrated composite that will eventually get diluted to a lower loading</i>
Particle	<i>A fundamental filler entity that has uniform crystallinity throughout its structure</i>
Particulate	<i>Any discrete filler entity, regardless of its provenance</i>
Dispersion	<i>A measure of separation between filler particles in a continuous phase</i>
Distribution	<i>A measure of particulate homogeneity in a continuous phase</i>
SEM; TOM	<i>Scanning electron microscopy; transmission optical microscopy</i>
TSE	<i>Twin-screw extrusion; a standard composite formation process</i>

CHAPTER ONE

Thesis Introduction

1 THESIS INTRODUCTION

1.1 A Background to the Project

Calcium carbonate mineral is the predominant component of several types of rock deposit, including chalk, limestone and marble. Although it can occur in various crystal forms, the most stable and therefore most abundant of these forms is calcite [1]. Marble is a mineral that has become formed from metamorphosed rocks that contain high proportions of calcium carbonate; chiefly limestone and dolomite. It is a relatively soft mineral with a Mohs hardness of 3. The rhombohedral structure of the calcite crystals of which it is chiefly composed make the material undergo rhombohedral cleavage during comminution, which gives it its relative softness.

Calcium carbonate is a heavily relied-upon industrial material [2]. It is estimated that 15 – 20 Mt of all forms of calcium carbonate are produced annually, with over half this figure being accounted for by finely ground material. About three quarters of calcium carbonate made for all industrial uses originates from marble [3]. The most quarried worldwide deposits of marble are in Italy, China, India, Spain and Portugal, which between them have consistently accounted for more than half of its annual global production for several decades [4].

Typical industrial applications for all calcium carbonate minerals are found in aggregates and additives/fillers. Traditionally, functional additives are materials that provide a specific functionality to a formulation (such as the addition of calcium carbonate to cement formulations that subsequently chemically reduces to form the required calcium oxide or its use in paper and paint materials to act as a white pigment), whereas fillers simply replace bulk material to reduce costs. However, the difference between these two has become less clear, due to the increasing use of fillers to simultaneously improve cost-effectiveness by targeting specific properties through engineered functionality or 'performance' [5].

Imerys Minerals Ltd is a major industrial minerals processing company whose business is in the extraction, processing and product distribution of an ever-growing portfolio of minerals (including calcium carbonate) for an ever-increasing range of applications. The philosophy of bringing performance to bulk materials by having already engineered performance into the minerals which go into them plays a significant role in how their technical operations and research endeavours are governed. By controlling the entire mineral processing stage, tailor-made mineral solutions can be provided efficiently, with no unnecessary processing steps or transportation.

The company known today as 'Imerys Minerals Ltd' has been operating since 1999, although it also benefits from experience and resources gained over many decades of the companies which preceded it at this time; Imetal and English China Clays, which provided minerals and mining experience dating back to 1880 and 1919 respectively [6]. The company today has continued to grow in the breadth and depth of the mineral solutions it aims to provide. Today they are active in 47 countries and operate in over 240 industrial locations around the globe. The sales ambitions that their 16,000-strong workforce aim to meet are strategically divided into four business groups; materials & monolithics, minerals for ceramics, refractories, abrasives & foundry, pigments for paper and performance & filtration minerals. Research and development play important roles in each of these categories, and in the group of performance minerals, the deliberate ambiguity in the title arguably paves the way for the most naturally novel and open-ended fields of research.

Along with kaolin (an alumina-silicate also known as china clay), amongst the most significant minerals in terms of the quantities produced by Imerys Minerals is calcium carbonate [6]. With high quality sources in Italy, Turkey, UK, US and elsewhere, the company provide many different grades of the mineral for many different applications. Their FilmLink range of ground calcium carbonates were originally developed for use in breathable polyolefin films. However, their excellent performance and versatility in other systems has also enabled them to be put to good commercial use elsewhere, such as for filler in commodity polymers such as polyolefins (polypropylene, PP and polyethylene, PE)

and also polyvinyl chloride (PVC). The annual production of PP in 2002 was 52.8 Mt, with an estimated annual growth of 4.7 % [7]. The figure has consistently remained between 40 – 60 Mt since this time. Consumption in 2005 was estimated at 42 Mt and predicted to rise to 109 Mt globally by 2015 [8]. It is thought that the demand for the material in current and potential future applications is exceeding its current supply, making it likely that the material will continue to play an important role in global materials applications for many years to come [7]. A supporting example may be seen in the recently-increasing number of various automotive parts being used that chiefly comprise a polypropylene matrix [9].

Calcium carbonate is extensively used in polymer manufacturing industries, due to the excellent performance it can provide for a reasonably low cost. In fact many minerals can provide both cost and functionality benefits to polymer systems simultaneously. Because of this, large mineral processing companies such as Imerys have many polymer processors and manufacturers for their customers. Any professional mineral producer will work closely with their customers to ensure that their products are being implemented in the way that they were designed to do so, to maximise their effectiveness. This is especially true for minerals that are put to use in the polymer industry, where the tolerance to variation of properties can be very low [10].

The primary purpose of adding minerals to polymer systems today is usually to improve one or several of its mechanical properties. To reduce an extraordinarily complex potential series of interactions and dependencies down to one summarised sentence, the exact effects that a mineral has on the polymer into which it is mixed depend on the distributions of its particle size and shape and also its surface chemistry. From this (perhaps overly) simplified statement come a seemingly infinite number of avenues of research; into why particles create the effects they do, how these effects can be improved and how they can be delivered at a lower cost to a company and at a lower cost to the world. The major goal of this thesis is to investigate each of these aspects across a commercial filled-polymer formulation that is relevant to modern day applications. In order to do so

in as much depth as possible, the breadth of research was generally limited to generally one principal filler type (calcium carbonate) and one principal polymer type (PP). Before specific project details are introduced (in subsequent chapters), the technological histories of these materials will first be discussed, followed by a discussion about what is hoped to be gained by a project in this area, supplemented by the presentation of a business case.

1.2 The Origins of Polymers and Their Composites

Naturally-occurring polymers have been put to deliberate technological use for hundreds of thousands of years, with one of the earliest known examples (dating back to approximately 200,000 BC) revealing evidence of the manipulation of natural gums and resins by early humankind to provide an adhesive function during the assembly of primitive tools and weapons [11]. The most significant change in the understanding of polymerisation behaviour since then could be argued to have occurred between the late 19th and early 20th Centuries, when the independent contributions of perhaps most significantly Berthelot and Staudinger led to the correct hypothesis that the thickening behaviour of the substance styrol under certain conditions, such as heating (that had been discovered in the mid 19th Century) was due to a genuine chemical reaction between the styrol molecules that created a long chain; a form of macromolecule, more specifically a synthetic polymer [12]. The potential for these new materials to play significant roles in current and novel global materials applications was already understood by parts of that scientific community and the field of polymer science was truly born, with specifically-dedicated journals appearing in the 1940s [13]. However, attempts to commercialise polymer formulations had already been attempted several decades before this time. This was in the form of chemical amendments to pre-existing natural polymers that was performed in the late 19th Century, such as celluloid which was first manufactured by Parkes (a thermoplastic that was originally called Parkesine) albeit somewhat unsuccessfully [14]. The first completely and genuinely synthetic polymer system to become a commercial success was Bakelite (a thermosetting plastic formed from phenol and formaldehyde) in the 1920s [15]. During and after this time, notable contributions from Carothers in that same decade and ICI employees

such as Perrin in the 1930s led to the first example of polyolefin commercialisation, in the form of PE, first commercially prepared (under high temperatures and pressures) in 1939 [16]. It was from the work of Ziegler and Natta in the '40s and '50s that the full commercial potential of polyolefin materials (amongst others) was realised by their development of polymerisation catalysts, which allowed polyolefin production to take place under milder (and therefore less expensive) reaction conditions. It was in 1957 that PP was first commercially produced on a large scale [17]. Notable developments in polymer science that took place after the onset of PP mass production are covered in the following Chapter. Countless synthetic polymers including combinations of additional polymeric and non-polymeric ingredients (which may have been added before or after the polymerisation process, creating co-polymers and blends, respectively) have been conceived of since this time; but even some of the earliest examples of commercial polymers such as celluloid and phenolic resins like Bakelite are still put to use to this day (although only to limited extents) [18,19].

Some of the reasons as to why synthetic polymers have become such ubiquitous materials today are their versatility in both physical form and potential functionality, their mechanical performance in relation to their weight and their relatively low production costs. Most of these could have been (and indeed were) predicted by those who contributed to the early stages of their development. What was perhaps less-considered during this time was the complexity in the structure and the mechanical response that these materials could display. Taking just one example some polymer molecules when undergoing cooling from a molten state, align themselves in chains with high degrees of order to create crystalline regions within an otherwise amorphous molecular phase. This is true for polymers comprising the least-branched molecular chains such as polyolefins, which can exhibit structures where more than half of their mass has cooled to become crystalline. It is decreasingly observed where these chains are sterically hindered, such as in polystyrene, which has no capacity for crystallinity [20].

As with the use of naturally-occurring polymers, the mixture of two or more separate materials to achieve synergy in a select variety of properties of the new material that they create also dates back to early humankind, for example mixtures of straw and mud to construct dwellings. Either of the constituent materials in isolation would not make a sufficiently strong or weatherproof construction, but by their integration, some of the properties of the disperse phase or 'reinforcement' (in this example, the straw) can manifest in the composite through being held in place by the continuous phase or 'matrix' (in this example, the mud), where they would not otherwise have been obtainable or relevant. More modern examples of the same concept are highly pervasive. To name a few, they can be found in mixtures of concrete and steel wires, metals in other metals (alloys) and even sawdust in ice [21]. Today, a large proportion of commercial plastics (i.e. completed polymer formulations comprising all their extra ingredients) comprise solid disperse phase 'filler' entities that provide synergy to some of their most useful properties to their given application. (The continued use of the term 'filler' is today something of misnomer, since they are now relied on for many otherwise unobtainable composite properties [22]). However, the use of disperse phases in polymers was not originally driven by the potential for synergy in selected properties, but instead was simply to replace (what was especially so at the time) highly expensive matrix material with an inexpensive material, so that the polymer matrix could literally be 'filled', in order to reach a given volume. This was most financially beneficial during the processing of polymer systems that already included a compounding stage (a type of high-intensity mixing of the molten polymer) as part of its necessary minimal formulation method, such that the capital investment, labour and energy costs that would be incurred by performing mixing were not done so just for the sake of the filler ingredient. PVC and thermosetting plastics are examples where this step is required even without the use of such a disperse phase. When the composite material properties that the filling process could provide were found to actually exceed some of those of unfilled polymers, the science of filler treatment for polymer composites was born. Furthermore, not only could the disperse phase have its own properties manifest in the composite, but it could also act as a substrate upon which additional substances could be incorporated and distributed evenly throughout the polymer. In the

field of mineral fillers for polymer composites, these would-be disperse phases were already being subjected to a series of processing steps that were in favour of the processes required to make an effective performance filler (such as powder fineness, resistance to aggregation and agglomeration, resistance to moisture pick-up, chemical surface modification, powder flow). Therefore additional processing to suit polymer systems would not require significant additional costs. This feature, combined with their relatively low cost, high abundance, natural variation in physical properties, their strength and their potential performance benefits made them ideal candidates for materials with which synthetic polymers could be filled to meet a global demand across a wide spectrum of desirable properties. Their potential benefit as fillers has led to the implementation of otherwise unnecessary compounding steps for certain polymers on a large scale, such as for PP. In 2003 it was estimated that approximately 15 Mt of all the minerals that were produced that year were consumed in polymer composites [23].

From a commercial point of view, the most important mineral fillers are clays, carbonates and talcs by the sheer volumes in which they are exploited. Calcium carbonate is used in many rubber and plastic applications to reduce costs [5]. However, certain grades (such as those with very fine particle sizes) can bring the synergistic properties to a matrix, which were mentioned above, including to both PVC and PP. Along with thermal conductivity and dimensional stability, its fine particles provide significant impact resistance improvements to PP under high-energy impacts. However, there are many known (and likely as yet unknown) complex mechanisms that contribute towards each of these effects and more and it is quite typical for the optimal conditions to be in fine balance. In order to get the best improvements of any property for any matrix/filler combination, it is crucial that the all of the consequences of making adjustments to the formulation are fully appreciated and understood, even if they may seem minor in the particular context in which they are made. Polymer composites are notionally very simple materials, but the degree of dependency between variables, the bulk effects of varying structural scales and the difficulty in isolating genuinely intrinsic material properties makes them a highly complex subject [24]. Like many great discoveries, the early origins

of synthetic polymer technology could be described as serendipitous. The goal of any scientist (including the author of this text) is of course to establish refined hypotheses, to perform methodical observations and make appropriate conclusions based on these. However, the best attempts were made to embrace serendipity in the earliest hypothesis-forming stages of research.

The subject of this thesis is on calcium carbonate / PP composites. Following a business case that will now be presented to commercially support this research endeavour, the remaining Chapters will cover in specific detail literature-based, theoretical and practical research on an as-broad-as-possible platform of composite production including; filler treatment, mineral and composite processing conditions, the actual processing methods, key analytical aspects at each stage and methods of maximising mechanical property benefits, each with the ultimate aim of providing novel formulae, formulations and methods of analysis for well-established materials that could ideally go on to perform at least as well as their predecessors, but at greatly reduced costs to the manufacturers, customers and ultimately our finite Earth resources.

1.3 Business Case

There are three main drivers that favour research into improving industrial polymer composites formulation to prepare lighter, stronger, less expensive alternative (or developed) materials with a lower overall carbon footprint. These drivers are of interest not only to the minerals and composites processing industries but also to any parties with an interest in reducing the environmental impact caused by the production and use of billions of tons worth of materials that occurs every year. They will now each be discussed in turn.

The first and arguably most obvious driver is the potential to reduce energy consumption associated with composites production and their long-term use. There are many ways in which an improved formulation of a heavily-produced material could act to reduce energy expenditure. Of great current interest in the composites science community is the potential to improve the specific properties of

materials (that is the properties of a material in relation to its mass), such that their mass may be reduced with no detriment to the key properties required in its application. In calcium carbonate/PP composites for example, the fineness of the mineral has been conclusively shown to affect the specific impact resistance of the composite in which they are dispersed such that finer dispersion provides greater specific impact resistance, thereby potentially allowing a lower proportion of mineral (which is typically 2-3 times as dense as the polymer) that is required in the composite. The underlying science is a subject for the subsequent Chapters, but due to the heavy use of these and other similar composite materials in the automotive industry (especially as dashboards and bumpers), the reduction of the mass that a fixed volume of material possesses not only could require less energy in preparing by using less mineral but also improve the mileage efficiency per unit of fuel that these automobiles consume. Any significant and globally-applicable improvement to such a composite is desirable to our planet, and would continue to be relevant regardless of how vehicles are fuelled. Regardless of whether this change could be implemented successfully or not, there is a potential for energy savings by other formulation improvements. While the finest fillers inherently require more energy-intensive mixing compared to coarser particles of the same material, there is potential to research new formulations that allow for a reduction of the required energy intensity of mixing. This could mean an upheaval of the very formulation process or simply minor protocol adjustments that act to provide such an effect.

The second driver behind the research presented in this thesis is the possibility for financial savings available to minerals and composites formulators. Due to the nature of business and the governance of developed nations, this driver is strongly related to the first in the sense that a 'greener' product is generally more favourable; carbon footprint or sustainability affects government regulations, public relations, customer perceptions and ultimately product profitability. However, there is potential for such a research endeavour to bring financial benefits to companies through means besides energy savings, one example being the way in which analyses are performed. In our technological age there is a wide range of complex apparatus that requires intense labour, expertise and / or time. Intricate

apparatus is naturally of great benefit to science, understanding and problem-solving, but it can also lead to a temptation to search for unnecessarily complex answers to problems which are in reality more straightforward. The point being that all avenues should be researched across a range of complexities. To paraphrase a highly influential 20th Century science, industrial research and development should rely on the simplest investigative means (but no simpler) [25]. There should be a focus on reducing equipment costs, reducing analysis time, reducing unnecessary operational complexities and seeking automation wherever possible. This makes more resources available to a company, allowing more investment in problems that require them more profoundly.

The third driver behind this type of research is the rather more subtle pursuit of strategic advantage. A process which is an industrial novelty, if successful enough, will allow a company to dictate the next generation of products and thereby remain ahead of its competitors. The company that developed the process will most likely know the most cost-effective ways of operating it. If the company believes it is sufficiently valuable and/or sensitive, they may go a step further and publicise the details in the form of a patent, preventing others from making any profit from their process for a fixed term. Therefore all companies with a research and development arm are constantly seeking out such strategic advantages. More specific advantages may also be sought. In the industry of minerals processing for the purposes of polymer composite applications for example, a common practice is for minerals processors to sell their products to independent formulators of a concentrated composite form known as 'masterbatch', who will then utilise or sell their product to producers of the final composite application. The performers of this central link in the overall formulation chain will be specialists at incorporating mineral product into polymer resins at a high concentration, or 'loading'. A typical masterbatch loading might be between 50 – 70 % w/w, but this depends highly on the materials involved [26]. If a minerals processing company could easily incorporate their products into polymers themselves, then logistical, financial and strategic advantages could be sought by selling their own masterbatch formulations to a wider customer base.

1.4 Closing Words

The work presented in this thesis is the result of a four-year industrially based research project in the field of formulation engineering, which principally took place at the University of Birmingham and at Imerys Minerals UK. All of the presented research in the following chapters was conducted first-hand by the author.

To summarise this Chapter, there are many reasons why continued mineral/polymer composite research should be performed. In the case where they are prepared for applications that rely on the property of impact resistance, this specific property should be of primary consideration when altering other aspects of the formulation, such as those described. Due to the complexity of the interactions between each of the constituent chemical and physical phases of these materials, it is prudent to confine the materials selection to a principal formulation which can then be adjusted, amended and developed as required. Calcium carbonate dispersed in polypropylene was selected as the target combination due to the low cost, versatility in processing, potential performance, current commercial relevance and predicted future growth of the constituent materials.

1.5 References

1. Johnston J, Merwin HE and Williamson ED. The Several Forms of Calcium Carbonate. *Am J Sci* 1916; 41(246): 473-512
2. Rohleder J, Kroker E and Tegethoff FW. Calcium Carbonate: From the Cretaceous Period into the 21st Century. Birkhauser, English ed. 2001
3. <http://www.ima-na.org/calcium-carbonate> (Accessed 4/8/2010)
4. Confederation of European Paper Industries (CEPI) Brief N^o.6. Strategic Positioning Study of the Marble Branch. 2005
5. Rothon RN. Particulate-Filled Polymer Composites. Rapra, 2nd ed. 2003
6. <http://www.imerys.com> (Accessed 13/9/2010)
7. Aitani AM and Lee S. Polypropylene Production. Encyclopedia of Chemical Processing. CRC Press, 2nd ed. 2005
8. <http://www.pardos-marketing.com/hot01.htm> (Accessed 3/9/2010)
9. <http://www.reinforcedplastics.com/view/11141/volkswagen-switches-to-polypropylene-composite-for-air-intake-manifolds/> (Accessed 13/9/2010)
10. Dubois P et al. Fillers, Filled Polymers and Polymer Blends. Wiley. 2006
11. Mazza PPA et al. A new Palaeolithic discovery: tar-hafted stone tools in a European Mid-Pleistocene bone-bearing bed. *J Archaeol Sci*, 2006; 33(9): 1310-1318
12. Staudinger H and Wiedersheim V. High Polymer Bonding 21 – The Reduction of Styrol. *Ber Dtsch Chem Ges*, 1929; 62: 2406-2411
13. *J Polym Sci*, 1946; 1(1) 1
14. Fenichell S. Plastic – The Making of a Synthetic Century. Harperbusiness. 1997
15. Baekeland LH. Bakelite, a Condensation Product of Phenols and Formaldehyde and its Uses. *J Frankl Inst*, 1910; 169: 55-60
16. Jenkins EW. The Discovery of Polythene – A Case History. *School Sci Math* 2010; 68(2): 135-140
17. Gillespie JF and Fordham JWL. Polypropylene – Production with Ziegler Catalysts. *Ind Eng Chem*, 1959; 51(11): 1365-1368
18. Reboul P and Perree R. Bakelite - The Material of a Thousand Uses. Snoeck-Ducaji & Zoon. 1996
19. Bockmann F. Celluloid – Its Raw Material, Manufacture, Properties and Uses. Bibliobazaar. 2008
20. Stevens MP. Polymer Chemistry – An Introduction. Oxford University Press. 3rd ed. 1999
21. Gold LW. Building Ships from Ice: Habbakuk and after. *Interdiscipl Sci Rev*, 2004; 29(4): 373-384
22. Kellar JJ, Herpfer MA and Moudgil BM. Functional Fillers and Nanoscale Minerals. SME, 2003
23. Karian HG. Handbook of Polypropylene and Polypropylene Composites. Marcel Dekker, 2nd ed. 2003
24. Kinloch AJ and Young RJ. Fracture Behaviour of Polymers. Applied Science Publishers. 1983
25. Mayer J and Holms JP. Bite-Size Einstein. Gramercy. 2003
26. Murphy J. Additives for Plastics Handbook. Elsevier, 2nd ed. 2001

CHAPTER TWO

Modern Challenges in the Production of Impact- Resistant Materials

FIGURES

Figure 2.1; An example of the effects of temperature on modulus for a polymeric material.....	25
Figure 2.2; An example of the effects of strain on modulus for a polymeric material	26
Figure 2.3; Basic particle shapes from mineral samples; A: calcium carbonate, B: wollastonite and C: talc.....	32
Figure 2.4; A representation of the multiple phases present in a typical composite comprising blocky filler particles which are coated, compatibilising agents and (semi-crystalline) polymer	35
Figure 2.5; A schematic representation of a conventional industrial mixing process that uses twin-screw extrusion	37

2 MODERN CHALLENGES IN THE PRODUCTION OF IMPACT-RESISTANT POLYMER MATERIALS

2.1 Aims of This Chapter

In the previous Chapter, the minimum material specifications for the purposes of meeting global production demands for cost-effective impact resistant materials were defined. The aims of this Chapter are to review the modern technical challenges that face a global manufacturer of impact-resistant materials, through material behaviour, implementation and measurement.

2.2 Interpreting the Behaviour of Polymers and their Composites

The behaviour of polymers, and materials that include them, is a complex and highly varied field that speaks to many different branches of science and technology. Reliable prediction of the mechanical performance of such ubiquitous materials is often a required for their intended application. The ideal solution would be to define fundamental material properties and have reliable models that could be applied to predict their behaviour in any given situation. To achieve this for polymers has been a key aim in the field of applied fracture mechanics; a branch of materials science and mechanical engineering [1]. Unfortunately, elucidating such properties to yield accurate predictions of how a material performs under impact (a highly significant characteristic for many materials) has not been achieved for all polymers, including some of those most commonly-used [2]. The difficulties of rigorous characterisations are demonstrated when considering that for one specific pure polymer, its stress-strain behaviour can vary drastically according to certain variables, even in simple systems [3]. This behaviour will have an influence over all of its mechanical properties, including impact resistance measurements.

The most important variables that can influence the behaviour of polymers and their composites are identified and summarised below, beginning with general ones which can affect all polymers and gradually becoming more specific, leading finally to those affecting the impact resistance of composites comprising calcium carbonate and polypropylene.

2.2.1 *General Case – Most Polymers*

The nature of the following states, properties and variables can have a profound influence on how almost any polymer or polymer mixture performs under testing.

(I) Aspects of Main Molecular Structure

The chemical identity of the molecular chain and its molecular weight will certainly affect the properties of the polymer that composes of them. However, this is a fact shared by every material. The multitude of ways in which long molecular chains interact or react with one another is what separates polymers from other materials.

Some polymers can undergo a chemical reaction on applying sufficient energy that causes the cross-linking of neighbouring chains, creating a widespread fused network throughout the structure (thermosetting plastics). A fused network will require a great deal more energy to become mobilised, compared to chains that are not fused. In fact, the process of cross-linking typically elevates this required energy to a level greater than that required to degrade the fused polymer and as such, these materials have limited potential for re-use. The manner of their formation can lead to high levels of resistance to scratching, to solvents and to weathering which makes them highly effective for use as coatings, adhesives and sidings [4].

Polymers whose chains do not possess sufficiently reactive chemistries on heating will not react; an appropriate degree of energy will simply mobilise the chains, which may be reversed or even repeated several times (thermoplastics) before noticeable degradation has occurred. This category of polymers is therefore generally more versatile in terms of processing and forming methods.

Of course, by specifying a particular polymer with given molecular characteristics whose changes are monitored, this 'variable' itself cannot prevent a rigorous material characterisation from taking place. It was mentioned here briefly nevertheless, as it is the most fundamental bifurcation of polymer types and their resulting properties.

(II) Sensitivity to Impurities and Oxidation

Low molecular weight inert impurities generally induce a softening effect on polymers, when present to a sufficient degree, which is typically detrimental to their toughness [5]. Some polymers (including polyamides such as Nylon) are highly hygroscopic, and as such special preventative measures must be used during their processing, to ensure their performance potential is reached. The necessity for special measures during processing may compromise the cost-effectiveness of a material, compared to a similarly-performing one that is not so sensitive.

All polymers undergo oxidation over time, when in an oxidising environment, such as the open air. They have varying natural propensities to oxidise and degrade, which determines the upper limits of their ideal processing temperatures and times. Provided that this phenomenon is controlled using inexpensive means, such as tightly-controlled processing (or chemical additives in small quantities), then it will not seriously hinder the cost-effective performance of a polymer.

(III) Phase Transitions

It is not valid to suggest that all polymers have *melting points*, but rather they undergo bulk phase transitions over a given temperature *range*. Firstly, only the crystalline content of a polymer (that is present in some, but not all) can be correctly said to 'melt'. Crystalline structures can include both different lengths and different configurations of chains, so polymers with a crystalline content will melt over a temperature range. The term, T_m quoted for these polymers may appear to be a single point, but a standard method will have been applied to acquire a single value from what is in fact a range, for the purposes of material comparisons [6]. Secondly, the variation in chain mobility in the bulk material means that the bulk phase transition of material from a glassy to a rubbery state (that all polymers can observe to some degree) will also occur over a temperature range. The term, T_g (glass transition temperature) is often similarly quoted as a value that may appear to be a single point despite this, similar to T_m .

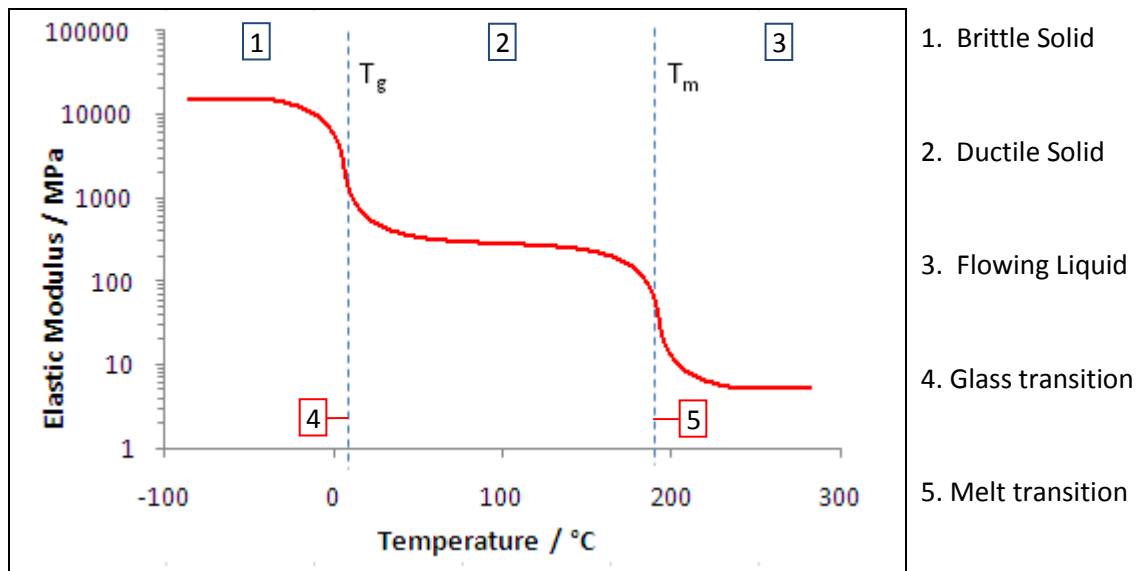


Figure 2.1; An example of the effects of temperature on modulus for a polymeric material

Figure 2.1 shows the phases and the temperature ranges of phase transition for a polymer, such as polypropylene. T_m is always greater than T_g . For $T < T_g$ the polymer is glassy and at its hardest, stiffest and most brittle, exhibiting elastic behaviour prior to fracture (which often coincides with yielding); returning to its original configuration after the removal of strain. For $T_g < T < T_m$, greater energy levels have facilitated the presence of 'free volume' where sections of chains can move freely, causing a more rubbery structure that is softer, more flexible and tougher than the glassy state. In this temperature range, the potential for a polymer to exhibit plastic behaviour is significantly improved; being more diverse in the manner in which it responds to strain (allowing fracture to occur after yielding). For $T_m < T$, semi-crystalline polymers, like polypropylene, will exhibit viscous flow.

Amorphous polymers (those with no crystalline content) will gradually become softer when $T_g < T$ and T is increased and will with enough thermal energy undergo the transition from a rubbery state into a flowing viscous state. When considering the practical applications of polymers, the temperature at which they are used will therefore affect their properties, especially the temperature compared to its T_g .

(IV) Viscoelasticity, Conditions of Testing and Fracture Mechanics

Polymers are viscoelastic materials; they exhibit properties characteristic of both viscous liquids and elastic solids, which together cause them to exhibit time-dependent strain [7]. The nature of their composition (i.e. formation from long, flexible chains) means that their response is highly dependent on the conditions of a test in which it is observed [8]. The dependence is such that the properties can vary significantly across practical and relatively narrow ranges of temperatures, as previously described and also, rates of strain [9]. The elastic properties of a polymer (such as Young's modulus) are most predictable at low temperatures and rates of strain. For all polymers, the linear strain responses to stress that may be observed in these elastic conditions can become plastic by increasing the temperature or strain rate.

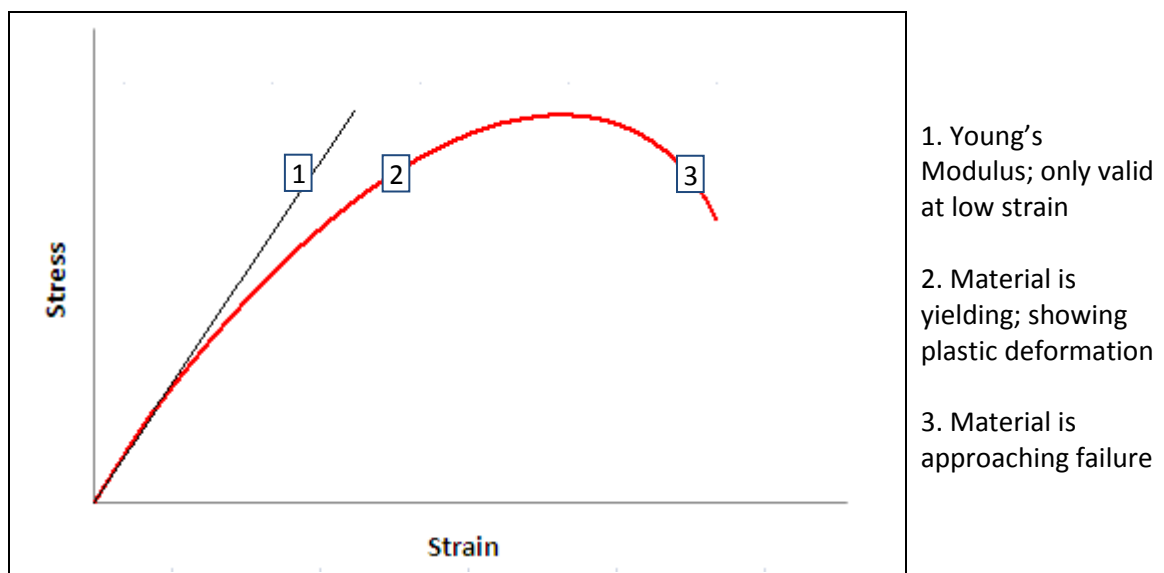


Figure 2.2; An example of the effects of strain on modulus for a polymeric material

Viscoelasticity can also be observed in measurements of creep, hysteresis and stress-relaxation [10].

Viscoelasticity is also reflected in the conditions necessary to not only cause the material to fracture, but also to dictate the manner in which it does so [11].

The conditions present when testing a material (in relation to its phase transition character) determine the mechanism through which it undergoes fracture [12]. The viscoelastic properties of that material determine the threshold limits of these conditions. Neat, isotactic polypropylene for

example can be characterised as a highly ductile material, if the conditions favour the movement and relaxation of polymer chains. Specimen geometry, impact velocity and temperature have each been found to significantly alter the response of polypropylene [13]. Generally, thinner specimens, low rates of strain and high temperatures (that are still sufficiently low, to as avoid systemic degradation) each favour ductile behaviour. A material can be described as ductile if it undergoes any significant degree of plastic deformation prior to fracturing [14]. The definition clearly does not stipulate any testing conditions. Any effect that restricts the movement of polymer chains will limit the extent to which plastic deformation occurs prior to fracture, thereby favouring brittle behaviour. Such effects induce a specific degree of restriction to chains, but how this restriction alters the mode of fracture will depend on the conditions of the test.

Fracture mechanics models were pioneered in the early twentieth century [15]. The Griffith fracture theory is still being applied today. Soon after they were made available, research into mechanical behaviour modelling began and is still ongoing today. The aim of a model is to encapsulate an entire host of known and unknown mechanics of a material undergoing a relevant process into a single algorithm with the intention of subsequently predicted its behaviour in similar processes to an accurate degree. The very existence of a wide array of different mechanical models in polymer science is testament to their complexity. Recently, successful modelling was achieved for practical polymer scenarios; including large deformations, strain rate dependence of stress and the yielding mechanism in bi-axial tests [16]. Modelling has also been applied to multi-axial tests, but the accuracy of these models diminished with increased rates of strain, which were arguably the most realistic reflection of a test designed to gauge significant levels of impact resistance [17]. The role of craze formation (micro-structural voids) in polymer toughness remains an active area of research. The extent to which they propagate into a distributed network during testing has been shown to play a significant role in the ultimate materials properties [18].

For very simple polymer types (i.e. those with maximum microstructural uniformity) that are subjected to well-defined tests, some fundamental material properties appear to have been identified [19]. However, very few modern day applications see the combination of simple microstructures and well-defined testing conditions. The mechanisms through which the materials are acting in tests that use multi-axial stressing are more complex and therefore more difficult to model than those that are uni-axial [1]. Polypropylene used for multi-axial impact resistance is precisely such an example, and no models could be found that attempted to elucidate polymer properties based on these tests. Some of the principles that apply to the simpler scenarios still have value. The critical stress concentration factor, K_c is defined as the critical value of concentrated stress that a given surface area of material is can withstand immediately prior to fracture. Despite some practical limitations, theories used to explain the behaviour of more complex systems could nevertheless draw on this and other concepts from that field [20].

2.2.2 *Specific Cases – Polymers with Additional Phases*

Some polymers contain multiple phases of structure. This includes instances where other materials have been deliberately incorporated (i.e. composites), but also applies to neat polymers whose molecular chains align on freezing to form distinct crystallographic regions (i.e. in semi-crystalline polymers). It has already been made clear that the precise mechanical response can be affected by the mobility of polymer chains. These phases can affect the results of mechanical tests, for example by leading to structural slippage [21].

(I) Crystallinity

It has been mentioned that crystallinity can occur in some polymers at sufficiently low temperatures. Crystal structures in polymers and their formation kinetics have been extensively studied. It is considered that by studying the crystalline nature of polymers, further knowledge regarding its microstructure may be ascertained. For example, the degree of steric hindrance in polymer chains and the distribution of crystallinity throughout the polymer structure have been attributed to a

particular crystallisation phenomenon observed of PP composites comprising various concentrations of fly ash [22]. Some specific effects of nucleating agents of carbon black with a poly (lactic acid) phase have also been identified using similar tests [23]. Even optical and mechanical properties have been determined from the use of crystallisation phenomena to investigate microstructure, which was performed on PP / PE blends [24].

In PP, various unique crystal phases have been identified, depending on the specific nature of the polymer. Three phases in PP have been defined as α -monoclinic, β -pseudo-hexagonal and γ -orthorhombic, which are based on their spectroscopic response [22]. Different phases have been observed and investigated in varying orientations of this polymer, for example in isotactic [25], syndiotactic [26] and random copolymer phases [27]. There has been some research into the effect of these individual crystal structures on the overall mechanical properties and it has been inferred that the so-called β -phase (of pseudo-hexagonal crystal structure) provides superior mechanical properties, compared to the more stable α -phase [28]. However, control over the specific crystalline phases in meaningful quantities in a real polymer cannot be performed cost-effectively and the true relationship between these phases and the resulting polymer properties has proven difficult to elucidate with any degree of certainty.

When meeting global production demands of PP, multiple crystal structures, including those regarded as being inferior to the final properties, will certainly exist. Any interactions that crystal structures may have with each other (and also the amorphous phase) during the use of the bulk material may contribute unknown benefits to its mechanical performance. The current state of its science and the commercial markets to which it would be sold suggest that the modest benefits that can seemingly be brought (to the mechanical performance of polypropylene homopolymer through manipulation of its crystalline structure) would cost more to implement than the perceived additional value of this new material and therefore it would not be a cost-effective measure. Copolymers from polypropylene are subtly different. Modifications to the crystal structure (caused

in this case by alterations in the polymerisation chemistry) have a strong effect on the properties. These invariably take the form of lowering the crystalline content since deviations away from a uniformly extended single carbon chain structure will make the chains less likely to form the close interactions required for genuine solid structure [29]. This effect also creates greater levels of 'free volume'. Therefore copolymers can behave more rubber-like compared to equivalent homopolymers, under the same testing conditions. However, just as increasing the temperature of a glassy polymer leads to arguably undesirable characteristics (for example softening and increased flexibility) as well as the desirable benefit to toughness, copolymers will also incur these changes compared to the homopolymer.

To improve the cost-effective performance of a selected polymer material using justifiable processes, some of the crystalline content should be monitored since this evidently can affect polymer performance and any such improvement processes may benefit cost-effective performance through any number of intermediate effects, including the content of the crystalline structure.

(II) Filler Particles and their Surfaces

There are many different characteristics of the mechanical behaviour of a polymer that can be altered by incorporating a sufficient number of particles into its structure to form a composite. The term, 'particles' is not extremely specific and as such, it is commonsense to consider their own characteristics and categorise them accordingly. Their surface chemistry, mechanical properties, morphology and concentration in the composite mixture are all particle aspects that determine how they affect the mechanical performance of a polymer when mixed into it. (The overall compatibility between the particle and polymer phases and the mixing processes used to implement these aspects also affect mechanical performance. They are discussed separately in subsequent sections).

The surface chemistry of fillers may be altered to improve any aspect that may ultimately lead to an improvement of the cost-effective performance of polymers. It may be manipulated simply to

improve the particles themselves, such as enabling easier particle handling, allowing for more efficient packing or reducing hygroscopicity (for example to prevent or limit subsequent aggregation) [30]. It may also be used to provide performance benefits to the composite, through surface compatibility and interaction, or to act as sites that nucleate crystal growth [31]. It could also be used to bring functionality to a polymer that would otherwise be absent [32].

The rigidity of particles can affect the performance of the composite that contains them. It has proven possible to improve the impact properties of polymers by both rigid and soft particles alike [33]. For rigid particles, such as minerals de-bonding composite systems (where the surfaces of the particles are not bound to the polymeric structure) are effective for impact. Firstly, this is because bonded particles cause isolated pinning of polymer movement, creating a flaw; a localised region where stresses concentrate when the material is subjected to strain and the brittle behaviour that gets observed can once again be attributed to the lack of freedom in chain movement. Secondly, the freedom of particle movement allows for distribution of stresses over a greater volume of material, allowing the material itself to seemingly be able to withstand greater strain. (In composites whose particles facilitate widespread crazing on impact, the effects of particle rigidity will lessen, however).

Particles can take the form of many shapes. Even within a collection of similarly-sourced particles, there naturally exists a distribution of shapes and sizes. To categorise their shapes into a small number of types can therefore be difficult. It is common practice to categorise them based on the relative lengths of their x, y and z co-ordinates positioned such that z is the longest possible dimension, y the next longest and x being the shortest [34].

The aspect ratio of a particle is a characteristic of its relative shape. It may be thought of as the ratio between the longest physical dimension of a particle (z, its principal axis) and the shortest of its orthogonal dimensions (x). Put simply, it is z/x based on the above definition. Perfect spheres have an infinite number of principal and orthogonal axes (and $z = y = x$) and the aspect ratio is 1. Blocky or

spheroidal particles have two orthogonal axes that are of similar length to the principle axis (and therefore $z \approx y \approx x$) and an aspect ratio greater than 1 but less than or equal to 3 [2]. Needle-shaped or acicular particles have two short orthogonal axes and a long principle axis ($z > y \approx x$) and aspect ratios from greater than 3 to 2-5 orders of magnitude higher can be produced [35]. Platy or laminar particles have one short orthogonal axis and two larger axes ($z \approx y > x$) and an aspect ratio of 2-3 orders of magnitude can be achieved [36].

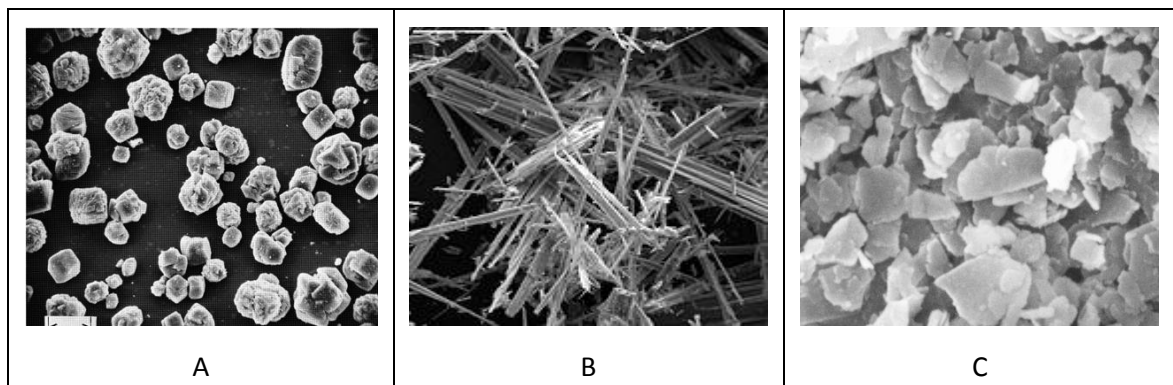


Figure 2.3; Basic particle shapes from mineral samples; A: calcium carbonate, B: wollastonite and C: talc

Figure 2.3 depicts an example of how basic particle shapes can be broadly categorised based on the relative lengths of their axes, into three types; blocky, acicular or platy.

The way in which these particles have been categorised also provides a rule-of-thumb for the different types of mechanical strength that they can provide to a polymer when they are mixed together to form a composite [37]. Blocky particles provide impact strength, acicular particles provide tensile strength and platy particles provide flexural strength [38]. The selection of the appropriate particles depends therefore on the desired application. Blocky particles are therefore highly desirable for the improvement of impact strength of car bumpers. Mechanical properties are insensitive to the alignment of spherical particles (that have an aspect ratio of unity) in the composite mixture, but they become increasingly sensitive to their alignment as their aspect ratio increases, which has been demonstrated experimentally [39].

As well as the shape of the dispersed phase particles, their size can affect the mechanical properties of the composite in which they are contained. The theory of stress concentration as a function of flaw size has been considered in modern research in this field, and is applicable to any composite material [40]. The theory suggests that finer particles, as well as having a less pronounced 'flaw' effect thereby keeping stress concentration to a lower value than that of coarse particles, finer particles that are also de-bonded in the system will assist the distribution of stresses throughout the composite structure during impact [41]. The presence of very coarse particles will fail to distribute and moreover act as a site of concentration of stresses and therefore create difficulties for the formulation engineer of cost-effective materials. Producing very fine particles ($< 1 \mu\text{m}$ in diameter, depending on the substance) can also create difficulties when it comes to mixing, by becoming hard to disperse into their fundamental sizes and hard to distribute evenly throughout the polymer [42]. These challenges of mixing are an aspect of implementation and are therefore addressed in more detail in Section 2.5. It is mentioned here because the mixing process itself may alter the particle size distribution. The size of the particles, especially when they appear fine, before the mixing process is not relevant to composite properties, but rather their size distribution that is present *in situ* will dictate its effects.

The concentration at which particles are included in a polymer phase affects the behaviour of the composite that comprises them, which manifests in changes in the mechanical [43] and rheological [44] behaviour alike. The order (and the general simplicity) of these effects can vary according to the mechanisms through which the particles act to alter a given mechanical property [45]. As mentioned, performing tests under uni-axial or bi-axial stress will generally result in simpler mechanisms than multi-axial ones. The nature of the effects of particle concentration is simple and intuitive in some tests, but complex and not well understood in others. The complexity of the structure of the composite material that is exposed during a test has a large influence over the complexity of the particle-dependent properties that are measured; including the particle concentration.

Due to the difference in surface properties that can occur between the continuous and dispersed phases of a composite, their compatibility is vital in achieving effective mechanical performance. Surface treatments performed on filler particles act as a primary measure of improving this compatibility, which is a subject that is addressed further under the next heading, 'Formulation Additives' that includes agents that are used to improve phase compatibility.

The process with which particles are mixed into a polymer is vital to the effective implementation of particle aspects that allows them to optimally contribute to the final composite performance. It is discussed in more detail in Section 2.3.

(III) Formulation Additives

Although fillers themselves could be described as 'additives', it is wide convention to use the latter term to apply to any additional materials beyond those of the filler and those that make up the filler surface. A formulation additive may be included to extend composite functionality, add new functionality to it or to aid its processing.

One way of extending the functionality that a filler material brings to a composite is to further improve the compatibility between the phases, beyond just using filler surface treatments [46]. The inclusion of additional polymer materials with intermediate or multiple functionality to accommodate the principal phases has been performed using polypropylene polymer chains that have been grafted with a polar moiety, much as maleic anhydride and several others [47]. Such materials are usually referred to as compatibilising agents; they may bring no additional functionality to composite other than to improve the mixing extent of the phases and their final performance. While significantly more expensive to acquire than the same volume of regular polypropylene, small quantities of compatibilising agents may be able to improve the composite properties to a degree that makes investing in them worthwhile [48].

Figure 2.4 shows a representation of phases in a polymer composite that include agents used to enhance phase compatibility.

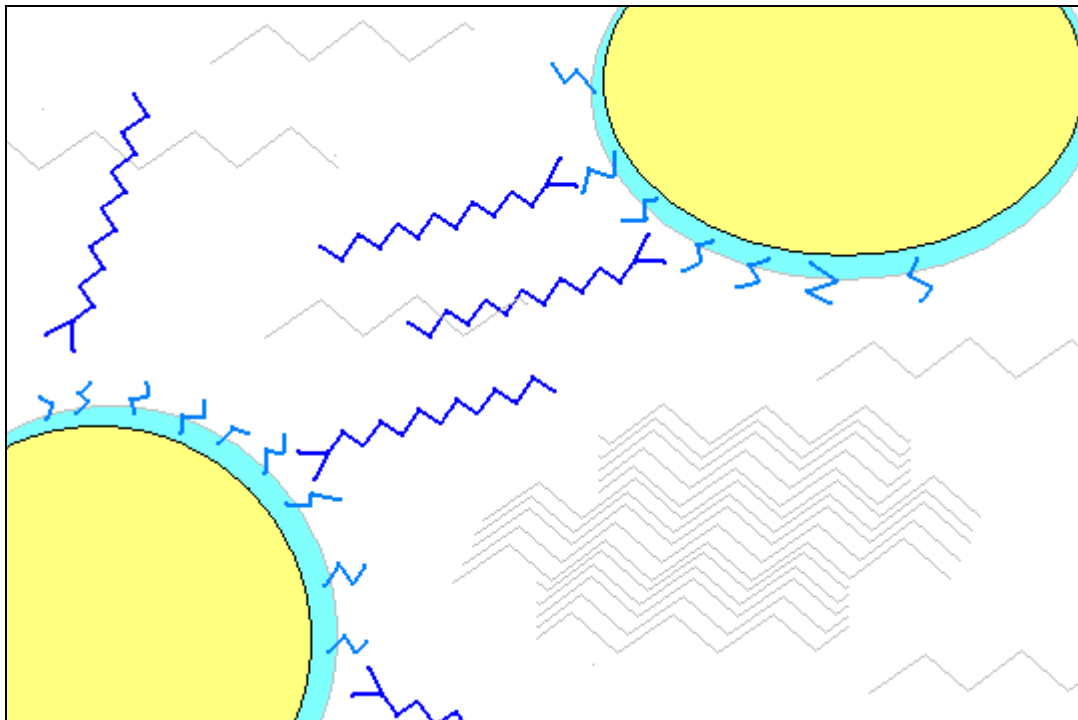


Figure 2.4; A representation of the multiple phases present in a typical composite comprising blocky filler particles which are coated, compatibilising agents and (semi-crystalline) polymer

Additives may be included to ‘plasticise’ a polymer [49]. These materials interfere with the alignment of polymer chains to give them improved mobility by extending the range of conditions in which they behave plastically, which invariably occurs in the form of a reduced glass transition temperature [50].

Other examples of frequently-encountered formulation additives include anti-oxidants and anti-foam and mould-release agents [51]. The requirement of these will depend on the nature of the composite components. They are designed to have a minimal effect on the mechanical performance of the composite that requires them, and typically include small, soluble organic compounds [52].

2.2.3 Concluding Remarks

It should be evident that the large number of different variables that affect the behaviour of polymeric materials can exhibit a degree of inter-variable dependency. As well as those which contribute to the conditions in which the rubber-like state of a pure polymer is favoured (i.e. the mobility of its constituent chains), the presence of additional phases within it such as crystalline structure, filler particles and other additives can also effect its behaviour (through chain mobility but also through other mechanisms relating to the distribution of stresses). The extent to which a structural aspect can vary in accordance to another is seen in one example where filler particles can profoundly influence the extent of crystalline structure that is formed on cooling.

It should be apparent that there are a significant number of variables that can affect the mechanical properties of composites that cannot all be adequately controlled. The full and precise extent of inter-variable dependency is not known in many of these materials, but it has been conclusively demonstrated that some of these phenomena are present. In order to research and improve the cost-effectiveness of reinforced materials, the researcher must at the very least be aware of the potential cascade of effects that a seemingly simple formula adjustment is capable of producing.

2.3 Considerations for Implementing the Chosen Materials

The inexpensive and abundant principal formulation materials that have been selected must then be implemented effectively in order to produce cost-effective, impact-resistant products. This section addresses some of the key considerations that should be made when implementing such materials through their processing.

2.3.1 Particle Preparation

The properties of the selected particles will relate strongly to the properties of the product. Those properties of a chosen particle material which are difficult to change (such as porosity and density) must therefore be taken into account during material selection. The most important properties of

the selected particles are their morphology and surface chemistry, which may both be altered significantly during their preparation by performing mechanical and chemical treatments [53]. Such processes will be frequently referred to in this thesis.

After the particles have been prepared to specification, the process of incorporating them into a polymer should impose minimal detrimental alteration to their state. The particle sizes and their spatial distribution are particularly important in delivering impact resistance to the final product.

2.3.2 The Mixing of Particles and Polymers to Form Composites

A mixing process used to form a polymer composite requires the continuous phase to be liquid during the mixing process. A ubiquitous mixing process for many polymers is twin screw extrusion [54]. Figure 2.5 shows a series of steps that includes this mixing process, to form polymer composites from its constituent materials. As indicated, the overall process uses three stages of heating and cooling.

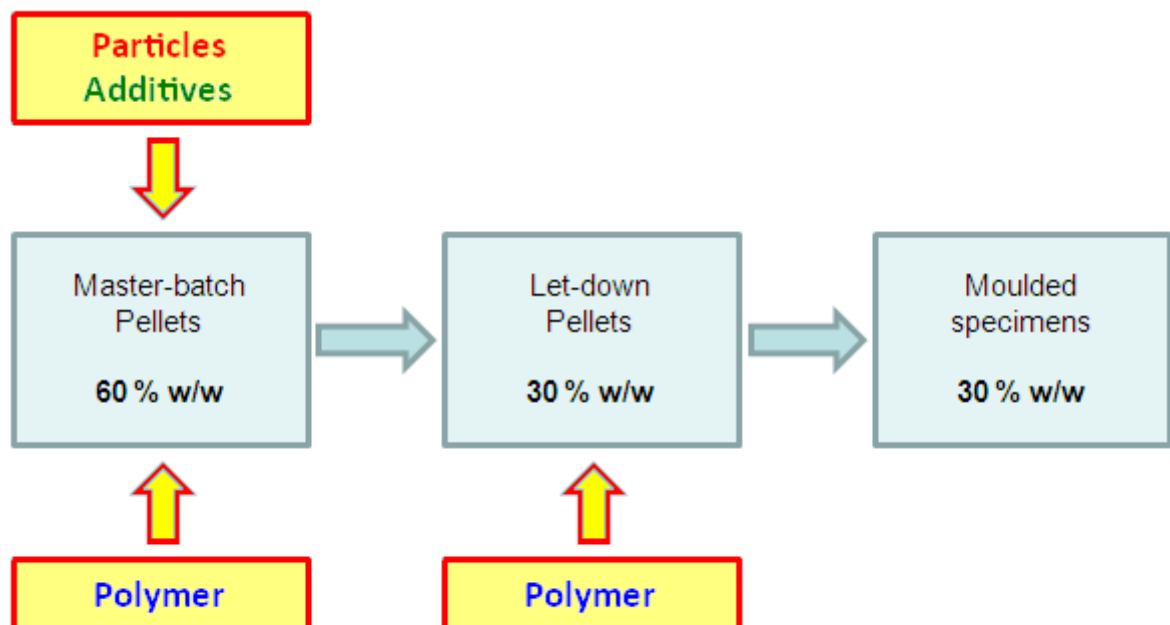


Figure 2.5; A schematic representation of a conventional industrial mixing process that uses twin-screw extrusion

Depending on the nature of the polymer, there are alternative processes that can be used to implement the required mixing process. Particles have been mixed with thermosetting plastic precursors during their cross-linking, in a process known as reactive extrusion [55]. Like twin-screw extrusion, this process has the advantage of being able to both mix and then shape the material. Particles have also been mixed into monomer compounds in liquid form, which subsequently became polymerised thereby achieving *in situ* polymerisation, which originally enabled polymer intercalation between platy particles [56]. The aspects of a mixing process that are most significant in the production of cost-effective materials to meet a global demand is the energy that the process consumes, the ease at which it may be applied, the feasibility of connecting the process to subsequent processes (such as shape formation) and of course the degree to which mixing is achieved.

In any mixing process, the degree or quality of mixing is determined by the energy density that is available to shear a given volume of mixture materials, combined with the proportion of material that gets exposed to this energy and the duration over which mixing occurs [57]. The process can be separated into two different components; 'dispersive' and 'distributive' mixing [58]. The former, 'dispersive' term may be thought of as the mixing that occurs over a very small volume and is what can cause the tearing of particulate structures into their primary particles. As such, it is tantamount to the energy density that can be achieved. The latter 'distributive' term may be thought of as the spatial uniformity to which the dispersed phase entities (regardless of their size) appear in the final product. A complete mixing process must achieve both of these aspects when implementing fine particles into a polymer in order for the material to reach its potential, in terms of mechanical performance.

It has been shown that transforming the starting materials to cost-effective products involves several different stages of processing. They can be categorised very generally into two stages; particle preparation and material mixing. Each of which may be split into several different fundamental

processes, each of which may impose effects on the condition of the materials. To acquire accurate information about these effects at each stage in the process, the materials must be studied appropriately.

2.4 Effective Measurements

Before and after every stage of the process, measurements can be performed on the materials in question to validate the efficacy of that individual stage. This section describes key analytical procedures that can be used to study the materials, given all the previous information that was collected and presented in the Chapter.

2.4.1 Particle Properties

The nature of the suspending media in which particles are present can have a profound effect on their morphological properties [59]. The way in which their effective particle size can change in different media has significant implications, especially in terms of alterations to the predicted composite performance. Measurements of the distribution of particle size which have taken place in one medium do not guarantee a representative figure in others. Media may be described as 'favourable' if particulate material that is suspended in it naturally disperses into fundamental particles with minimal mixing energy. Water, for example is a more favourable medium for the dispersion of (uncoated) calcium carbonate compared to non-polar medium and the measured particle sizes will be finer for a given particle grade (assuming their surfaces are sufficiently repellent, such as when an effective dispersant is present). Favourability in this sense will be a function of the surface energy of the suspended material and the nature of the material that suspends them.

Polypropylene differs from water as a material in many ways, including its viscosity (which is higher) and its polarity (which is lower) [60]. Both of these contribute to making polypropylene a less-favourable dispersion medium for (untreated) calcium carbonate. In this case, significantly more mixing energy will be required to produce the particle sizes in polypropylene that are similar to those measured in water. It may even be impossible to impart sufficient energy to achieve this without

compromising the molecular integrity of the polymer [61]. This consideration becomes increasingly pronounced and relevant with finer and finer particle sizes. The ability to impart sufficient mixing to nanocomposites whilst avoiding degradation is critical in the extent of the role these materials will play in future materials technology. Therefore, measuring the particles after they have been mixed into a polymer is valid and likely to observe closer dependencies to the mechanical properties of a composite, compared to measurement that were acquired from a medium that is chemically unrepresentative of the application material. The most representative particle size measurements will be obtained directly from its application medium; which is said to be '*in situ*'.

When measuring particle size distributions, both fine particle detail and high particle counts are required for accuracy. In technical terms, these are termed as how resolved and how representative the measurement is, respectively. With a fixed capacity of particle information, these parameters are in direct competition with each other. Indeed in practice, a technique that is strong in one of these elements is usually much weaker in the other. A degree of optimisation (when using one technique) or complementation (when using multiple techniques) is required. An example of the extremes may be found when considering the analysis of a clear, thin polymer film containing 5 % opaque particles. Transmission electron microscopy may be applied to achieve the highest visual resolutions available to science [62]. Alternatively, the film could be simply be studied in front of a light source by eye, thereby accounting for an area of film with practical relevance. In reality both of these measurements could prove useful when used with the other, but the data they provide may not be sufficient in isolation.

2.4.2 *Composite Microstructure and Flow*

Besides being capable of affecting its mechanical properties in the solid state, the microstructure of a polymer composite can affect the degree to which it is able to flow when in its molten state [63]. An ideal polymer material will flow quickly and predictably when molten, but retain its shape perfectly when solid. The flow properties of a polymer will affect the minimum cycle times required during a

shape forming process, which becomes relevant when producing materials to meet global demand [64].

Rheology (the study of flow) of polymers is a subject of extensive review [65]. Data acquired from rheological tests of polymers is highly susceptible to variation because of the complex nature of chain interactions (especially when additional phases are present, such as particles) and the fact that the heating and cooling history of a polymer greatly influences its results [66]. The extent of crystallisation that was discussed previously also has a significant influence over these results. Particle-particle interactions can also introduce thixotropy to a polymer system; a time-dependent structural breakdown [67].

In some circumstances, it is useful to just have a number to allow comparisons of polymer or composite flow between similar materials, which is referred to as its melt flow index [68]. Quoted values each have units that describe a mass of polymer that was adjudged to have undergone flow under a stated load, at a stated temperature and for a stated period of time. At 190 °C, under a load of 2.16 kg with a pre-heating duration of 6 minutes, polypropylene derivatives for example will usually produce between 2 and 20 g of output material that has undergone flow [69]. Within this range, the available processes to which the material is amenable may vary, for example film formation using casting, which requires a low melt flow index ($< 6 \text{ g} / 10 \text{ min}$) [70].

2.4.3 *Impact Properties*

Impact resistance is a term that is synonymous with impact strength. However, defining it in this way allows for observations other than those directly of strength to be performed. Strength is the energy required to create yielding (or fracture) over a given surface area. Because in some test the active area is not always easy to define or measure, strength is not a generally recommended value when quoting multi-axial impact test data [71]. For the application as car bumpers, the desired functionality of a composite is to be resistant to multi-axial stresses that are caused during high

energy impact events. As such, data provided by falling-weight impact measurements may prove more relevant data than uni-axial impact tests [72]. Cruder testing routines will involve dropping weights (on to different samples) from increasing heights until a certain height results in a specified failure quota (for example 50 % of samples failed at height, h) [71]. More modern devices utilise impact events by being designed to consistently cause fracture, whilst monitoring sample deflection as a function of impact force up to and beyond the point of fracture [73].

2.4.4 Concluding Remarks about Measurements

When performing processes on materials it is possible that by achieving the desired process goals, unexpected and unwanted changes to another aspect of the material is introduced. In order to become aware of these changes and to successfully research process improvements, a well-chosen set of processes and measurements is required. Three highly important measurements in the process of mixing particles and polymers together to make composites for impact-resistance applications have been identified as; particle size, crystallinity (and other related microstructural aspects) and impact resistance.

2.5 Conclusions

With a foundation of previous research in place, experiments can be constructed in order to research and to improve cost-effectiveness of the impact-resistant materials of today. This appears to be possible by deliberately targeting the materials themselves, the processes that are used to transform them, effectively measuring the changes that are incurred to enable strategic modifications to the formula and finally other aspects of cost-effectiveness, such as reducing energy by creating more efficient industrial conventions. Armed with this knowledge, the real challenge lies in designing the impact-resistant materials of tomorrow.

2.6 References

1. Kinloch AJ and Young RJ. Fracture Behaviour of Polymers. Applied Science Publishers. 1983
2. Rothon RN. Particulate-Filled Polymer Composites. Rapra, 2nd ed. 2003
3. Perez J. Physics and Mechanics of Amorphous Polymers. Taylor & Francis. 1998
4. Unnikrishnan KP and Thachil ET. Toughening of Epoxy Resins. Des Monomers Polym, 2006; 9(2): 129-152
5. Stukalin EB, Douglas JF and Freed KF. Plasticization and Antiplasticization of Polymer Melts Diluted by Low Molar Mass Species. J Chem Phys, 2010; 132(8): #084504
6. Turley SG and Keskkula H. Study of Polypropylene Annealed at a Temperature Near its Melting Point. J Appl Polym Sci, 1965; 9(8): 2693
7. Nissan AH. Molecular Approach to the Problem of Viscoelasticity. Nature, 1955; 175(4453): 424
8. Miyake A. A Note on the Molecular Theory of Viscoelasticity of Polymers. J Polym Sci, 1957; 26(113): 239-240
9. Morton-Jones GJ. Polymer Processing. Springer, 1989
10. Passman SL. Stress-Relaxation, Creep, Failure and Hysteresis in a Linear Elastic Material with Voids. J Elasticity, 1984; 14(2): 201-212
11. Zezin YP. Conditions of the Ductile-Brittle Transition in Failure of Polymer Materials. Mech Composite Mater, 1988; 24(5): 579-585
12. Bucknall CB. Impact Testing of Polypropylene Mouldings. Pure Appl Chem, 1986; 58(7): 985-998
13. Daiyan H et al. Low-Velocity Impact Response of Injection-Moulded Polypropylene Plates – Part 1: Effects of Plate Thickness, Impact Velocity and Temperature. Polym Test, 2010; 29(6): 648-657
14. Callister WD. Materials Science and Engineering. John Wiley & Sons. 1999
15. Griffith AA. The Phenomena of Rupture and Flow in Solids. Philos T R Soc A, 1921; 211: 163-198
16. Sweeney J, Spares R and Woodhead M. A Constitutive Model for Large Multiaxial Deformations of Solid Polypropylene at High Temperatures. Polym Eng Sci, 2009; 49(10): 1902-1908
17. Sanchez-Soto M, et al. On the Application of a Damped Model to the Falling Weight Impact Characterization of Glass Beads-Polystyrene Composites. J Appl Polym Sci, 2004; 93(3): 1271-1284
18. Takahashi J, Yamamoto T and Shizawa K. Modeling and Simulation for Ductile Fracture Prediction of Crystalline Polymer Based on Craze Behavior. Int J Mech Sci, 2010; 52(2): 266-276
19. Akao HT and Kobayas AS. Stress-Intensity Factor for a Short Edge-Notched Specimen Subjected to 3-Point Loading. Mech Eng, 1965; 87(10): 72
20. Bramuzzo M, Savadori A and Bacci D. Polypropylene Composites – Fracture Mechanics Analysis of Impact Strength. Polym Composite, 1985; 6(1): 1-8
21. Chen LS, Mai YW and Cotterell B. Impact Fracture Energy of Mineral-Filled Polypropylene. Polym Eng Sci, 1989; 29(8): 505-512
22. Nath DCD et al. Isothermal Crystallization Kinetics of Fly Ash Filled Iso-Polypropylene Composite – and a new Physical Approach. J Therm Anal Calorim, 2010; 99(2): 423-429
23. Su ZZ et al. Non-Isothermal Crystallization Kinetics of Poly (Lactic Acid) Modified Carbon Black Composite. Polym Bulletin, 2009; 62(5): 629-642
24. Wang JB and Dou Q. Polypropylene/ Linear Low-Density Polyethylene Blends: Morphology, Crystal Structure, Optical and Mechanical Properties. J Appl Polym Sci, 2009; 111(1): 194-202

25. Hou WM et al. The Influence of Crystal Structures of Nucleating Agents on the Crystallization Behaviors of Isotactic Polypropylene. *Colloid Polym Sci*, 2006; 285(1): 11-17
26. Palmo K and Krimm S. Energetics Analysis of Forms I-IV Syndiotactic Polypropylene Crystal Structures. *Macromolecules*, 2002; 35(2): 394-402
27. Razavi-Nouri M. Thermal and Dynamic Mechanical Properties of a Polypropylene Random Copolymer. *Iran Polym J*, 2005 14(5): 485-493
28. Karger-Kocsis J et al. Instrumented Tensile and Falling Weight Impact Response of Injection-Moulded Alpha- and Beta-Phase Polypropylene Homopolymers with Various Melt Flow Indices. *J Appl Polym Sci*, 1999; 73(7): 1205-1214
29. Hutley TJ and Darlington MW. Further Observations on Impact Strength-DSC Correlation in Mineral-Filled Polypropylene. *Polym Comm*, 1985; 26(9): 264-267
30. Moczo J and Pukansky B. Polymer Micro and Nanocomposites – Structure, Interactions, Properties. *J Ind Eng Chem*, 2008; 14(5): 535-563
31. Rethon RN. Fillers and their Surface Modifiers for Polymer Applications. *Plastics Information Direct*. 2007
32. Kellar JJ, Herpfer MA and Moudgil BM. Functional Fillers and Nanoscale Minerals. *SME*, 2003
33. Riew CK and Kinloch AJ. *Toughened Plastics II*. American Chemical Society. 1996
34. Katz HS and Milewski JV. *Handbook of Fillers for Plastics*. Van Nostrand Reinhold, 2nd ed. 1987
35. Hamilton WR. *The Hamlyn Guide to Minerals, Rocks and Fossils*. Hamlyn. 1974
36. Cao T, Fasulo PD and Rodgers WR. Investigation of the Shear Stress Effect on Montmorillonite Platelet Aspect Ratio by Atomic Force Microscopy. *Appl Clay Sci*, 2010; 49(1-2):21-28
37. Jancar J. Influence of Filler Particle Shape on Elastic Moduli of PP/CaCO₃ and PP/Mg(OH) Composites 1 – Zero Interfacial Adhesion. *J Mater Sci*, 1989; 24(11): 3947-3955
38. Fernando PL. Fracture Toughness of Filled Polypropylene Copolymer Systems. *Polym Eng Sci*, 1988; 28(12): 806-814
39. Gonzaga CC et al. Effect of Processing Induced Particle Alignment on the Fracture Toughness and Fracture Behavior of Multiphase Dental Ceramics. *Dent Mater*, 2009; 25(11): 1293-1301
40. Lin JC. Investigation of Impact Behavior of Various Silica-Reinforced Polymeric Matrix Nanocomposites. *Compos Struct*, 2008; 84(2): 125-131
41. Renner K et al. Analysis of the Debonding Process in Polypropylene Model Composites. *Eur Polym J*, 2005; 41(11): 2520-2529
42. Chaochanchaikul K, Kositchaiyong A and Sombatsompop N. Blending Techniques Affecting Mechanical and Morphological Properties of Fly Ash/LDPE and CaCO₃/LDPE Composites. *Polym Polym Compos*, 2009; 17(5): 281-290
43. Khalil HPSA et al. Recycle Polypropylene (RPP) Wood Saw Dust (WSD) Composites – Part 1: The Effect of Different Filler Size and Filler Loading on Mechanical and Water Absorption Properties. *J Reinf Plast Comp*, 2006; 25(12): 1291-1303
44. Wang Y and Yu MJ. Effect of Volume Loading and Surface Treatment on the Thixotropic Behavior of Polypropylene Filled with Calcium Carbonate. *Polym Composite*, 2000; 21(1): 1-12
45. Dubnikova IL, Berezina SM and Antonov AV. Effect of Rigid Particle Size on the Toughness of Filled Polypropylene. *J Appl Polym Sci*, 2004; 94(5): 1917-1926
46. Karian HG. *Handbook of Polypropylene and Polypropylene Composites*. Marcel Dekker, 2nd ed. 2003

47. Ko TM and Ning P. Peroxide-Catalyzed Swell Grafting of Maleic Anhydride onto Polypropylene. *Polym Eng Sci*, 2000; 40(7): 1589-1595
48. Liaw WC et al. PPgMA/APTS Compound Coupling Compatibilizer in PP/Clay Hybrid Nanocomposite. *J Appl Polym Sci*, 2008; 1871-1880
49. Hong HQ et al. Influences of Ternary Graft Copolymers on the Morphology and Properties of Polypropylene/ Calcium Carbonate Composites. *Polym-Plast Technol*, 2006; 45(3): 379-387
50. Fowler JN, Chapman BR and Green DL. Impact of Plasticizers and Tackifiers on the Crystallization of Isotactic Poly(1-butene). *Eur Polym J*, 2010; 46(3): 568-577
51. Murphy J. *Additives for Plastics Handbook*. Elsevier, 2nd ed. 2001
52. Alexander M and Thachil ET. The Effectiveness of Cardanol as Plasticiser, Activator and Antioxidant for Natural Rubber Processing. *Prog Rubber Plast Recyc Tech*, 2010; 26(3): 107-123
53. Xu XM, Tao XL and Zheng Q. Influence of Surface-Modification for Calcium Carbonate on the Interaction Between the Fillers and Polydimethylsiloxane. *Chinese J Polym Sci*, 2008; 26(2): 145-152
54. Agassant JF, Andersen PG and Manas-Zloczower I. *Mixing and Compounding of Polymers – Theory and Practice*. Hanser-Gardner Publications. 1994
55. Janssen LPBM. *Reactive Extrusion Systems*. CRC Press. 2004
56. Messersmith PB and Giannelis EP. Polymer Layered Silicate Nanocomposites – In situ Intercalation Polymerization of Epsilon-Caprolactone in Layered Silicates. *Chem Mater*, 1993; 5(8): 1064-1066
57. Plochocki AP, Dey SK and Wilczynski K. Evaluating Screw Performance – Extrusion Process Stability and the Degree of Mixing from Melt Rheology Data and from Measurement on an Instrumented Extruder. *Polym Eng Sci*, 1986; 26(14): 1007-1011
58. Ess JW. *Characterization of Dispersive and Distributive Mixing in a Co-Rotating Twin-Screw Compounding Extruder*. PhD Thesis, Brunel University, 1989
59. Domka L et al. Influence of Pyridinium Chlorides on the Physicochemical Character, Morphology and Particle Size Distribution of Natural Chalk. *Tenside Surfact Det*, 2002; 39(3): 33-39
60. <http://www.sigmaaldrich.com/united-kingdom.html> (Accessed 13/9/2010)
61. Hari J et al. Kinetics of Structure Formation in PP/Layered Silicate Nanocomposites. *Express Polym Lett*, 2009; 3(11): 692-702
62. Egerton RF. *Physical principles of electron microscopy: an introduction to TEM, SEM, and AEM*. Springer. 2005
63. Wang J et al. Microstructure and Mechanical Properties of Ternary Phase Polypropylene/ Elastomer/Magnesium Hydroxide Fire-Retardant Compositions. *J Appl Polym Sci*, 1996; 60(9): 1425-1437
64. Ferreira I et al. Multidisciplinary Optimization of Injection Molding Systems. *Struct Multidiscip O*, 2010; 41(4): 621-635
65. Sedlacek B, Pukansky B et al. *The Effect of Fillers on the Rheological and Mechanical Properties of Polypropylene Composites*. Polymer Composites. Walter de Gruyter. 1986
66. Wypych G. *Handbook of Fillers*. ChemTec Publishing, 2nd ed. 1999
67. Rognon P, Einav I and Gay C. Internal Relaxation Time in Immersed Particulate Materials. *Phys Rev E*, 2010; 81(6): #061304
68. Schreibe HP and Rudin A. Effect of Carbon Black on the Time Dependence of Melt Flow Index. *J App Polym Sci*, 1967; 11(7): 1043

69. Jikan SS et al. Relationship of Rheological Study with Morphological Characteristics of Multicomponent (Talc and Calcium Carbonate) Filled Polypropylene Hybrid Composites. *J Reinf Plast Comp*, 2009; 28(21): 2577-2587
70. Private communication with Imerys Minerals UK
71. Brown R. *Handbook of Polymer Testing*. CRC Press. 1999
72. Turner S, Reed PE and Money M. Flexed Plate Impact Testing – Some Effects of Specimen Geometry. *Plast Rub Proc Appl*, 1984; 4: 369-378
73. Wnuk AJ, Ward TC and McGrath JE. Design and Application of an Instrumented Falling Weight Impact Tester. *Polym Eng Sci*, 1981; 21(6): 313-324

CHAPTER THREE

Materials and Methods

EQUATIONS, FIGURES AND TABLES

Equation 3.1; Calculating volumetric flow rate from the motor speed of a peristaltic pump.....	61
Equation 3.2; A simple calculation of total operation yield, Y_1 by mass.....	64
Equation 3.3; Calculation of steady operation yield, Y_2 in two stages, A and B	64
Figure 3.1; The molecular structure of squalane	53
Figure 3.2; The reduced molecular structure of PP-g-MA	53
Figure 3.3; Materials and analytical techniques contextualised within the main processing backbone. (Dashed boxes represent processes that may be omitted, depending on the chosen formulation method).....	54
Figure 3.4; A representation of a grinding collision	55
Figure 3.5; Laser light scattering	57
Figure 3.6; The Hegman gauge from above and from the side. (Not to scale). A flat edge has been swept from right to left, resulting in a concentration of particles at the indicated spot	58
Figure 3.7; A spray drying chamber	60
Figure 3.8; A pneumatically-driven spray drying atomiser, as used in the thesis.....	62
Figure 3.9; Air-impact pulverisation.....	67
Figure 3.10; Rotational cone and plate suspension rheometry.....	69
Figure 3.11; Twin-screw extrusion and pelletization	71
Figure 3.12; An example of a calorimetric response of a semi-crystalline polymer during heating and cooling, at 10 °C / min, designed from sample experimental data.....	74
Figure 3.13; Differential scanning calorimetry.....	74
Figure 3.14; Falling-weight (multi-axial) impact analysis.....	76
Table 3.1; The disperse phase entities that were used in the experimental work. ‘Proportion’ describes the range of mass percentages of each ingredient in a moulded test specimen, should it be required.....	50
Table 3.2; The continuous phases that were used in the experimental work. ‘Proportion’ describes the range of mass percentages of each ingredient in a specimen, should it be required	50
Table 3.3; Instrumentation that was used for mineral and polymer processing.....	51
Table 3.4; Instruments and software used in the thesis. For ImageJ; PD: public domain software, NIH; (American) National Institute of Health. *Analytical programs that were written in Visual BASIC for semi-automated processing of LLS, Impact and TOM data can be found in the Appendix.....	52

3 MATERIALS AND METHODS

3.1 Aims of this Chapter

This Chapter is included to ensure that the materials and methods that were used are fully understood in the context of the thesis experimental work. The Chapter consists of two sections ('Overview' and 'Further Details') that introduce and describe the materials and methods used. The 'Overview' section features concise summaries of firstly; the materials used and their approximate quantities, and secondly; the methods used. The 'Further Details' section features information on both materials and methods, intended to place them in the context of the polymer composites field and in the context of this thesis. The operating conditions for each method are included in separate paragraphs following each method description.

3.2 Overview

3.2.1 Materials

In this section, basic supplier details are provided for each of the materials that were used in the thesis. They were categorised into two main types; dispersed phase entities and continuous phases. Each of these types includes further categorisation, which was determined by the nature of their intended purpose.

In Table 3.1, basic details of the materials that were acquired for the ultimate purposes of studying and improving some mechanical properties of neat polypropylene are shown. Table 3.2 shows basic details of the continuous phases into which filler and other additives were incorporated. The dispersion media were used for studying various effects of filler particles, while the carriers were investigated as potential substances in which filler could be incorporated at high concentrations.

Material Name	Function	Full/Product Name	Supplier	Proportion
0.40 µm PCC	Filler	Winnofil S	Solvay	10 - 30
1.40 µm GCC	Filler	FilmLink 400	Imerys UK	10 - 30
1.89 µm GCC	Filler	FilmLink 520	Imerys UK	10 - 30
13.34 µm GCC	Filler	Carrara flour	Imerys UK	10 - 30
Stearic acid	Surface Treatment	Stearic acid	Sigma-Aldrich	0.04 – 1.20
PHSA	Surface Treatment	Poly(hydroxyl stearic acid)	Noveon	0.02 – 0.60
Sodium polyacrylate	Surface Treatment	Sodium polyacrylate	Ciba	0.02 – 0.60
Silicone fluid	Additive	Dow Corning 200/10 cSt	Dow Chemicals	0.5 – 1.0
Functionalised silicone fluid	Additive	KPN-3504	Shin-Etsu	0.5 – 1.0
PP-g-MA	Additive	PP-g-MA, Scona TPPP 2112 FA	Kometra	5 – 10
Anti-oxidant	Additive	Irganox 1010	Ciba	0.1

Table 3.1; Dispersed phase entities that were used in the experimental work. ‘Proportion’ describes the range of mass percentages of each ingredient in a moulded test specimen, should it be required

The columns marked ‘Proportion’ refer to the approximate mass percentage of each ingredient, should it be required in typical formulations of specimens of injection moulded polypropylene measuring 60 x 60 x 2 mm.

Material Name	Function	Full/Product Name	Supplier	Proportion
Distilled water	Dispersion Medium	Distilled water	-	-
Isopropyl alcohol	Dispersion Medium	Propan-2-ol	Sigma-Aldrich	-
n-Hexane	Dispersion Medium	Hexane	Sigma-Aldrich	-
Squalane	Dispersion Medium	2,6,10,15,19,23-Hexamethyltetracosane	Sigma-Aldrich	-
PP homopolymer	Dispersion Medium	HE125MO	Borealis	60 – 90
PP copolymer	Dispersion Medium	RB206MO	Borealis	60 – 90
PP wax 1	Carrier	Ceridust 6071	Clariant	1 – 6
PP wax 2	Carrier	Hoechst Wax PP 230	Clariant	1 – 6
PE wax	Carrier	Licowax PE 130 P	Clariant	1 – 6
E copolymer wax	Carrier	Luwax ES 91014	BASF	1 – 6
PE/paraffin wax	Carrier	Vestowax A 118	Evonik Degussa	1 – 6

Table 3.2; The continuous phases that were used in the experimental work. ‘Proportion’ describes the range of mass percentages of each ingredient in a specimen, should it be required

3.2.2 Methods

In this section, basic supplier details are provided for each of the processing techniques used. The methods were categorised into two according their purpose; processing and analysis. Each of these were categorised into further types.

Table 3.3 shows the various processes that were used to provide the appropriate materials that could enable research into the effects of dispersion behaviour of fine calcium carbonate filler in polypropylene.

Process Name	Type	Instrument / Item	Supplied By
Low-Solids Grinding	-Comminution	-10 L stirred vessel -Carbolite grinding media	-Netzsch, Germany -Imerys, UK
Spray Drying	-De-Watering	-Mobile Minor Basic sd unit -Rotary atomiser -Peristaltic pump 501RL2	-GEA Niro, Denmark -“ -Watson-Marlow, UK
High-Speed Melt-Coating	-Coating	-10 L Jacketed Mixing Vessel	-Steele & Cowlshaw, UK
Air-Impact Pulverisation	-Milling	-Jet Mill TX	-Trost, US
Air-Classification	-Classification	-Alpine 100 MZR	-Hosokawa, Japan
Polymer Melting and Kneading	-Filler Binding	-Torque Rheometer	-Brabender, Germany
Twin-Screw Extrusion	-Resin Mixing -Pelletization	-Baker-Perkins 2000 -Strand Pelletizer Primo 60E	-Baker-Perkins, UK -Automatik, Germany
Injection Moulding	-Shape Formation	-All-Rounder 320M	-Arburg, Germany
Film Casting	-Shape Formation	-Extruder and chill roll	-Dr Collins, Germany

Table 3.3; Instrumentation that was used for mineral and polymer processing

Finally, Table 3.4 shows the analytical techniques that were used to characterise and test the processed materials.

Analysis Name	Property Measured	Instrument / Software	Supplied By
Laser Light Scattering (LLS)	Particle Size Distribution	-Mastersizer S -Small Dispersion Unit	-Malvern, UK -“
Hegman Gauge Test	Particle Top-Cut	-Hegman	-Pearson Panke, UK
Moisture Content Analysis	% Moisture	-Moisture Balance	-Sartorius, UK
Cone-and-Plate Rheometry	Suspension Rheology	-Bohlin Advanced Rheometer	-Malvern, UK
Differential Scanning Calorimetry (DSC)	% Crystallinity	-Calorimeter DSC 5 -Thermal Analysis Controller 7 -Gas Station	-Perkin-Elmer, UK -“ -“
Scanning Electron Microscopy (SEM)	High-Res Visualisation	-SEM XL30	-Philips, UK
Transmission Optical Microscopy (TOM)	Low-Res Visualisation	-Microscope SMZ-U -NIS Elements F Software -ImageJ; PD Analysis Software	-Nikon, Japan -Laboratory Imaging, CZ -NIH, US
Melt Rheometry	Molten Polymer Rheology	-ARES Rheometer -TA Orchestrator Software	-TA Instruments, UK “
Tensile Testing	Tensile Properties	-Tester, 10 kN load cell -Q-Mat 7 Software	-Tinius Olsen, UK -“
Falling-Weight Impact Testing	Impact Resistance Properties	-Rosand IFWIT Type 5	-Rosand Precision, UK
*Analytical Automation Programs	n/a	-Microsoft Excel, with Visual BASIC	-n/a

Table 3.4; Instruments and software used in the thesis. For ImageJ; PD: public domain software, NIH; (American) National Institute of Health. *Analytical programs that were written in Visual BASIC for semi-automated processing of LLS, Impact and TOM data can be found in the Appendix

3.3 Further Details

3.3.1 Materials

The principal formulation ingredients of calcium carbonate and polypropylene have been described in detail in Chapters 1 and 2. This section will introduce the general role of other materials of importance.

(V) Alternative Dispersion Media

To understand the role of particles in a medium, the most representative measurements will be available from analyses in that medium, as the physical and chemical properties of the medium affect the particles. Due to the high viscosity of polypropylene at room temperature, it is not possible to apply many types of particle analysis. However, it is possible to perform tests in a medium with a lower viscosity. Normally water is used, but this polar substance will induce quite different effects to

the non-polar polypropylene. This is demonstrated by the differing values of relative permittivity (dielectric constants) of the materials. For water and polypropylene they are approximately 80 and 2 respectively.

Squalane was selected as a low-viscosity medium that was otherwise representative of polypropylene (Figure 3.1). The dielectric constant of squalane is approximately 2; very similar to that of polypropylene.

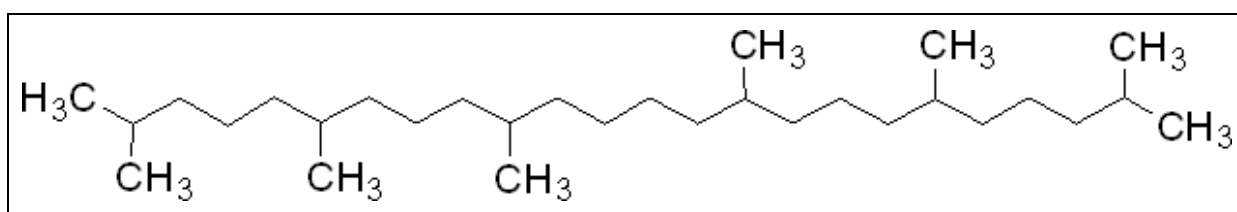


Figure 3.1; The molecular structure of squalane, sourced externally [1].

(VI) Composite Processing Additives

Anti-oxidants are designed to prevent or limit the extent to which atmospheric oxygen causes attack on organic substances. They typically contain a butylated hydroxytoluene moiety that is organically soluble and will act as a scavenger to undergo reactions with radical species (that cause ageing oxidation), to produce non-radical products [2]. Unless stated otherwise, they were incorporated into all polypropylene samples at a level of 0.10 % w/w, based on the net weight of resin.

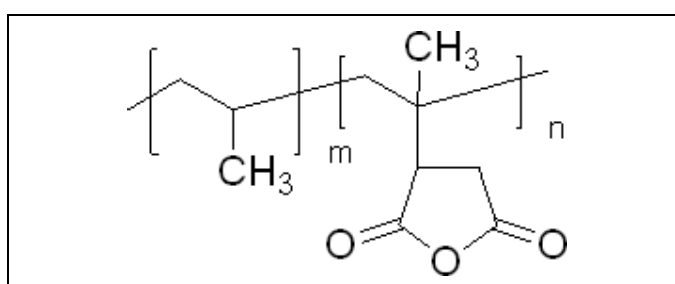


Figure 3.2; The reduced molecular structure of PP-g-MA, sourced externally [1].

Polypropylene-*graft*-maleic anhydride (PP-g-MA, Figure 3.2) has been used as an additive in the research of composites containing polyolefins [3-5]. It acts as a compatibilising agent between the low surface energy polymer and the typically higher-energy mineral surface.

3.3.2 Methods

How each of the materials, processes and analytical techniques link together to form an overall research and development platform is depicted in Figure 3.3.

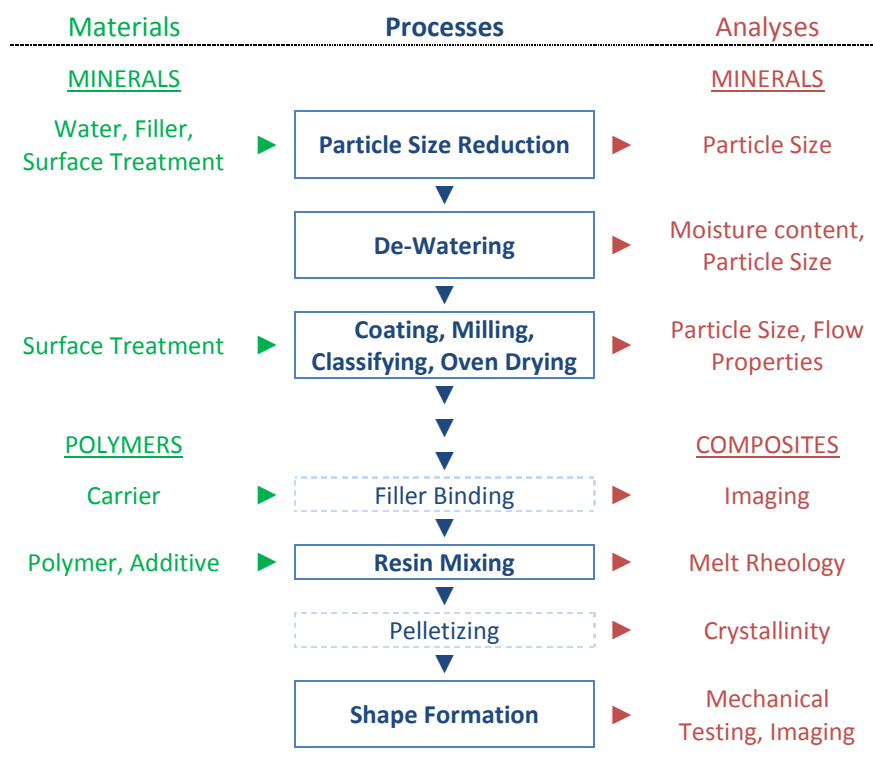


Figure 3.3; Materials and analytical techniques contextualised within the main processing backbone. (Dashed boxes represent processes that may be omitted, depending on the chosen formulation method)

The processes and analytical techniques that were used will now be discussed in more detail in the sequential order of their first appearance in Figure 3.3. The level of detail provided for each is a reflection of their significance to the experimental sections that follow. Under each title, the closing paragraph will list operating conditions that were used.

(I) Particle Size Reduction

The transformation of commercial quantities of large hydrophilic particulates into fine, fundamental particles usually involves aqueous stirred-media milling at some stage. (If the material was sourced from dry mining, one or several dry crushing stages may first be required before this can be employed).

Stirred-media milling is usually performed in the presence of water, although this is not essential. It works by the following principles; hard and relatively dense materials (i.e. grinding media) are agitated with a high speed impeller, in a concentrated phase of the particulates of interest. Media agitation facilitates impact events between each of the phases. When two of the hard media particles collide or shear with enough energy, softer mineral present at the impact area will undergo attrition, demonstrated in Figure 3.4. Continued agitation improves the statistical likelihood that each particulate will undergo sufficient size reduction, as do higher impact energies and using effective ratios of media-to-mineral.

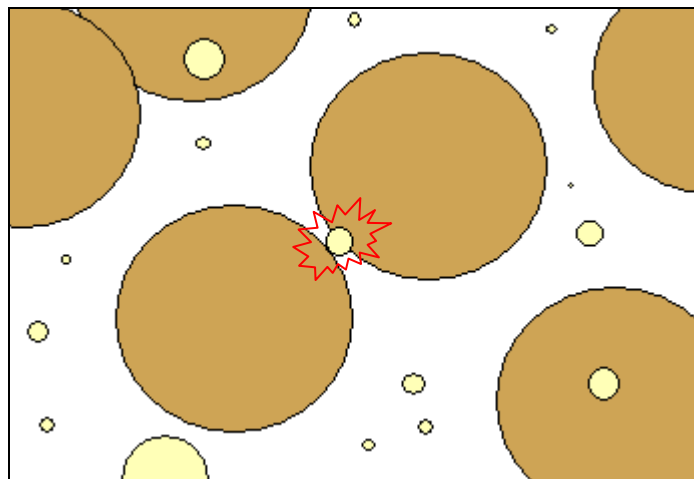


Figure 3.4; A representation of a grinding collision

In aqueous conditions, the suspension viscosity increases as more surface area is generated, but the viscosity may be lowered during the grind, by using more water and then optionally more grinding media. Dispersants may also be used to lower the suspension viscosity for a given concentration. This effect can be used to improve energy efficiency.

An alternative to using mechanical energy to achieve size reduction is to use chemical energy. If a mineral is soluble in ambient or moderate conditions, then dissolving and re-crystallising it from solution becomes a realistic possibility for commercial production.

Stirred-media milling was not the key focus of the work. Therefore, details of factors which can affect its performance were not included. Due to its role in industry and to the overall processing backbone (Figure 3.3) however, a brief mention is justified. It is also the first process in the series to which particle size measurements are relevant.

Aqueous stirred-media milling was performed using equal volume proportions of grinding media and 30 % (w/w) aqueous calcium carbonate suspensions. 10.00 kg Carbolite grinding media therefore required 3.19 kg water and 1.36 kg calcium carbonate, regardless of its size. Both 16/20 and 20/40 mesh size fractions were used (0.84 - 1.19 and 0.40 - 0.84 mm, respectively). No dispersants were used during the process.

(II) Particle Size Distribution Analysis

Accurately and representatively recording the sizes of particles is of critical importance in the field of fine filler composites. Size distributions are valuable to any situation in which particles play a key role and as such are used in a wide range of industries and research fields. A widely-used method of achieving particle size distributions is laser light scattering (LLS) [6]. Typical apparatus of this instrument is shown in schematic form in Figure 3.5.

Particle sizes may be recorded directly (for example by physical screening or image analysis). It may also be recorded indirectly (for example by sedimentation time, laser light scattering diffraction patterns or other particle properties, such as surface energy and surface area).

Any ideal measurement would record highly resolved detail ($< 1 \times 10^{-9}$ m) of large numbers of particles ($> 1 \times 10^3$). In reality however it is difficult for one measurement to collect such a high quantity of information in a realistic time frame.

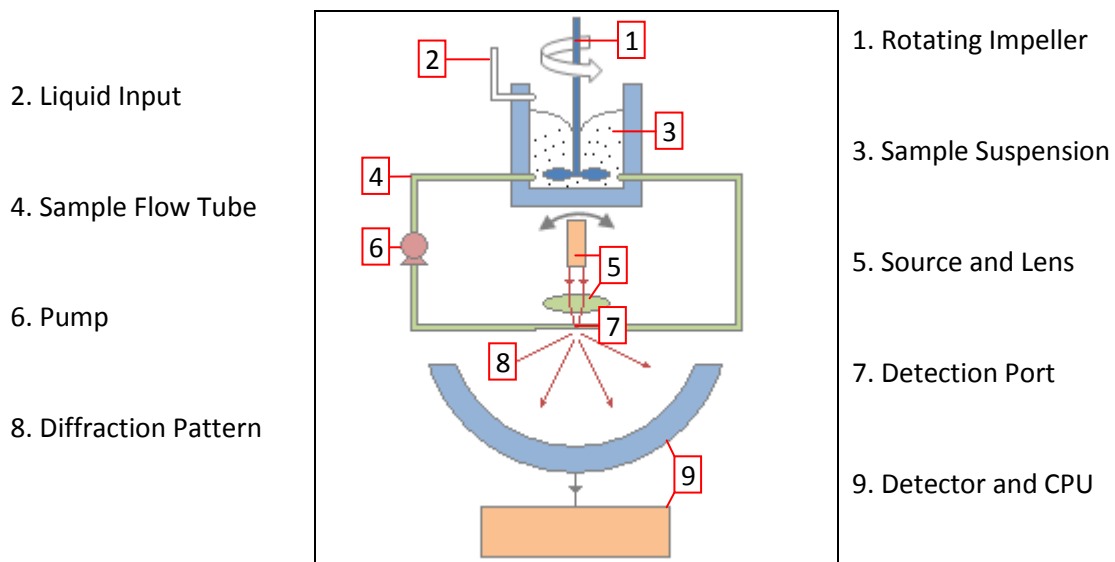


Figure 3.5; Laser light scattering, adapted from an external source; the website of the Cilas 1064 manufacturer [7].

All measurements are influenced by the medium in which the particles are present. In some media they might disperse immediately into their fundamental particles, whereas others may cause them to aggregate via flocculation or coagulation. Their behaviour in different media can provide useful information about their surface properties, but in terms of understanding particles in a particular application, the medium used in analysis must be as physically and chemically similar to the one used in that application, thereby maximising the likelihood of acquiring representative data.

(III) Hegman Top-Cut Analysis

For the purposes of studying impact resistance, the coarsest particulates in a distribution are of significant interest. The Hegman gauge test provides data relating to the coarsest particles only. The principles of its operation are as follows. A mineral suspension is mixed under high shear at a high concentration. The concentration is subsequently reduced under mixing and a sample is placed on the gauge. The gauge has a flat, shallow well which is fractionally inclined from one end which is flush to the rest of the gauge surface. By placing a small amount of material on the deepest part of the incline and running a sharp, flat edge down the gauge to and beyond its shallow end, the particles are spread over the area of incline. Optical inspection will then reveal a line (perpendicular to the direction of incline) at a point where the particles were most concentrated. Gradations on the

well indicate at what particle size this is. The finest manual gauges available are from 0 – 25 μm and the coarsest are 0 – 200 μm .

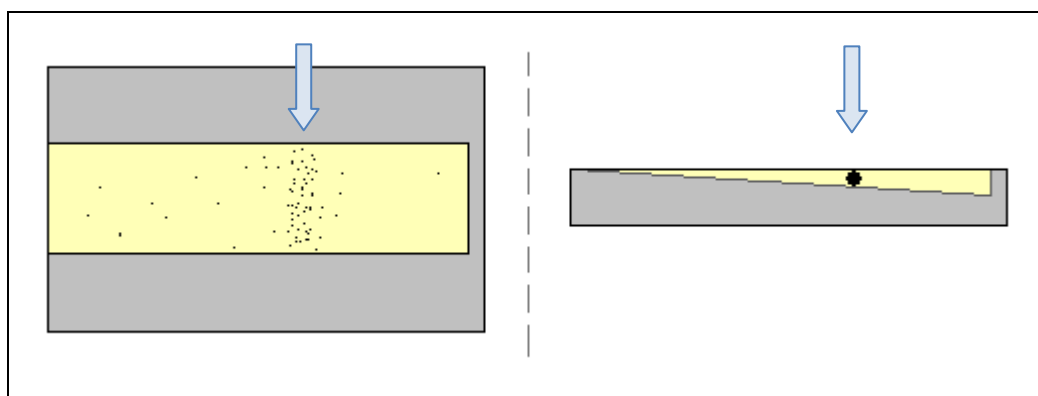


Figure 3.6; The Hegman gauge from above and from the side. (Not to scale). A flat edge has been swept from right to left, resulting in a concentration of particles at the indicated spot

The conditions used will now be listed for each appropriate technique.

LLS was performed in both distilled water and n-hexane using a Malvern Mastersizer-S (with a Mie algorithm) coupled with a small dispersion unit. Suspensions were formed by adding small quantities of dry powder to the 150 ml liquid capacity of the chamber, in a quantity that resulted in laser obscuration equalling $25 \pm 2\%$, as per manufacturer recommendation. This would result in suspensions between 1 – 5 % (w/w) being formed, depending on their specific laser obscuring properties. The pump speed of the small dispersion unit was 1500 rpm. Data was collected following an equilibration period. Equilibration of the instrument was performed after introduction of new samples and was determined by data variance and mixing time (see Appendix). The effects of using integrated ultrasound were studied by not applying it for initial measurements and then subsequently applying it for 2 minutes and recording any differences in the measured properties.

Hegman gauge tests were performed in simplified alkyd paint formulations of the following weight percentages; 68.5 % calcium carbonate, 22.1 % Synolac 60WD alkyd resin (Cray Valley Acrylics, France), 6.9 % white spirit and 2.5 % Durham VX72 drier (Rockwood Pigments, UK). Suspensions were mixed for 20 minutes at 5000 rpm before being diluted under shear to 5 % solids using

additional resin. Hegman gauge tests were performed on the diluted suspensions. Tests were also performed after applying a similar protocol to calcium carbonate in squalane and n-hexane separately; suspensions were originally mixed at 70 ± 5 % (w/w) calcium carbonate in each liquid under a fume-hood, before being diluted to 5 % and tested.

Transmission optical microscopy (TOM) was performed on films comprising 2 and 5 % (w/w) of calcium carbonate minerals in PP. The films measured 100 ± 50 μm in thickness. Development of an image analysis protocol using TOM is the subject of Chapter 6.

(IV) Spray-Drying

To acquire a dry powder following an aqueous size-reduction process, water must be removed from the suspension. There are many ways in which de-watering may be achieved, such as; filter-pressing, oven-, spray- or solvent-drying. They are each capable of removing different proportions of water from suspensions, but the removal of water is the only concept that is shared by each method.

In the interests of the work; controllability, reproducibility, efficacy and speed were desirable features of the de-watering process. Combining such features effectively will allow reliability of a product and flexibility in research. Spray-drying was selected as the most suitable drying process in the thesis for these reasons.

Spray drying is a process that separates solid particles from their suspension in volatile liquid media to produce a powder. Along with the minerals processing industry, spray drying plays a significant role in both the pharmaceutical and dairy industries.

Spray drying differs from conventional drying techniques in several ways. Amongst the most industrially significant of these differences are; the number of processing steps required, the extent of powder dryness achieved, throughput, operating conditions (the required pressures and temperatures) and the extent to which the final product is able to flow. An optimised spray drying

process can be commercially advantageous over other techniques in each of these factors, with the exception of operating temperature.

There is a range of apparatus with which spray drying may be implemented. However, there are two features that are consistently present, regardless of the apparatus. Firstly, a gas is heated and conveyed throughout a system. Secondly, on equilibration of the system temperature, the liquid suspension is introduced and carried by the gas throughout the system, in the form of an atomised stream.

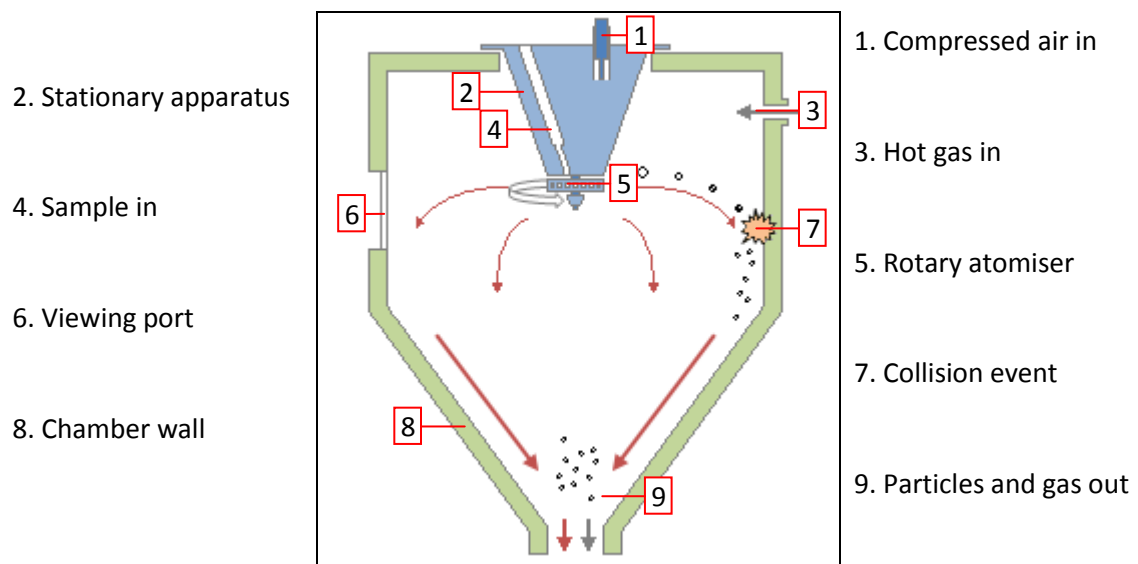


Figure 3.7; A spray drying chamber, adapted from an external source [8].

Figure 3.7 depicts a representation of the device that was used for small-scale drying processes in the thesis. Key aspects of the process are discussed below in an order consistent with that of operation. These aspects are; sample introduction, atomisation, gas heating, gas conveying and particulate drying.

Aqueous suspensions of calcium carbonate were conveyed to the atomiser by peristaltic pump, through flexible tubing (Pumpsil #16, wall thickness and internal diameter 1.6×10^{-3} and 3.2×10^{-3} m, respectively). The range of flow properties of the suspension media, the extent of the need for flow consistency and the cost of this instrument contributed to its selection. The interface of the pump

instrumentation allowed manual adjustment of the speed of the internal motor by integer values of revolutions per minute. The speed of the motor corresponded to a peristaltic cycle of contraction and relaxation over a given length of tube (with a uniform internal diameter). Therefore, the motor speed was expected to be directly proportional to the volumetric flow rate. The validity of this assumption was assessed for a range of suspension concentrations (see Appendix). For 0 – 30 % w/w aqueous GCC suspensions at pump speed of 0 – 250 rpm, it was determined that each revolution in the pump motor caused $1.80 \pm 0.05 \text{ cm}^3$ of liquid to be mobilised. The volumetric flow could therefore be calculated (Equation 3.1).

$$Q_{\text{sus}} = S \cdot V$$

Q_{sus}	=	Suspension volumetric flow rate	$\text{cm}^3 \cdot \text{min}^{-1}$
S	=	Motor speed of pump	rpm
V	=	Peristalsis volume	cm^3
V	=	1.80 ± 0.05	cm^3

Equation 3.1; Calculating volumetric flow rate from the motor speed of a peristaltic pump

Atomisation of a liquid into fine droplets or a spray significantly increases the surface area-to-volume ratio of the liquid, thereby kinetically favouring media evaporation. The two most common methods of finely distributing liquid/particle suspensions within spray driers are; to combine a pressure gradient with a narrow injection bore to create a spray, or instead to use high-speed rotation to create fine droplets by centrifugal force. Put simply, narrow-bore injectors can provide much finer fluid distributions, whereas rotational devices can function effectively over a wider range of suspension properties. Examples of such properties are; the concentration and size of suspended particles, and suspension viscosity (which is a function of particle concentration and size, but it can also be controlled by independent means such as by altering the suspension chemistry).

A rotary pneumatically-driven atomiser (Figure 3.8) was used so that suspensions with various particle sizes, concentrations and viscosities could be dried without interruption. The conveyance of the gas provides transportation of the atomised suspension stream and the dried particulates that they become, to a point of collection (or further processing). A spray drying system is said to operate in either an 'open' or 'closed' mode. In open-mode devices, the gas is collected, filtered and heated

before it is introduced into the main system. Following particle removal and possible additional filtration it is released as exhaust gas. Open-mode devices typically use air as the gas. Closed-mode devices operate in a similar fashion, except that the exhaust gas gets treated and re-introduced to the system, in a circulating loop. The suspending media is removed by a vapour extraction process.

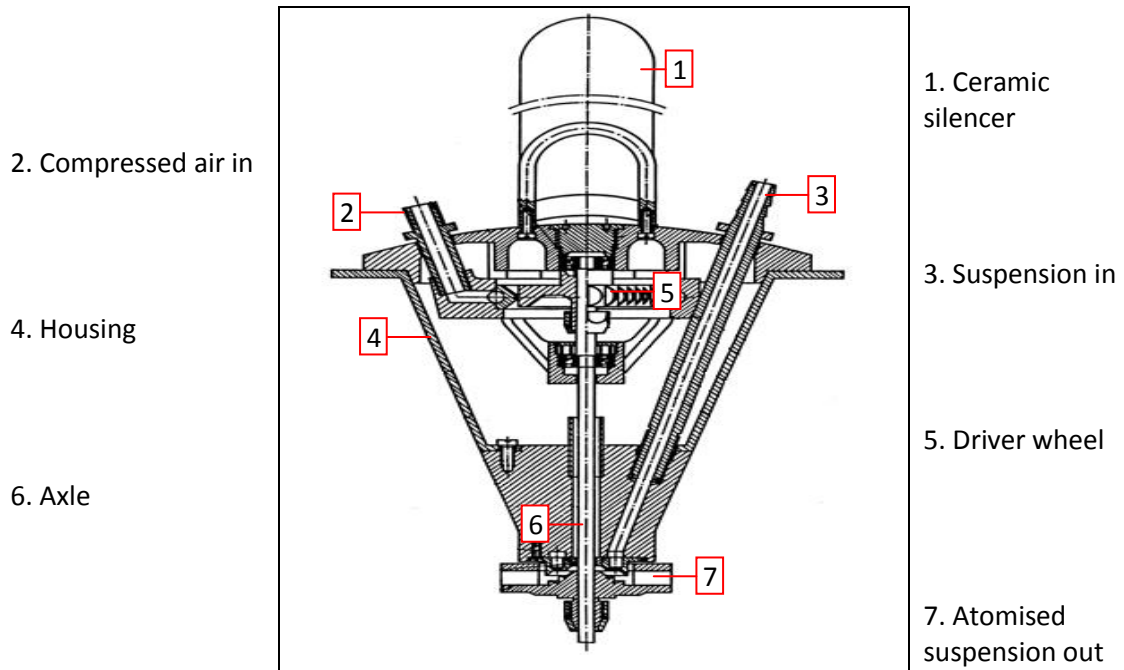


Figure 3.8; A pneumatically-driven spray drying atomiser, as used in the thesis, sourced externally [9].

These devices are most commonly used to safely dry organic suspension media in inert environments. They can also be used to ensure that a product cannot become contaminated by extraneous materials in the carrier gas that are below micron scale (10^{-6} m) in size. (Only materials with a size equivalent to or greater than micron scale can be filtered from the carrier gas in conventional open-mode designs). Although closed-mode designs have an intrinsically higher degree of energy efficiency in heating, modern open-mode driers are also designed to utilise the heat from the exhaust gas to provide some energy for subsequent heating. The assurance in preventing contamination that is afforded by closed-mode designs render them commonplace in the spray drying production of goods for human consumption, such as pharmaceuticals or foods [10]. An open-mode drying system (using air as the carrier gas) was selected because it was the most cost-effective mode that still fulfilled the necessary drying criteria. The prevention of contamination from

sub-micron scale extraneous air-borne material was not regarded as a necessary measure for the project.

The process of particulate drying in the carrier gas removes the vast majority of the volatile liquid from the suspension droplets, leaving particulate material and typically a very small amount of residual liquid, the degree of which indicating the extent of powder dryness. This product may contain fundamental particles, collections of particles or a mixture of the two. To understand the formation of aggregated structures on drying, the thermodynamics of structure formation and the alternatives to that formation must be considered. In short, the propensity to aggregate will be affected by; the surface energy of the particles, their size and shape, the suspension concentration, the original liquid droplet size, the volatility of the suspending liquid and the rate at which it is removed, the droplet/particulate residence time during drying and the amount of residual liquid after drying. Rapid drying of spherical droplets will favour the formation of roughly spherical particulates. Many forms of drying will cause some degree of particle aggregation, but spray drying enables some control over the extent to which this occurs. It is because of this control that the powder flow properties of a material can be significantly improved by this process, without the need for further intervention.

The temperature of the carrier gas contributes to the kinetic favourability of liquid evaporation. Combined with the atomisation process, the effects maximise the extent to which it occurs, for a given residence time. The minimum required temperature of the gas depends on the boiling temperature of the suspension liquid.

On exiting the drying chamber, the apparatus directs the dry material to a cyclone that separates particulates by size. The coarse fraction is collected as product and the fine fraction is directed through a vertical bag filter to on-site ventilation. The magnitude and variance in this threshold particulate size within the cyclone will depend on the speed of the carrier gas and the amount of

particulates in the gas stream. The yield for a spray drying process is defined as the amount of solid material collected as product divided by the total solid material that entered the system. This may be crudely approximated from the original suspension properties (Equation 3.2).

$$Y_1 = 100 \cdot \left(\frac{m_{min}}{x_{sus} \cdot m_{sus}} \right)$$

Y_1	=	<i>Yield (total operation)</i>	% w/w
x_{sus}	=	<i>Suspension mass fraction</i>	w/w
m_{sus}	=	<i>Suspension initial mass</i>	kg
m_{min}	=	<i>Mineral output mass</i>	kg

Equation 3.2; A simple calculation of total operation yield, Y_1 by mass

The total solid material that entered the system may be more accurately calculated in a narrower time frame if that the volumetric flow rate and concentration of the introduced suspension are unchanged or are otherwise known and the corresponding output is measured (Equation 3.3).

A

$$M_{min} = Q_{sus} \cdot \phi \cdot \rho_{min}$$

M_{min}	=	<i>Mineral mass flow rate in</i>	$g \cdot min^{-1}$
Q_{sus}	=	<i>Suspension volumetric flow rate</i>	$cm^3 \cdot min^{-1}$
ϕ	=	<i>Suspension volume fraction</i>	v/v
ρ_{min}	=	<i>Mineral density</i>	$g \cdot cm^{-3}$

B

$$Y_2 = \frac{m_{min(t)}}{M_{min} \cdot t}$$

Y_2	=	<i>Yield (steady operation)</i>	% w/w
$m_{min(t)}$	=	<i>Mineral out (in time, t)</i>	g
M_{min}	=	<i>Mineral mass flow rate in</i>	$g \cdot min^{-1}$
t	=	<i>Collection time</i>	min

Equation 3.3; Calculation of steady operation yield, Y_2 in two stages, A and B

Both yield values will be a reflection of not just the cyclone efficiency, but also the moisture content.

The moisture content of the processed material is the most intuitive way to validate the performance of a drier, although the subsequent processing or final application of the material may not specifically require a minimised value, and the natural propensity of a powder to absorb moisture (hygroscopicity) may vary significantly. For a given surface however, this approach was believed to be a valid way of assessing drier performance.

The pressure of the air supply to the atomiser directly affects the speed of atomising rotation. This speed affects droplet size and therefore final particulate size and the extent of powder dryness. In

the work, air was consistently introduced under the maximum available pressure in order to maximise the extent of powder dryness. The following stage of powder processing was almost invariably a mechanical process of removing or breaking up collections of particles (see the following sections). This is most effective for powder materials with a low degree of residual moisture.

The spray drying process was typically performed under the following conditions; the air pressure to atomiser was $7.5 \times 10^3 \text{ kg.m}^{-1}.\text{s}^{-2}$, the volumetric input flow rate of the liquid suspension was typically $6.7 \times 10^{-7} \text{ m}^3.\text{s}^{-1}$ ($40.2 \text{ cm}^3.\text{min}^{-1}$) and the carrier gas inlet temperature to the drying chamber was maintained during operation at $330 \text{ }^\circ\text{C}$. Suspensions that were introduced consisted of $25 \pm 5 \%$ (w/w) calcium carbonate in water.

(V) Moisture Content Analysis

The mass percentage presence of any volatile or organic phase as part of an inorganic mineral is easily calculable, by recording the total mass before and after exposing it to a sufficient degree of heat that removes these components. Attempting to specifically extract the moisture composition from such experiments may be subject to complication by the removal of unaccounted-for volatile species during heating. When attempting to use moisture composition data in practical situations, such as to assess the extent of a drying process, relative measurements (either relative to other samples or at best to a carefully selected control sample) can be the most useful, as they can subtract the extent of any volatile species that are present in the same degree. They also account for the hygroscopic tendencies of the type of sample; its moisture pick-up.

Moisture composition data was recorded using a 2 decimal place moisture balance at $130 \text{ }^\circ\text{C}$. The instrument applied heat to maintain this temperature. When the mass change per unit time dropped below a certain threshold, the instrument ceased heating, recorded the total mass difference incurred and converted that to a percentage of the original mass.

(VI) High-Speed Melt-Coating

The process of applying a chemical treatment to a mineral surface is an important stage of the overall formulation. While hydrophilic dispersants may be applied to suspensions prior to spray drying, (which can prove commercially advantageous), hydrophobic coatings are usually applied after the drying process. The type of surface treatment can have a profound effect on the performance of a mineral filler in its final application. Waxy, semi-solid or viscous materials (which many hydrophobic treatments are) will not flow sufficiently at room temperature to provide an even surface coating. Therefore coating is usually applied using elevated temperatures. High speed, heated agitation of a mineral and coating mixture over a period of time will improve the extent of coating distribution. An example calculation of the required amount of coating is that which provides monolayer coverage. By knowing the filler surface area and the amount of this area that one molecule of coating substance occupies, a dose can be derived. However, several factors can potentially cause such a figure to not give the most cost-effective formulation. Firstly, if the coating has not been fully applied there will be a coating deficiency for some of the filler area, so a greater initial amount of the coating substance would be required in a given process. Secondly, it is possible that the beneficial effects of the coating substance for the final application may be reached with an incomplete surface coverage, or that any excess results in some detrimental downstream effects. No expensive treatment should be used in unnecessary excess, and therefore a lower initial amount of coating would be preferable.

In the thesis, the amount of surface treatment required in each case was determined by the benefit of various doses to the impact resistance of polypropylene homo-polymer in preliminary tests.

Coating was performed using a high-speed mixer, at 110 °C using between 0.75 and 1.50 kg of mineral. The amounts of coating as a percentage of this mass for each selected treatment are discussed in detail in Chapter 4. Mixing took place in three 5-minute periods. The first period involved using mineral alone, to maximise the surface area that would be subsequently available. The second was following the addition of the coating substance to the mineral. Stopping the

instrument before the third period allowed manual intervention to ensure mineral was relieved from any areas in which it might have collected.

(VII) Removal of Coarse Particulates by Milling and Classifying

To maximise the available surface area of a spray-dried powder, milling can be used. While the stirred-media milling process that takes place upstream provides sufficient mechanical energy to break fundamental particles of a mineral, the milling applied post-drying is performed to improve the efficacy of subsequent processes by providing sufficient energy to disassociate coarse collections of particles in powder form. Air impact pulverization is a synonym for jet milling. The basic features of the milling technology within a typical instrument are represented in Figure 3.9.

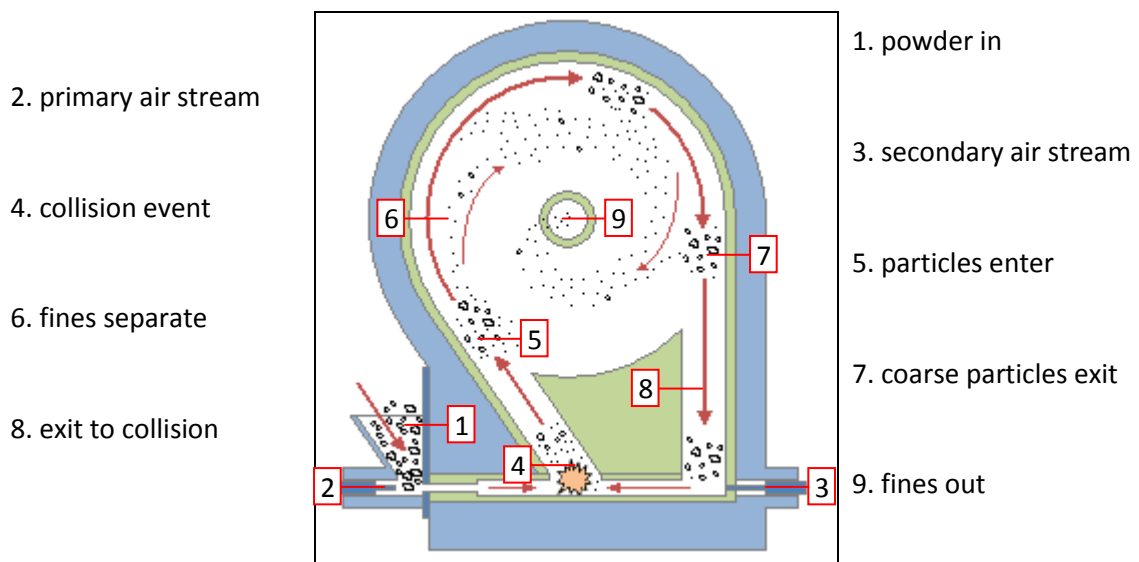


Figure 3.9; Air-impact pulverisation, adapted from an external source [11].

Powder is introduced into two opposing streams of compressed air. The primary stream must be marginally greater in pressure than the secondary, to prevent the stream being directed back towards the sample introduction channel. The opposing nature of the streams creates two opposing particulate paths that facilitate particle-particle collisions. The material containing fine particles and coarse particulates alike will be directed to enter the circular milling section. The radius of the curvature of each particle will relate directly to its mass, at constant gas pressure. Finer particles will have a smaller mass and a smaller radius of curvature. Only particles below a threshold size will be

directed out from this apparatus. Coarser particulates will be directed back to the original site of opposing gas streams, with the hope of them colliding and disassociating to create sufficiently fine particles that will pass out through the apparatus. This cycle will continue until all the available fine particles have passed through. On leaving the apparatus, there will typically be a feature of an additional cyclone that is attached to the mill. This allows safe removal of ultra-fine particles, which may be detrimental to some applications and provides an exit for the compressed air streams through a filter. The classification process also operates on the relationship between the size of a particle and its radius of curvature.

The order in which coating, milling and classifying are performed can vary. The processes can have an effect on the others. Milling may precede coating as it maximises the available surface area. But coating may precede milling as coating can result in the formation of large particulates removable by milling. Classification to remove the coarsest materials could be used at any stage, but its yield of the desired fraction will improve if there are much less coarse particles to separate. However, a single classifier might require extensive cleaning if it was exposed to a large amount or a large variety of coated surfaces. It was for these reasons that a standard post-drying protocol was used as follows; mill, classify, coat, mill. Since the efficacy of each can be improved with increased powder dryness, the samples were kept at 60 °C in an oven overnight between each step in this standard protocol.

In the thesis, jet milling was performed using a primary air stream of $7.5 \times 10^3 \text{ kg}\cdot\text{m}^{-1}\cdot\text{s}^{-2}$ and a secondary stream of $7.0 \times 10^3 \text{ kg}\cdot\text{m}^{-1}\cdot\text{s}^{-2}$. Uncoated material was fed to the mill under vibration at a mass flow rate equivalent to $60 \pm 2 \text{ g}\cdot\text{min}^{-1}$. Coated materials were fed into the mill in the same manner at $138 \pm 5 \text{ g}\cdot\text{min}^{-1}$. Air classification was performed on 50 g batches with a feed rate of approximately $33 \text{ g}\cdot\text{min}^{-1}$ using 70 % power of a maximum 1 kW motor.

(VIII) Shear Rheometry

The measurement of the flow of a material is known as rheometry. Both liquids and viscoelastic solids may be studied provided they flow to a sufficient degree. There are such a wide range of

instruments and tests available that a description of each would not be justified in this thesis, but they are described elsewhere [12,13]. The shared principle is that a specific stress is applied to cause a material to flow and the resulting strain rate is measured (or vice versa). The complexity of the response is a reflection of the micro-structural complexity of the material.

For materials consisting of one phase dispersed in another, measurements over a range of concentrations can provide extremely useful practical data (albeit indirect) about the dispersed phase itself the interface between the two phases. If used effectively, rheological data of suspensions can provide information about the morphology, packing behaviour and surface chemistry of particles in a continuous phase, provided that the mixture has a viscosity within a range that is appropriate for the apparatus and testing conditions. With all the testing configurations available, the test is highly versatile providing there is a sufficient degree of flow.

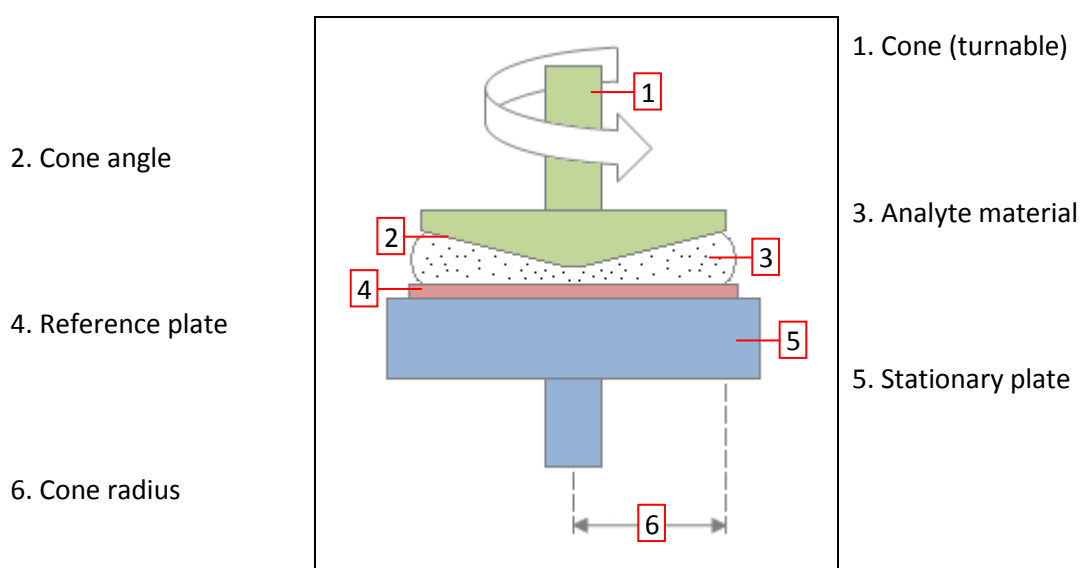


Figure 3.10; Rotational cone and plate suspension rheometry

In the thesis, cone-and-plate rheometry (Figure 3.10) was performed using a cone that was 40 mm in diameter with an angle of 4°. Analysed were suspensions of varying concentrations (typically 0-60 % w/w) of calcium carbonate in water, n-hexane and squalane at 20 °C. In each case, shear stress was recorded as a function of shear rate. The profile of shear rates used included 14 values distributed between 0.01 and 1000 s⁻¹. The gap size was controlled and corrected automatically by the instrument; correcting was controlled according to automated normal force measurements. For

some of the more highly concentrated mixtures tested at higher strain rates, noticeable wall slip occurred. Therefore data for suspensions > 50 % w/w in concentration were taken using a reduced shear rate profile of $0.01 - 277 \text{ s}^{-1}$. The precise nature of wall slip was not investigated further with this instrumentation. Data from these experiments feature in Chapters 4 and 7 and the Appendix.

At a later stage in the overall formulation (following polymeric composition), parallel-plate rotational rheometry was also applied to composites of calcium carbonate in polypropylene. Results from this are shown in Chapter 5 and the Appendix.

(IX) Filler and Polymer Mixing

Solid filler particles may be incorporated into polymers in a variety of different ways, but each requires mixing into polymers that are liquid, and typically viscous. The intensity of mixing can be described as the degree of shear forces that a process is able to impart per unit volume of material. The extent of mixing refers to the proportion of material that becomes effectively mixed. Mixing quality is a combination of both of these factors. The subject of mixing fillers and polymers has been extensively reviewed [14-16]. In short, high intensity mixing favours kinetic (or dispersive) aspects, whereas long mixing times favour thermodynamic (or distributive) aspects. The goal of a mixing process is to maximise both dispersion and distribution of one phase in another, while still maintaining the molecular integrity of the polymeric phase.

Twin-screw extrusion (TSE, Figure 3.11) is a mixing process that utilises two heated interlaced rotating screws to knead viscous material and extrude it through at least one die. It is commonplace to then cool and pelletize the extrudate for subsequent processes. In many formulations, a 'masterbatch' is first produced, which is a medium-to-high concentration (50 – 70 % w/w) of filler in polymer. Using a higher original concentration increases the melt viscosity in the barrel. In turn, this allows a greater degree of mixing intensity. Masterbatch mixing is usually performed with the barrel

being under vacuum, to assist the removal of air from the mixture. This makes TSE a highly versatile process, as it allows for the introduction of minerals in powder form, for example.

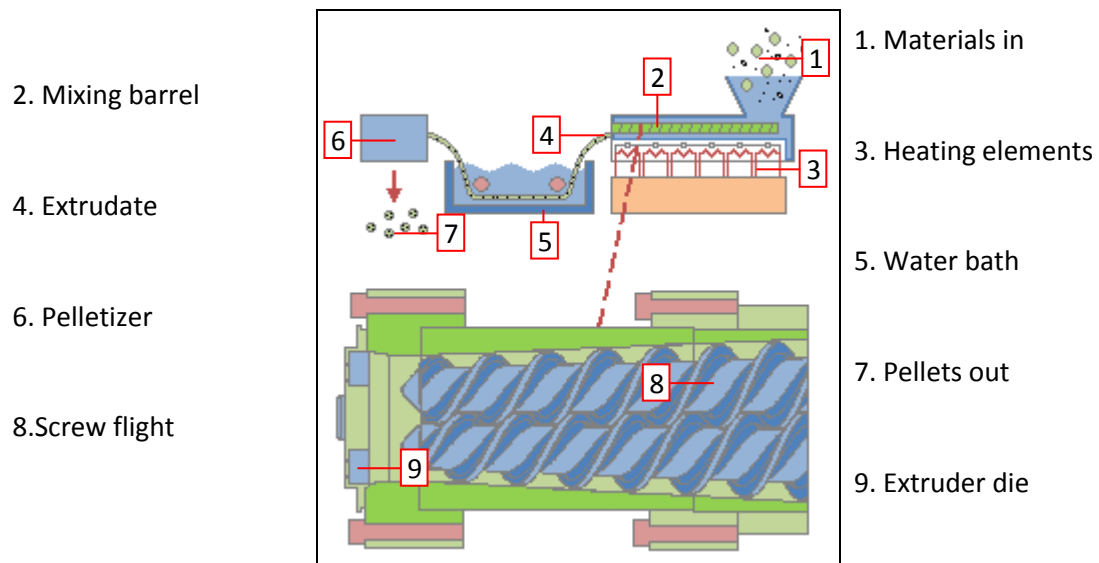


Figure 3.11; Twin-screw extrusion and pelletization, adapted from an external source [17].

Subsequent processing involves mixing masterbatch pellets with additional polymer, at a proportion that is in accordance with the concentration required by the next process, which is usually a shape formation process. The two-stage mixing approach also has some conventional value in commerce, since masterbatch formulation is typically performed by a specialist company, whereas required concentrations (which are subject to vary) and subsequently-required shape-forming processes may be performed elsewhere by manufacturers of composites (that is, the final application). Trading materials of a high concentration can be more advantageous in terms of transportation and storage costs compared to those of a low concentration, as they simply occupy less volume.

The most significant indicators of mixing in the TSE process are barrel pressure and % torque. For a given combination of mineral and polymer, the barrel temperature profile (which is usually controlled by six heating elements on pilot-scale machines), the speed of the screws and the rate at which material is fed to them are also important. These measurements enable reproduction of work, as well as acting as performance indicators when in operation. For semi-crystalline polymers, the rate at which the polymer cools will affect the size and proportion of crystallites. Although the

subsequent processing can be used to mitigate any unwanted effects introduced at this stage, it must still be considered particularly when materials are to be studied or tested directly after extrusion.

TSE mixing of masterbatches of calcium carbonate at 30 – 60 % (w/w) in polypropylene was performed using mineral powder of various sizes and surfaces that had been stored at 60 °C in an oven for a minimum period of 24 hours beforehand. The barrel temperatures from input to die were 170/175/175/180/185/200 ± 5 °C, operating under a pressure of 6.9 ± 0.8 MPa with an average torque of 45 ± 10 % at 420 ± 20 rpm. Pellets produced using TSE and water-bath quenching were stored for 24 hours under vacuum at 50 °C to remove surface moisture collected during the quenching process. Chapters 4, 6 and 7 each describe experiments that used this type of mixing.

The mixing of mineral into molten polyolefin waxes was performed using a Brabender torque rheometer, at temperatures 10 – 15 °C greater than the melting point of the wax. This facilitated the formation of small quantities of highly-concentrated materials (70 – 90 % w/w). Chapter 5 describes in further detail the experiments that utilised this method.

(X) Scanning Electron Microscopy

Scanning electron microscopy (SEM) enables the acquisition of high-resolution images. The workings of this instrument are not explained here, but it is a highly pervasive analytical tool and information regarding its operating principles is widely available [18, 19].

Two highly relevant aspects of the instrument to this thesis are sample preparation and data representation. When attempting to visualise minerals within a polymeric structure, sample preparation must be carried out for two main reasons. Firstly, brittle fracture surfaces of composites must be created and secondly, the sample must be made physically amenable to the analysis.

Generating a brittle fracture surface minimises the extent to which plastic deformation occurs in a polymer, which can affect what subsequently becomes visualised, rather than providing an accurate

representation. To this end, polypropylene composites (of a 4 x 10 mm cross-section) were submerged in liquid nitrogen for 5 minutes prior to being fractured manually. Highly-concentrated (> 80 % w/w) mineral/polymer mixtures did not require liquid nitrogen as they were regarded as being sufficiently brittle at room temperature. This was confirmed by perfect match-up of the broken surfaces after breaking; thus no significant deformation had occurred.

To make samples physically amenable to SEM, they must be coated with an electrically-conductive surface, the type of which is determined by the type of SEM that will be performed, the cost of the coating material and the ease with which it may be applied. In the thesis, gold was used as the coating substance. Images were acquired using SEM with a secondary electron detector with an accelerating voltage of 20.0 kV, at magnifications between 100 – 3500 x.

(XI) Differential Scanning Calorimetry

Differential scanning calorimetry (DSC) is a technique that provides data of the energy associated with a phase transition of a material. The softening of polymers (and the melting of crystalline structure that some of them possess at low temperatures) is commonly studied with DSC. Along with various kinetic and thermodynamic data, it is possible to determine the mass percentage of a polymer that is composed of crystals, from the energy that is associated with the transition of specifically that phase.

Figure 3.12 shows the calorimetric response (in red) of a semi-crystalline polymer when subjected to a controlled heating and cooling cycle (in grey). As indicated, the melting peak is endothermic showing that chemical energy has been absorbed. The crystallisation process is the energetic reverse of melting. Although both transitions are highly sensitive to the rate at which the temperatures are changed. Crystallisation kinetics can be calculated from experiments performed using DSC apparatus [20].

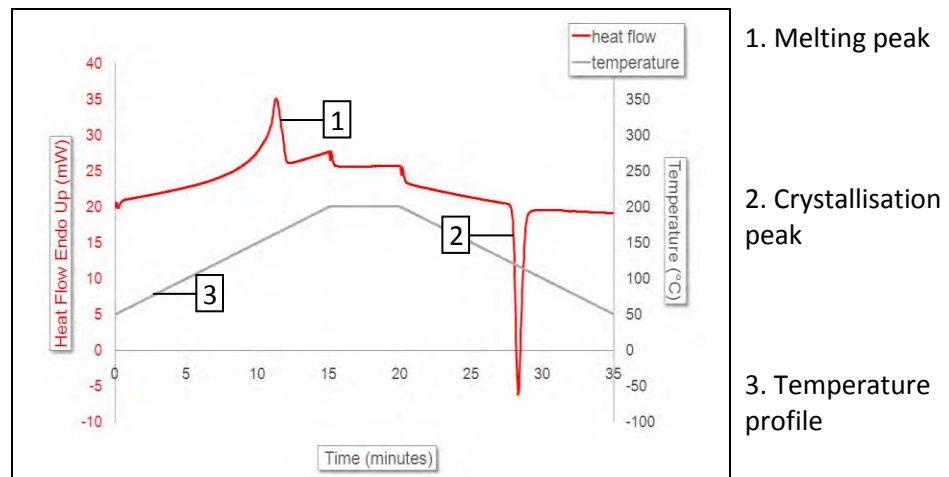


Figure 3.12; An example of a calorimetric response of a semi-crystalline polymer during heating and cooling, at 10 °C / min, designed from sample experimental data

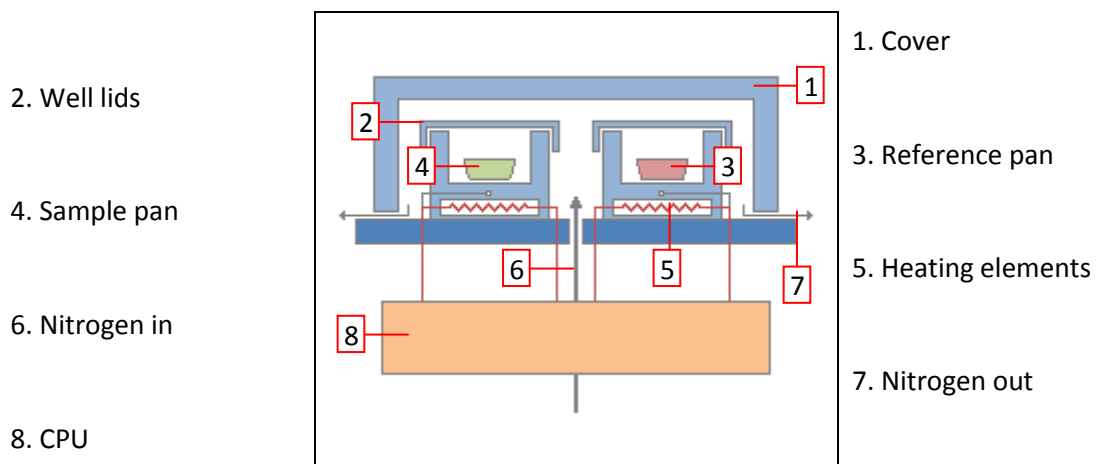


Figure 3.13; Differential scanning calorimetry, adapted from elsewhere [21].

All instruments require two pans to contain the sample and the reference, as shown in Figure 3.13. Most operate using power-compensation, whereby a constant rate of temperature change is to be maintained by both pans over a range in temperature that encompasses the transition of interest. In an endothermic transition (such as melting) energy is being absorbed by the sample and therefore a greater rate of heat flow must be supplied to it than the non-absorbing reference. The difference between the required heat flows for both pans is calculated; thereby eliminating all energy transitions that are not specifically a result of the sample.

This configuration is perhaps so widely-favoured due to the ease at which the enthalpy of a transition may then be derived; by integrating between defined points either side of the transition response to

give a direct energy measurement. Also because the specific enthalpy in a crystalline transition is constant under defined conditions, the energy can be used to determine the mass of material that underwent the transition and therefore the mass percentage of the original sample that this represents. The necessity of a non-oxidising atmosphere depends on the propensity of the sample to oxidise and the type of measurement that is intended.

In the thesis, power-compensation DSC was used to investigate the effects of different aspects of formulation on the mass percentage of crystalline structure in polypropylene. Unless stated otherwise, all measurements were taken after an initial heating and cooling cycle performed at 50 °C / minute, to limit the effects of processing history. All measurements were recorded with a temperature gradient of 10 °C / minute under a supply of nitrogen gas, unless otherwise stated.

(XII) Composite Shape Formation (Injection Moulding and Film Casting)

Forming shapes from polymer composites is done either to create a product for a final application or to create a specimen for testing. There is a wide array of different techniques [22].

Mechanical properties of polymeric materials are usually highly sensitive to variation according to their spatial dimensions. Therefore, injection moulding was selected so that the dimensions could adhere to particular testing specifications, as referenced in the related section.

Dry materials comprising mineral and polymer (0 – 60 % w/w of mineral) were injection moulded for the purposes of mechanical testing. They were moulded into 60 x 60 x 2 mm specimens (for falling-weight impact tests), 40 x 10 x 4 mm specimens (for Charpy impact tests) and dog-bone shapes that were overall 150 x 4 mm with terminal widths of 20 mm and a central width of 10 mm. The central region had a cross-section of 10 x 4 mm that was uniform for 80 mm (for tensile tests).

Masterbatch pellets comprising mineral and polypropylene co-polymer (0 – 5 % w/w of mineral) were cast as films using a kneader-extruder and chill roll to thicknesses of $100 \pm 50 \mu\text{m}$. The

extrusion barrel temperatures steadily ranged from input to die between 200-240 °C. A melt temperature of 217 ± 1 °C, a barrel pressure of 6.2 ± 0.1 MPa and a current of 3.8 A were recorded.

(XIII) Mechanical Property Analysis (Tensile and Impact)

The mechanical properties studied for the purposes of the thesis have been described in detail in the previous Chapter, so they will only be mentioned briefly in this section.

Mechanical properties of viscoelastic materials are notoriously difficult to quantify absolutely. Their dependence on temperature, spatial dimensions, strain rate and other conditions during testing is what makes this so. Underlying intrinsic properties that remain consistent across all testing conditions and specifications are plausible for certain pure polymers, allowing their behaviour in certain conditions to be modelled accurately. However there is no model that can account for all polymers under all conditions, due to the complexity and variety in their structures and therefore their mechanical responses.

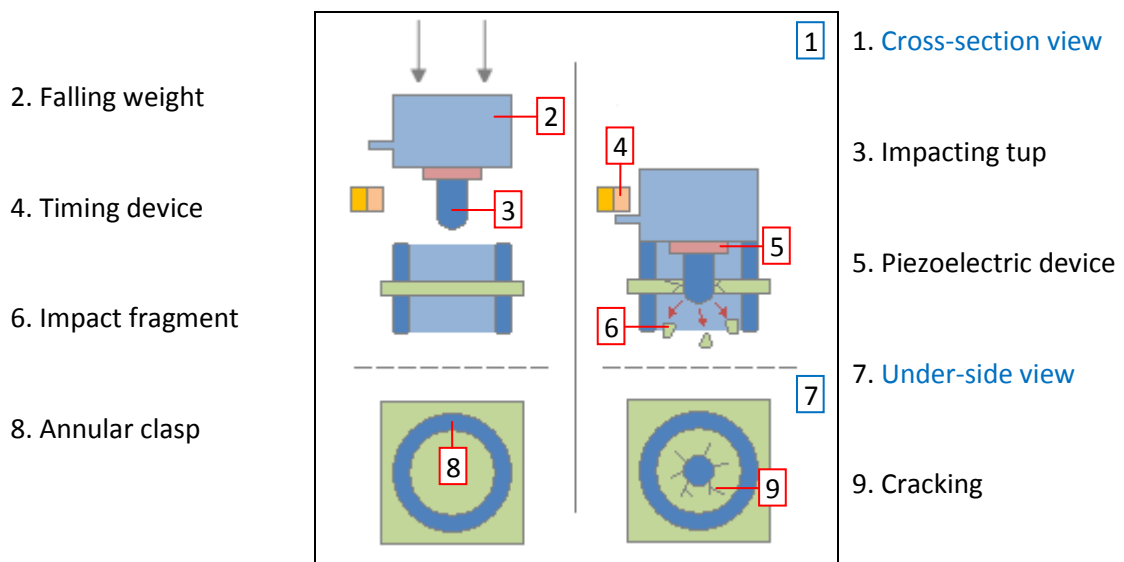


Figure 3.14; Falling-weight (multi-axial) impact analysis, drawn for the purposes of this thesis

Filled semi-crystalline polymers that have a moderate glass transition temperature (such as filled polypropylene, as used in the thesis) amount to materials with high degrees of structural complexity

and therefore mechanical response. For this reason, tests were used to represent similar conditions to the desired material application (*i.e.* to resist impact).

In Figure 3.14, an impacting event leading to fracture is represented. The timing and piezoelectric devices work in harmony to measure the resistance of the material to impact [23]. Unless stated otherwise, measurements were taken in accordance with ISO 6603-2, using specimens of 60 x 60 x 2 mm at 18 ± 3 °C, with a 25 kg weight that was dropped from a height of 1.0 m; contacting at a speed of $4.43 \text{ m}\cdot\text{s}^{-1}$. Tests were performed at least ten times for each sample type. Tensile measurements were taken in accordance with ISO 527-2, using ISO 3167-1A specimens with a cross-sectional area of 10×4 mm, using a 10 kN load cell under a strain rate of $50 \text{ mm}\cdot\text{min}^{-1}$. As above, tests were performed a minimum of ten times for each sample type.

The items described in this Chapter represent a platform of research and development, with which mineral/polymer composites and their cost-effective modifications could be considered and probed using experimental data. The following Chapters describe distinct, yet associated investigations into some important technical aspects of these materials to meet the demands of global production.

3.4 References

1. <http://www.sigmaaldrich.com/united-kingdom.html> (Accessed 13/9/2010)
2. Fujisawa S, Kadoma Y and Yokoe I. Radical-Scavenging Activity of Butylated Hydroxytoluene (BHT) and its Metabolites. *Chem Phys Lipids*, 2004; 130(2): 189-195
3. Ishak ZAM et al. Effects of Compatibilizers and Testing Speeds on the Mechanical Properties of o-MMT Filled PA-6/PP Nanocomposites. *Polym Eng Sci*, 2010; 50(8): 1493-1504
4. Wang YH et al. Effect of Interfacial Interaction on the Crystallisation and Mechanical Properties of PP/Nano-CaCO₃ Composites Modified by Compatibilizers. *J App Polym Sci*, 2009; 113(3): 1584-1592
5. Li WJ, Jozsef KK and Thomann R. Compatibilization Effect of TiO₂ Nanoparticles on the Phase Structure of PET/PP/TiO₂ Nanocomposites. *J Polym Sci B*, 2009; 47(16): 1616-1624
6. Johnson CS and Gabriel DA. *Laser Light Scattering*. Dover Publications, 1995
7. http://www.particle-size-analyser.com/cilas_1064_particle.htm (Accessed 28/4/2010)
8. <http://www.niroinc.com/html/chemical/cpdfs/mobminor.pdf> (Accessed 28/4/2010)
9. *Spray-drying Manual – Mobile Minor Basic*, GEA Niro, Denmark
10. Sharma SK, Mulvaney SJ and Rizvi SSH. *Food Process Engineering: Theory and Lab Experiments*. Wiley-Blackwell, 1999
11. http://www.amicon.com/toll_manufacturing.htm (Accessed 28/04/2010)
12. Okagawa A and Mason SG. Suspensions – Fluids with Fading Memories. *Sci*, 1973; 181(4095): 159-161
13. Gupta RK. *Polymer and Composite Rheology*. CRC Press, 2nd ed. 2000
14. Ess JW. *Characterization of Dispersive and Distributive Mixing in a Co-Rotating Twin-Screw Compounding Extruder*. PhD Thesis, Brunel University, 1989
15. Ma CG et al. Phase Structure and Mechanical Properties of Ternary PP/Elastomer/Nano-CaCO₃ Composites. *Compos Sci Technol*, 2007; 67(14): 2997-3005
16. Chan CM et al. PP/Calcium Carbonate Nanocomposites. *Polym*, 2002; 43(10): 2981-2992
17. <http://www.freepatentsonline.com/6609819.html> (Accessed 28/4/2010)
18. Egerton RF. *Physical principles of electron microscopy: an introduction to TEM, SEM, and AEM*. Springer. 2005
19. Deev IS and Kobets LP. SEM in the Study of the Microstructure and Strain Microfields in Polymer Composites. *Ind Lab*, 1999; 65(4): 234-240
20. Zhang F et al. Isothermal Crystallization Kinetics of High-Flow Nylon-6 by DSC. *J App Polym Sci*, 2009; 111(6): 2930-2937
21. <http://materials.npl.co.uk/matsol/thermal.html> (Accessed 28/4/2010)
22. Morton-Jones GJ. *Polymer Processing*. Springer, 1989
23. Wnuk AJ, Ward TC and McGrath JE. Design and Application of an Instrumented Falling Weight Impact Tester. *Polym Eng Sci*, 1981; 21(6): 313-324

CHAPTER FOUR

The Application of Cost-Effective Technology to Research the Properties of GCC and its PP Composites Made by Twin-Screw Extrusion

EQUATIONS, FIGURES AND TABLES

Equation 4.1; A calculation of maximum possible tests per hour, with no accounting for instrument set-up, applicable to heavy use.....	84
Equation 4.2; A calculation of time required to prepare and analyse sufficient material for ten separate tests, applicable to light use.....	85
Figure 4.1; Test 1 – A particle size distribution of uncoated GCC obtained by laser light scattering. ‘At Size’ percentage values (in green) have been multiplied by ten to improve their clarity	87
Figure 4.2; Test 4 – The rheological response of uncoated GCC in water at various concentrations, presented for A) yield stress and B) maximum practical concentration.....	88
Figure 4.3; Test 5 – A scanning electron micrograph of PP comprising 30 % w/w uncoated GCC, taken at 1000x magnification.....	90
Figure 4.4; Test 6 – Differential scanning calorimetry data of PP comprising 30 % w/w uncoated GCC. The baseline of the melting region has been omitted	91
Figure 4.5; Test 7 – The mechanical response of an uncoated GCC/PP composite under uniaxial tension.....	92
Figure 4.6; Test 9 – The mechanical response of an uncoated GCC/PP composite under multi-axial impact, showing samples that were part of the same batch that underwent high degrees of plastic deformation prior to fracturing (black) and more brittle character (red)	93
Figure 4.7; Differing fracture behaviour for two (ostensibly) identical testing scenarios, displaying fracture behaviour that is A) brittle and B) ductile	94
Figure 4.8; Fracture energy plotted against the outer crack perimeter, measured using image analysis software	95
Table 4.1; A summarised technical evaluation of relevant tests, performed on minerals and composites. All times and quantities are approximate. †Values are given to the nearest 5 minutes. ‡The time taken to prepare composite material (~7200 s in total for TSE mixing and injection moulding) was included in the calculations.	86
Table 4.2; A summary of the key characteristics of uncoated, fine GCC material (Tests 1-4) and a basic PP composite formulation that comprises it (Tests 5-9), taken from N measurements. ‘Ideal’ represents which direction (increase or decrease), if any, is most desirable for composite performance.....	97
Table 4.3; A list of the names of the formulations that were used and what they contained. † Values in % w/w referring to the weight of the treatment relative to that of the mineral on which it was applied. ‡ Values in % w/w referring to the weight of the overall composite. NaPAA refers to sodium polyacrylate, PHSA refers to polyhydroxystearic acid.	100
Table 4.4; How Formulations A-L performed in Tests 1-9	103

4 THE APPLICATION OF COST-EFFECTIVE TECHNOLOGY TO RESEARCH THE PROPERTIES OF GCC AND ITS PP COMPOSITES MADE BY TWIN-SCREW EXTRUSION

4.1 Introduction

A theoretical material was considered; a composite that was composed of polypropylene (PP) with 30 % of the polymer mass replaced by ground calcium carbonate (GCC) and 0.1 % of the new overall mass replaced by an antioxidant solute. The ingredients were mixed using at least one cycle of twin-screw extrusion (TSE) and the resulting pellets injection moulded into a specific shape. In this case, the effectiveness of this formulation could be measured by the ability of this shape to absorb energy prior to fracturing under high speed impact, while otherwise having possessed a sufficient degree of flexural strength. From the perspective of an industrial formulation engineer, the key aspects of this example were defined as: the properties of the materials, the manner in which they were combined and some measure of how well the final mixture performed, in relation to its implementation costs. This simple example was relevant to all parts of this Thesis and therefore will now be discussed for each of these defined aspects, by using fine particulate size as a case study.

It was shown in Chapter 2 that the properties of the filler material have a significant influence over those of the composite and that blocky particles such as GCC can enhance the toughness of a polymer, the latter of which is believed to occur via a stress distribution mechanism, as referred to in Chapter 2. Therefore, one role of the formulator is to maximise the amount of stress that can be distributed during impact, by seeking to ensure that only fine particulates will be present in the final composite. This property is sensitive to the environment that surrounds the particulates and it can change over time. The presence of moisture in a powder and its compaction history are two examples of strongly affecting conditions.

Once a filler material such as GCC has been prepared and treated to ensure its particulate fineness has reached an acceptable degree, it can be incorporated into a polymer, such as PP. As previously described, the mixing process aims to ensure the delivery of certain particulate properties that were

present in its original powder form. Twin-screw extrusion (TSE) is commonly used, due to its versatility. Conventionally, materials are mixed under a first extrusion pass to prepare a material referred to as 'masterbatch', which may be of 50 – 70 % w/w filler concentration in the polymer. The mixing process must maximise the shear energy to which the particulates are exposed, to maximise the extent of filler dispersion and thereby maximising the degree of their fineness. A second pass is then performed to 'dilute' the mixture to the desired final concentration, (for example, 30 % w/w) prior to the shape- formation process.

Formed composite shapes can be tested. All the materials and processes that have been used to create these specimens are known, so their associated costs are easily calculable. With an appropriate application test in place, the material and processing costs can be evaluated and the cost-effective performance of the overall formulation can be deduced. The appropriateness of an impact-based measurement to reflect on the fineness of the filler dispersion has been established in previous chapters.

4.2 Aims of this Chapter

In the previous chapters, mineral/polymer composite materials were closely reviewed, the desire for their further development was established, the ways in which different research has been conducted were reviewed and several of the key ways in which they can be prepared and characterised were described in detail.

This Chapter is the first of four that describe the implementation of the previously introduced methods. These are for the purposes of researching materials by way of processing and analysis. The first aim of this Chapter is to provide the reader with a sound comprehension of a conventional composite formulation and its processing methods, as well as which types of adjustments to this formulation are possible, which are effective and which are justifiable; in terms of the benefits they bring compared with their complete associated costs. The second aim of the Chapter is to establish

the effectiveness of measurements taken upstream in the process as precursors for final application performance, and to identify which of those are the most effective.

Performance indicators can be very useful in industrial R&D because when used effectively, they can lead not only to fast identification of an ineffective formula adjustment (thereby allowing for more efficient experimentation and generating more research time) but also a reduction of material waste. They will also be highly applicable to the controlling of processes when scaling-up material production. Provided that these indicators are researched and implemented appropriately, there is no reason why relying on them should sacrifice the understanding of phenomena; a personal view of the author is that this is the first step when attempting to do so.

4.3 Hypothesis

It is predicted that by applying a series of carefully selected, relevant tests to a conventional composite formulation process, the techniques and the materials can be better understood in terms of the role they might play in the research and development of composites with an improved cost-effective performance. While this is a very general hypothesis, the original experimentation is designed to shape the form of subsequent experiments. It is also predicted that some of the tests used upstream in the overall process could act as indicators for final performance within an application designed to withstand impact or at the very least as quality control measures that could significantly reduce the amount of unnecessary time and materials being spent in later stages of research.

4.4 Results

Presented in this section first are results from tests performed on an established GCC grade (its uncoated substrate) and on PP composites that comprise it, used to investigate technical and logistical aspects of testing. Presented second are comparisons of the results of each test to falling weight impact measurements (which was assumed to be a valid comparison to how a material would

perform in its final application). Presented third is usage of the results from the previous two parts to determine which tests if any would be effective as performance indicators in an industrial processing environment. The final part of the section discusses results that show how the selected tests can be used to assess various actual formulations.

4.2.1 Measurement of an Uncoated GCC Grade

FilmLink 520 (uncoated GCC substrate) was tested to acquire a range of data. This included tests of the mineral in its powder form, suspensions of the mineral in flowing media and composites that were cooled following melt mixing to become solid matrices. For these composites, a simple formulation was used that originally contained 69.93 % (w/w) PP homo-polymer, 29.97 % (w/w) GCC and 0.10 % w/w anti-oxidant. These numbers conform to the theoretical composite considered earlier in the Chapter. This section provides some useful aspects of each test and how exactly the uncoated substrate performed in them. The characteristics of uncoated GCC will be consistently referred to in following sections.

To assess a test objectively, the quality of the data that can be derived from it is of critical importance, and is discussed throughout this Chapter. When assessing the appropriateness of this test for extensive use in research and development other factors must be considered, such as instrumentation costs and the associated testing time. Equation 3.2 shows how a testing rate may be calculated that takes material preparation time into consideration, but does not consider that of instrumentation set-up.

$$X = \frac{3600}{T_t + B_t (T_q / B_q)}$$

$X =$ Testing Rate hr^{-1}
 $T_t =$ Time taken to perform 1 test s
 $B_t =$ Time taken to prepare 1 batch s
 $T_q =$ Quantity of material in 1 test g
 $B_q =$ Quantity of material in 1 batch g

Equation 4.1; A calculation of maximum possible tests per hour, with no accounting for instrument set-up. It is applicable to heavy usage

By using this value, it is assumed that this can be performed simultaneously with (or prior to) the material preparation stage. The equation also accounts for the ratio of material required per test to that which can be made per batch.

Another calculation is featured in Equation 4.2. It is a method of calculating the time taken to prepare sufficient material for and to then perform ten instances of that particular test. The resulting value is quoted differently from that above, to reflect the differences in the calculation.

$$T_{10} = B_{t(10)} + I_t + 10 \cdot T_t$$

T_{10} = Minimum time to do 10 tests s
 I_t = Time req'd to set up instrument s
 $B_{t(10)}$ = Time req'd to make enough batch material for ten tests s

Equation 4.2; A calculation of time required to prepare and analyse sufficient material for ten separate tests. It is applicable to light usage

It is believed that of the two above equations, the first one should be most applicable to situations where a test is employed in heavy or constant operation, whereas the second is most applicable to situations where the test is used lightly. Table 4.1 provides overall testing rate analyses of various tests for both heavy and light use.

From the approximate values of X and T_{10} , several observations can be made. Firstly, how a test performs for one of these attributes does not necessarily indicate its performance for another. This can only be the case where instrument set-up times are negligible in comparison with the time required to perform ten tests, ($I_t \ll 10 \cdot T_t$) such as for Tests 3 and 6 (moisture content and differential scanning calorimetry). For Test 5 (scanning electron microscopy), there is a noticeable discrepancy between the two values of testing rate. In this case, it takes less time to perform ten tests than it does to set up the instrument, ($I_t > 10 \cdot T_t$). This, along with the fact that a minimum batch contains enough material for $> 10^5$ tests explains the discrepancy between the two. In other words, performing such a test routinely (heavy usage) allows for highly efficient use whereas using it as a one-off demands significantly more time per measurement. The results show that other tests, such as Tests 3 and 6 do not become much more efficient when they are used more heavily.

	Test Name	Analyte Material	Properties Measured	Per Batch...		Per Test...			Overall	
				B_t /s	B_q /g	T_t /s	T_q /g	I_t /s	X /hr ⁻¹	T ₁₀ [†] h:m
1	Laser Light Scattering	Powder susp. (dilute)	Particle Size Distribution	180	10	120	0.1	60	30	0:25
2	Hegman Gauge Test	Powder susp. (concentrated)	Coarsest Particle Size	1500	100	10	1	0	144	0:25
3	Moisture Content	Powder	Residual Moisture	0	3	1200	3	60	3	3:20
4	Suspension Rheology	Powder susp. (concentrated)	Particle Packing Properties	300	10	300	1	300	11	1:00
5	S. Electron Microscopy	Any composite material	Visual Aspects e.g. Particle Size	14400 ‡	200	10	0.001	1200	357	4:20
6	D. Scanning Calorimetry	Any composite material	Thermal e.g. Crystallinity	7320 ‡	200	2400	0.02	1200	1	9:00
7	Tensile Testing	Moulded composites	Tensile Properties	7230 ‡	200	180	20	300	4	2:35
8	Flexural Testing	Moulded composites	Flexural Properties	7230 ‡	200	30	20	300	5	2:10
9	Impact Testing	Moulded composites	Impact Properties	7230 ‡	200	30	20	300	5	2:10

Table 4.1; A summarised technical evaluation of relevant tests, performed on minerals and composites. All times and quantities are approximate. †Values are given to the nearest 5 minutes. ‡The time taken to prepare composite material (~7200 s in total for TSE mixing and injection moulding) was included in the calculations.

The meaning of these data will be more realistically understood when considering the nature and volume of experimental information that each single test provides. This will now be presented for tests 1 – 9, as labelled in Table 4.1.

Figure 4.1 shows data of uncoated GCC from Test 1 (laser light scattering). It can be seen that a distribution of particle sizes are presented; both discretely ('At Size') and cumulatively ('Under Size'). From the cumulative curve, the size of particle below which a certain volume percentage of particles lies can be easily calculated. Shown are two examples of this; one coloured black, at 50 % v/v (i.e. the volumetric median) and the other coloured red, at 98 % v/v. The blue arrow also featured relates to the discrete curve and it shows the smallest detected size below which 100 % of the particles lay; which provides a method for calculating the top-cut (or coarsest particles). In particular, the results from Test 1 show that the d_{50} , d_{98} and d_{100} of uncoated GCC were found to be 1.89, 6.93 and 10.5 μm

respectively, when suspended in aqueous solution using 30 s of sonication, with no chemical dispersant added.

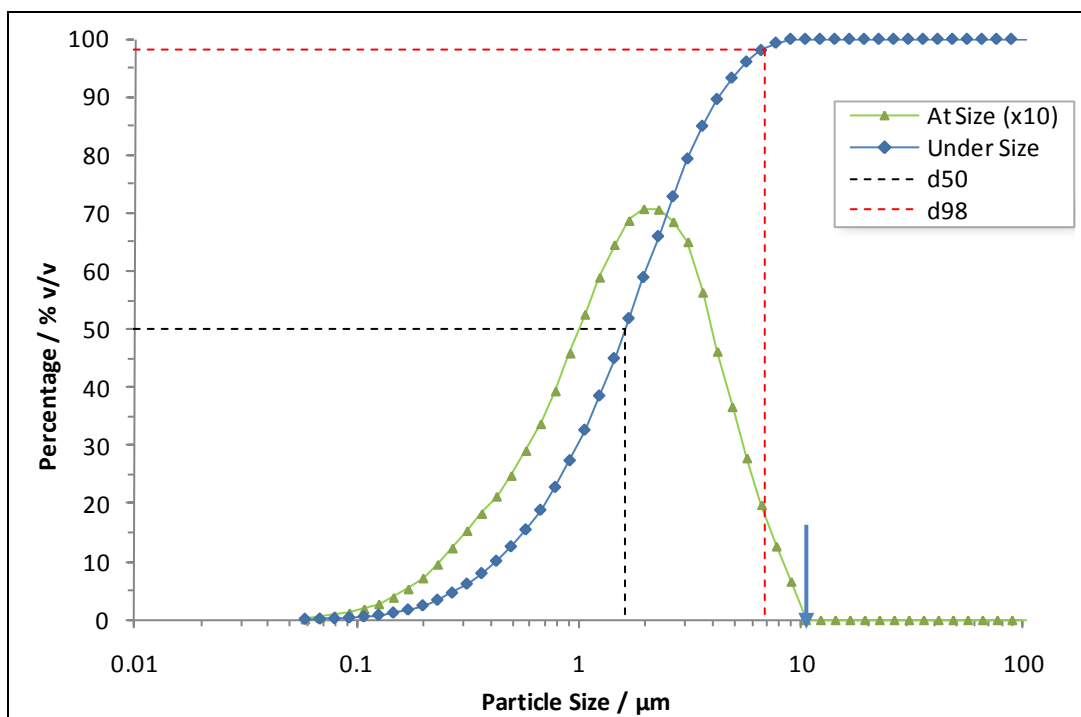


Figure 4.1; Test 1 – A particle size distribution of uncoated GCC obtained by laser light scattering. 'At Size' percentage values (in green) have been multiplied by ten to improve their clarity

Test 2 (Hegman gauge test) was performed on the uncoated GCC material. The top-cut of the material was found to be $8 \pm 1 \mu\text{m}$ from this method of measurement. This is a slight discrepancy from the d_{100} data acquired by laser light scattering, but it does however fall in the range between the recorded values of d_{98} and d_{100} . The test provided no further information.

Test 3 (moisture content) of the uncoated GCC was consistently found to be less than 0.2 % w/w of the powder. Values between 0.08 and 0.15 % w/w were recorded on material stored at $10 \pm 2 \text{ }^\circ\text{C}$ for a minimum period of two weeks, in polyethylene bags. For material heated in an oven at $60 \text{ }^\circ\text{C}$ for 24 hours prior to measurement, values between 0.03 and 0.12 % w/w were recorded. These data imply that the powder material comprised a trace amount of at least one volatile component that was only volatilised at temperatures between $60 \text{ }^\circ\text{C}$ and $130 \text{ }^\circ\text{C}$ (the temperature at which the moisture content analysis was performed). It was hypothesised that some degree of moisture could become

‘trapped’ within particulate structure, although milling the powder prior to measurements did not induce a significant reduction in measured moisture content. This was attributed to the lack of aggregated structure within the powder sample, which was observed from Tests 1 and 2.

There is a range of tests that fall into the category of Test 4 (suspension rheology). Figure 4.2 shows data for uncoated GCC that has been suspended in water at 0, 10, 20, 30, 40 and 50 % w/w, which have been subjected to varying shear rates with their responses measured in shear stress. Doing so allows the packing behaviour of these particles to be observed, at the concentration increases and the suspension viscosity increases as a result. Monodisperse spheres cannot pack more efficiently than ~65-70 % v/v (random close packing) but any deviations such as polydispersity in a spherical distribution or the presence of imperfect spheres (spheroids) or completely non-spherical particles may allow for a higher three-dimensional packing efficiency.

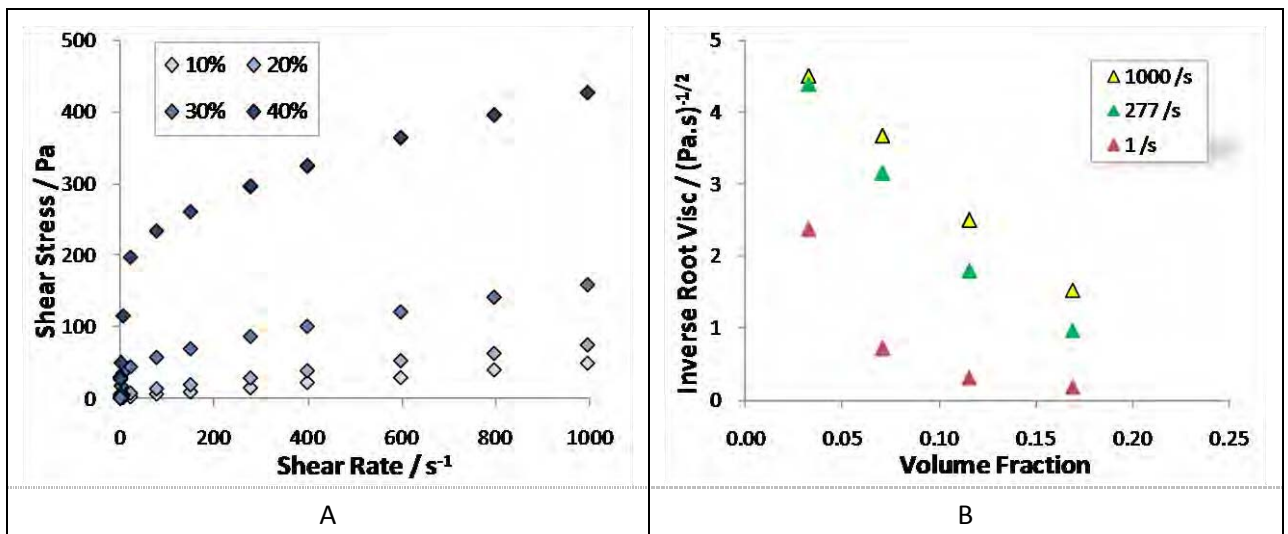


Figure 4.2; Test 4 – The rheological response of uncoated GCC in water at various concentrations, presented for A) effect of shear stress and B) viscosity-concentration relationship

The results from Test 4 show that uncoated GCC suspended at 40 % w/w in water exhibited pseudo-plastic fluid behaviour and that the material could pack to an efficiency of between 8.76 – 22.1 % v/v at the shear rates used. This corresponded to a mass-based packing percentage of between 23.8 – 48.1 % w/w. Figure 4.2 B therefore shows that the shear rate at which the experiments were performed profoundly affected the predicted maximum packing efficiency. This was attributed to

the higher shear energy being capable of breaking up aggregated structure that was not possible at lower shear rates. When this occurs, the volume of unoccupied space between particles becomes reduced and the packing efficiency increases as a result. Ideally the highest shear rates should be used to get the most accurate data, however particularly viscous samples proved difficult to analyse at greater than 300 s^{-1} . Therefore the value of 277 s^{-1} was used from that point on to acquire this type of packing information. (A more detailed study of rheological measurements in this context, including the viscosity-concentration relationship, is provided in Chapter 7).

The remainder of this section describes results that were taken from the uncoated GCC material that had been incorporated into a simple PP composite formulation consisting of HE125MO PP and 0.10 % w/w Irganox 1010 anti-oxidant. Figure 4.3 shows visual data that was acquired using Test 5 (scanning electron microscopy). Electron microscopy provided highly resolved images of the particles *in situ* in polymeric matrix. Visual details of the particles in a state that was representative of their final intended application were obtained, albeit across particle numbers that were not assuredly representative. Some assumptions must be made when quoting three-dimensional particle size characteristics from two-dimensional images, such as visually detecting an unrepresentative particle section. A good example of this is the analysis of thin plates; they may appear very narrow or very broad, depending on how they are aligned relative to the image. Due to the low aspect ratio of GCC particles (2-3), three dimensional properties acquired from two-dimensional images were believed to be sufficiently representative.

By applying image analysis techniques to the data obtained in Test 5, a mean particle diameter of $3.32 \mu\text{m}$ was determined. By applying further assumptions, a volume-based median was calculated from a number of images from the same composite specimen, which was $4.04 \mu\text{m}$. The coarsest particles detected were $11\text{-}12 \mu\text{m}$. When deriving such data from these images, it is important to acknowledge the assumptions that were made, due to both the low numbers of particles that are

counted and the assumption that the size and shape detected is representative of the particles from any angle of observation.

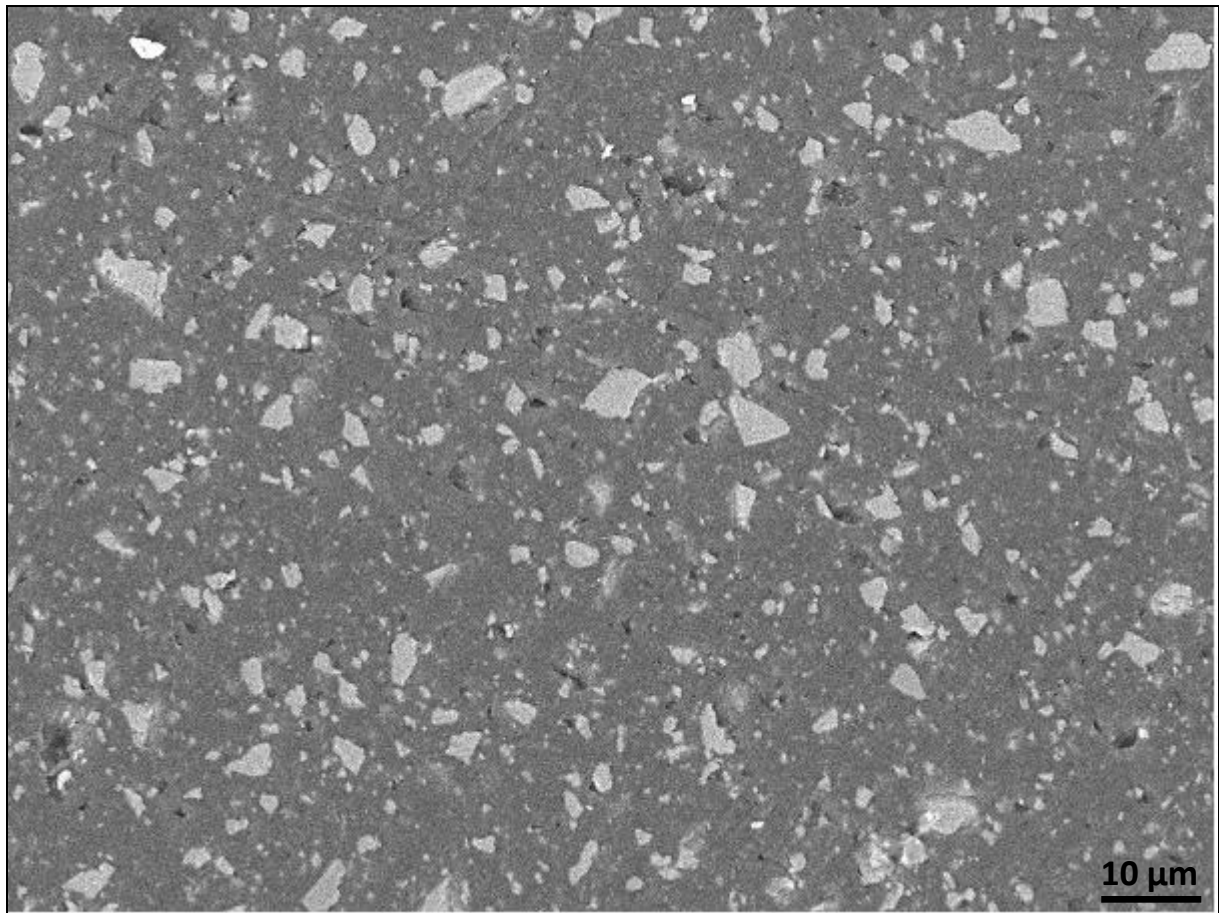


Figure 4.3; Test 5 – A scanning electron micrograph of PP comprising 30 % w/w uncoated GCC, taken at 1000x magnification

Figure 4.4 shows data for Test 6 (differential scanning calorimetry). From the energy required to overcome the forces that maintain the solid structure of a crystalline phase, the total crystalline content and therefore its proportion in the overall sample can be calculated. It also provides the temperature range over which this occurs. The results from Test 6 show that for polypropylene composites containing 30 % w/w of the uncoated GCC, the crystalline structure melted within the temperature range of 120 – 170 °C and further calculations showed that this solid structure accounted for 44.9 % w/w of the total polymeric phase. The second of these characteristics was found to be the most susceptible to variation due to the method in which the tested composite was formed and the section of a moulded specimen from which the sample was derived. Both of these effects were believed to be due to the rate at which the particular sample was allowed to cool; this

having a well-established effect on the nature and extent of crystallinity of any solid structure formed from a cooling liquid.

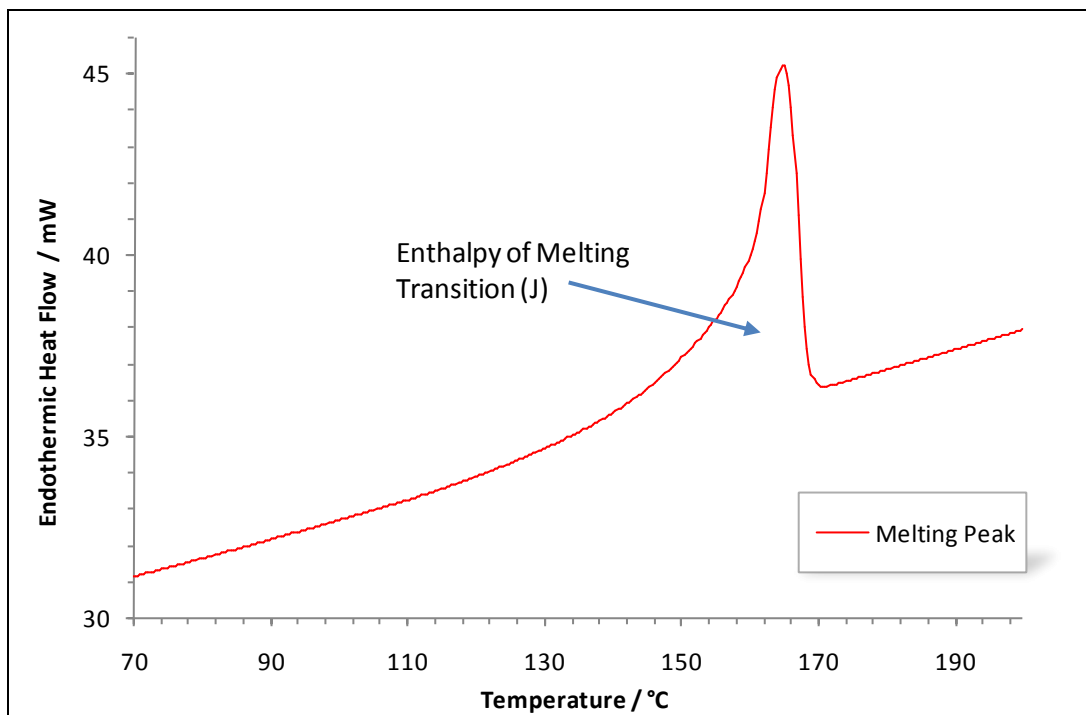


Figure 4.4; Test 6 – Differential scanning calorimetry data of PP comprising 30 % w/w uncoated GCC. The baseline of the melting region has been omitted

Figure 4.5 shows the mechanical response of a polymer under uni-axial tension. This was derived from Test 7 (tensile testing), but many of the themes that will be described are also applicable to Tests 8 and 9 which were also used to study mechanical response of composites, albeit in slightly different ways.

Results from Test 7 show that the tensile strength of PP composites comprising 30 % w/w of the uncoated GCC was 27.30 ± 0.10 MPa. There was a high degree of reproducibility in the data from tests performed on different samples of the same batch, as well as different samples of different batches. This was attributed to two testing aspects. Firstly, the crosshead speed (and hence strain rates) of this test could be controlled to be relatively slow and consistent, slow enough to allow for molecular relaxation time, which meant that the data did not become distorted from the relaxation

effects of varying pockets of molecular entanglement, as a more rapid test might. Secondly, the area over which forces act is consistent from one sample to the next.

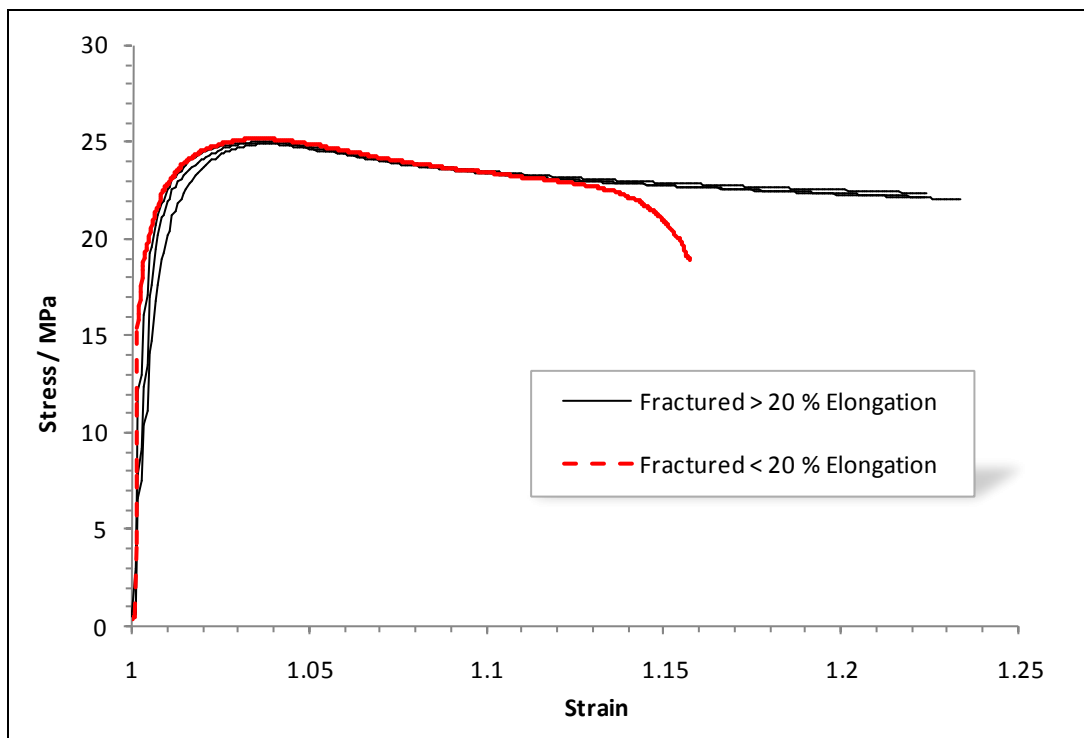


Figure 4.5; Test 7 – The mechanical response of an uncoated GCC/PP composite under uniaxial tension

A disadvantage of this test is that the degree of the tested material over which the measured strength is derived is inconsistent; the viscoelastic nature of the material makes it susceptible to small changes in experimental conditions. The material is understood in its own right in specified conditions, but not in a context that can be applied to all situations where it is used practically.

Test 8 (flexural testing) was performed. Uncoated GCC in PP demonstrated a flexural modulus of 1.38 ± 0.18 GPa. These data relate to the stiffness of the material. In polymer research and development terminology, the toughness (which is addressed in the following paragraph using Test 9) and stiffness are seen as a natural compromise, especially when considering whether the temperature of a test is greater or less than that of the glass transition of the polymer. It is only when a modification to the formulation of a polymer has improved both its stiffness and toughness simultaneously that it can be correctly described as being 'reinforced'.

Figure 4.6 shows data for Test 9 (impact testing). This type of test can take on several forms, most commonly Charpy, Izod and multi-axial. Each of them require an impact with moderate or high rates of strain to create a new surface. Here, multi-axial falling-weight impact measurements are described, taking place at temperatures greater than that of the glass transition of PP (but lower than that of the crystalline melting point). It was believed that this test, in these conditions was the most representative of the practical applications described in Chapters 1 and 2. From the graph, it can be seen that as with all mechanical tests, there are several ways in which the event may be defined. For example, the positions of yield onset, full plastic deformation and material fracture.

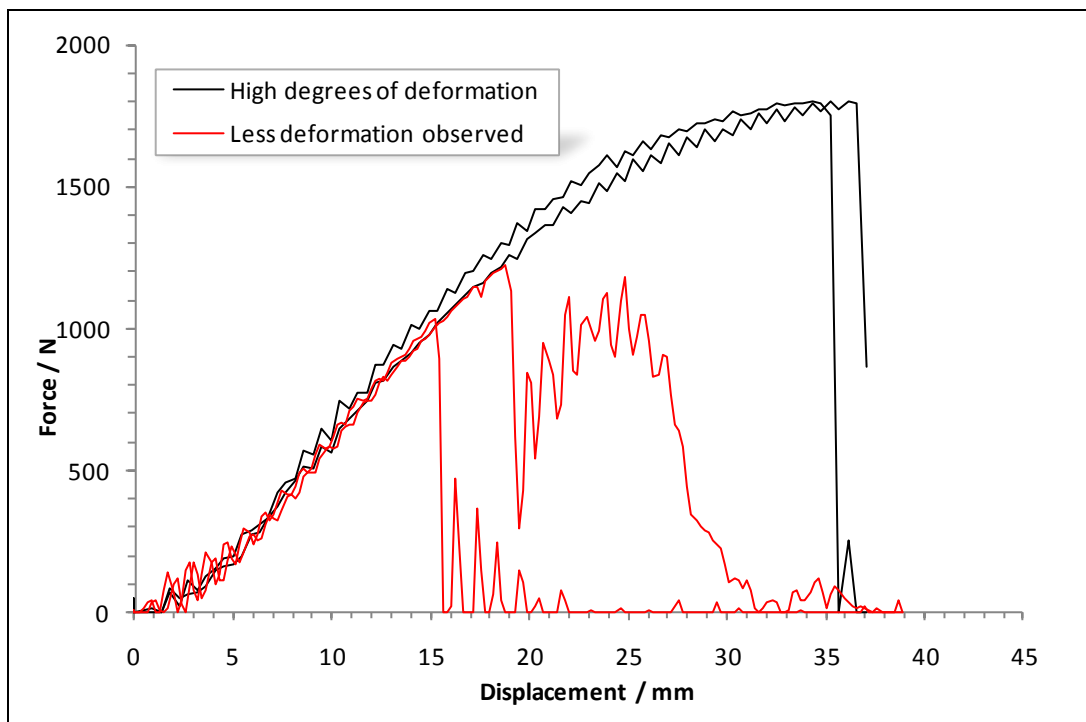


Figure 4.6; Test 9 – The mechanical response of an uncoated GCC/PP composite under multi-axial impact, showing samples that were part of the same batch that underwent high degrees of plastic deformation prior to fracturing (black) and more brittle character (red)

In particular, the results from Test 9 show that for the uncoated GCC in PP at 30 % w/w, the average energy required to break 60 x 60 x 2 mm specimens (up to the point of their fracture, as defined) over ten tests was 8.19 ± 1.14 J. It was found however that this value was subject to a noticeable degree of variation around this average. It was also found that during some tests little or no energy

was absorbed throughout the entire fracturing process. This prompted a more detailed investigation into the practical effects of this phenomenon and some speculation about its underlying causes.

Figure 4.7 compares two fracture patterns that were observed when applying identical testing procedures to two samples that were of the same batch and otherwise regarded as the same material. The energy values (shown inset) corresponded to the fracture patterns, which was characteristic of every test for all PP/GCC composite materials.

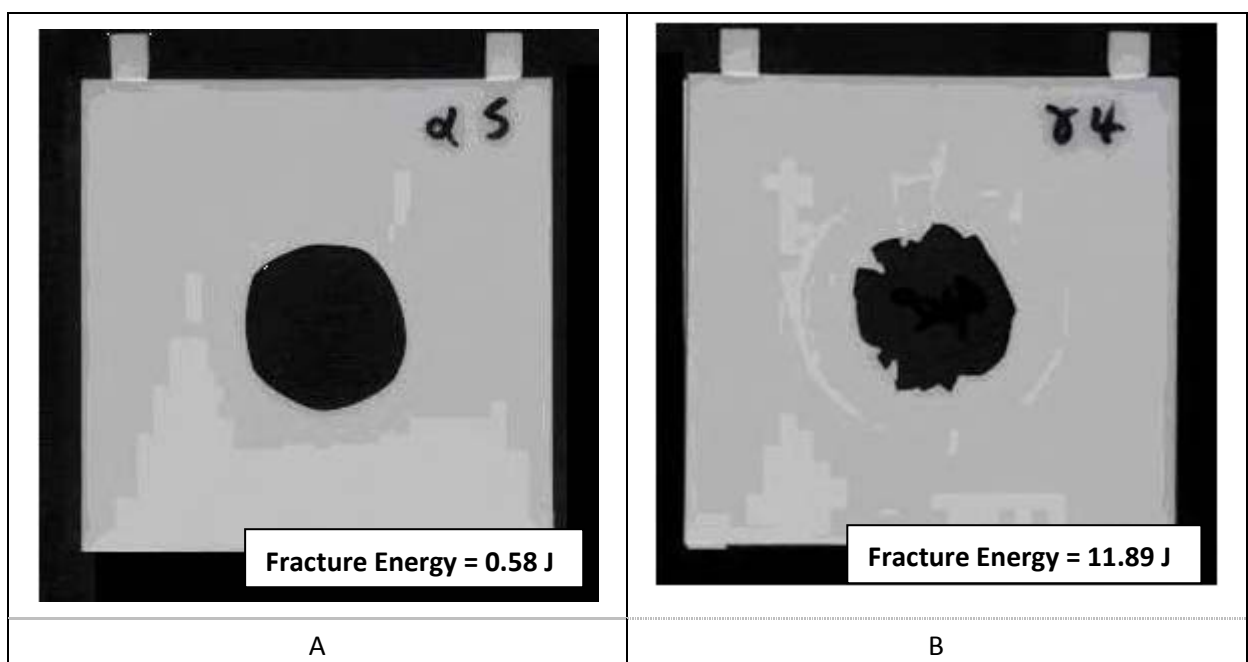


Figure 4.7; Differing fracture behaviour for two (ostensibly) identical testing scenarios, displaying fracture behaviour that is A) brittle and B) ductile

Since the ductility of a material is defined as the extent to which it is able to undergo deformation prior to fracturing, then for these particular testing conditions the high energy-absorbing group (Figure 4.7 B) was defined as 'ductile' and the low energy group was defined as 'brittle'; being unable to accommodate high rates of strain and fracturing readily. Given this definition of the two fracture modes and the patterns that have been shown, an intuitive visual measure of ductility was derived as the outer perimeter of the void that remained after the fracture. Brittle fractures resulted in a smooth and approximately circular void; thereby having a lower perimeter than the jagged and misshapen void that was the result of ductile fractures. This property was easily measured by

digitally capturing the void pattern and quantifying its perimeter to scale using image analysis software. The fracture energy (for multiple composite types) was plotted against this derived perimeter value for each specimen and the results are shown in Figure 4.8. It was observed that a distinct threshold was consistently present between the two modes of fracture. By selecting points that were closest to the theoretical threshold, its position was validated; revealing ductile fracture modes for any point above it and brittle modes for any point below it. Over 500 data points, taken from various PP/GCC composite types, were successfully divided in this way.

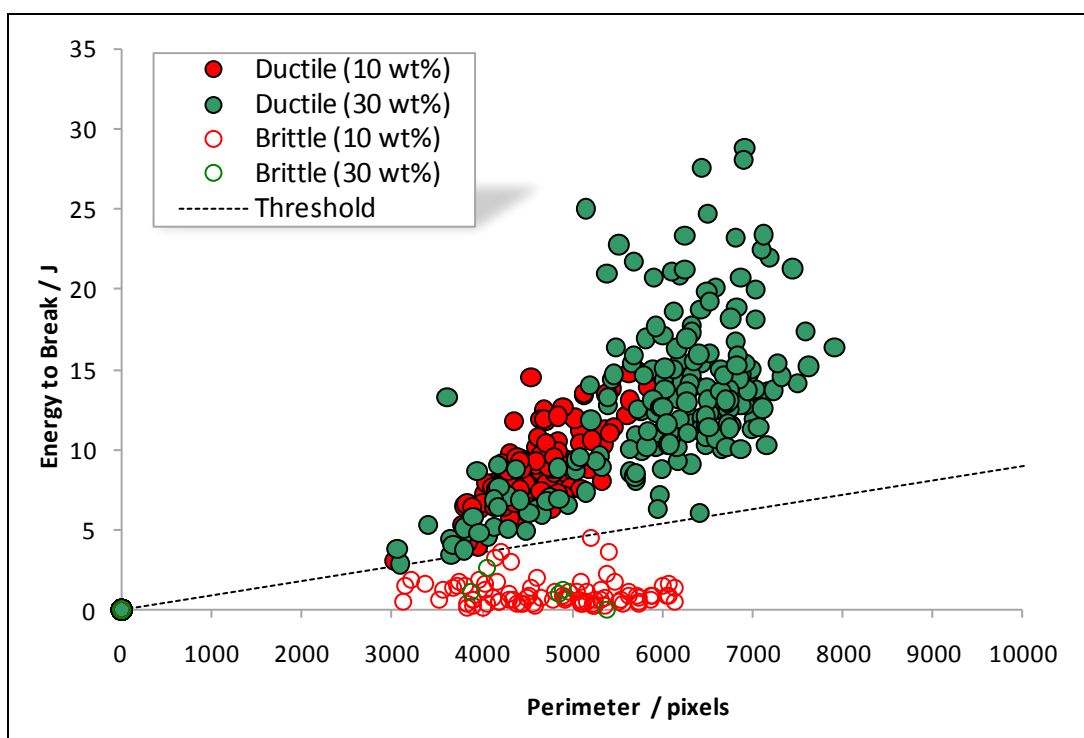


Figure 4.8; Fracture energy plotted against the outer crack perimeter, measured using image analysis software

In previous chapters, the concept of a brittle / ductile threshold was introduced and similarities of this and the glass transition state of the polymer were considered. The rate of strain in comparison to molecular relaxation time was highlighted as a major cause for the differing behaviours. The threshold phenomenon was adjudged to have been linked with the glass transition state of the polymer matrix, although comparisons between different types of polymers do not always hold true, in terms of the temperature of the material relative to the glass transition. The incorporation of filler

provided an additional complication to the already convoluted nature of polymeric material behaviour.

In order to transform the raw data from falling-weight impact measurements into meaningful and representative quantifications of the property of a material, these data must be interpreted carefully. Referring to the threshold between fracture modes, it was observed in some instances that a material in ten tests could give eight results with only a small degree of variance (for example 9.0 ± 1.0 J), but the other two tests in the series of ten underwent fracture through a brittle mode, absorbing 1.0 ± 0.2 J. Simply quoting an average value of these ten energy values would not represent the data set effectively. In the case of brittle fracture, this behaviour was understood in terms of the theory of large particles acting as mechanical flaws (introduced in previous chapters). When such a flaw, such as a sufficiently-large particle happens to be present at the site of impact and fracture initiation, the fracture mode is pre-determined as brittle and the polymeric phase does not get appropriately measured, if it gets measured at all. To understand the polymeric phase, it may therefore be tempting to completely discard data with a value below the threshold; classified as brittle. However, in the field of polymer composites a degree of importance must be apportioned to the particulate phase. The propensity of brittle fracturing is too important a concept in these mixtures to simply discard said data points. To fulfil both of these requirements of impact data presentation it is therefore suggested that a mean value and its range is quoted of data points lying above the threshold, which is accompanied by the percentage of fractures in the series of tests that were discarded from this mean due to their classification below the threshold. It was regarded as unnecessary to include the value of brittle fracture energy for a given polymer type, as it is consistently low with little variance. So in the above example, the quoted data could be presented as ' 9.0 ± 1.0 J (20 % brittle fractures)'. In the case of the uncoated GCC in the simple PP formulation, 50 tests could be fully summarised as 8.19 ± 1.14 J (16 % brittle fractures). It is acknowledged that this system may not be applicable to polymers where differences between ductile and brittle failures are less-clearly defined, where brittle fracture data may prove more illuminating.

The measurement from Test 9 was regarded as the most representative of applications that require a material designed to resist impact. In Table 4.2, the key results from the section for the uncoated, fine GCC substrate are summarised. The data presented for uncoated GCC and simple PP composite formulations that comprise it will also feature consistently in the following section.

	Test Name	Property (Units)	Ideal	Value	N
1	Laser Light Scattering	Median particle diameter (μm)	↓	1.9	10
2	Hegman Gauge Test	Top-cut (μm)	↓	8	10
3	Moisture Content	Total moisture present (% w/w)	↓	0.11	3
4	Suspension Rheology	Maximum packing value (% v/v)	↑	41	3
5	Scanning Electron Microscopy	Median particle diameter (μm)	↓	4.0	10
6	Differential Scanning Calorimetry	Total crystal content (% w/w)	n/a	44.9	3
7	Tensile Testing	Tensile strength (MPa)	↑	27.3	10
8	Flexural Testing	Flexural strength (MPa)	↑	37.3	10
9	Impact Testing	Impact Energy (J and % brittle)	↑ (↓)	8.19 (20)	10

Table 4.2; A summary of the key characteristics of uncoated, fine GCC material (Tests 1-4) and a basic PP composite formulation that comprises it (Tests 5-9), taken from N measurements. 'Ideal' represents which direction (increase or decrease), if any, is most desirable for composite performance

4.2.2 Identifying Key Indicators of Application Performance

In this section, Tests 1-8, as previously introduced, will be considered briefly in terms of how they relate to Test 9, which was assumed to be a representative measurement of application performance. Being able to detect downstream performance based on upstream indicators was regarded as very useful. This section was therefore included to assess the validity of using these tests in this manner, and also to attempt to identify any situations in which these tests could produce misleading data. Tests 1-8 are divided into two groups; particle and polymer composite testing, which each contain four tests that were seen as potential 'indicators' of performance in the impact resistance test.

(I) Particle Indicators

Any upstream indicator of downstream performance must make some assumptions about how that upstream material gets delivered. For particle indicators, this is particularly relevant because the mixing process of particles with a polymer has high potential for the apparent qualities of the particles to not get adequately delivered, thereby invalidating previous measurements. That said, there are certain properties of particles that affect how effectively they can be mixed and some that mixing will not be able to change.

The particle size information acquired by Tests 1, 2 and 4 should provide data that relates to the finest possible particle sizes i.e. the fundamental particles, assuming the particles have been fully dispersed. They could be thought of as measurements of the *potential* of that material. In Tests 1 and 2, a significant amount of coarse particles might be detected. It is unlikely that these will be removed with polymer mixing, if they could not be removed during the preparation for these tests. Test 1 was found to be less representative than Test 2. This was attributed to the manner in which the materials were prepared. Test 1 used aqueous solution and sonication to disperse the particles, which proved effective for GCC particles, but was not representative of a mixing process that used shear to mix viscous mixtures to achieve dispersion. Test 2 did use principles similar to these in sample preparation, and was more versatile in terms of the type of suspending medium that could be used. Acquiring measurements from Test 2 however was regarded as being exposed to subjectivity. Test 4 was similarly versatile to Test 2 regarding the suspending medium. Test 4 was regarded as less useful than Test 2 due to its greater degree of insensitivity to trace levels of coarse particles. However, it could be used to provide information about particulate strength and packing that eluded the other techniques. For some situations (which are considered later in the Thesis), maximising the level of particle packing is highly desirable, and Test 4 enabled a representative upstream indicator that could measure this property accurately. Test 3 was not regarded as an appropriate indicator of subsequent performance. Moisture generally has a deleterious effect on the properties of polymers, but this is often so severe that it requires materials preparation protocols to include a powder drying

stage prior to mixing. In summary, Tests 2 and 4 had the most potential for frequent use in the context of this Thesis; for the purposes of marking downstream performance.

(II) Polymer Composite Indicators

Measurements taken on particles after their composition into polymer matrices have natural integrity, since the particles are essentially frozen in place and will remain in this state up to the point where they are put to their final test in the desired application.

Test 5 has the potential to be the most useful test that indicates performance under impact. It can map out a two-dimensional surface and provide high degrees of highly resolved physical data, upon which many theories of fracture mechanism chiefly rely. Several disadvantages exist in the long preparation times, the low particle counts that each image can collect and its inability to easily measure equally-resolved chemical and crystallographic information, which are also believed to play a significant role in fracture mechanisms. Even for the excellent physical information it can provide, it is arguably unnecessarily resolved (and costly) for the purposes of predicting performance during impact tests. The crystalline content measurable in Test 6 is meaningless in isolation, since both very high and very low levels of crystallinity can occur in materials that perform well under impact. As a supplement to other tests, where the desired crystalline extreme is known it can however prove useful. The test can also be used to acquire various thermal properties that will be useful to the polymer processor, such as the available operating window; the temperature at which the solid phase melts and how long it can withstand processing temperatures before degrading. Tests 7 and 8 are tests of other mechanical properties and their usage to predict the outcome of an alternative property is unlikely to prove successful or indeed useful. Their use is to supplement research into impact since improving this property could have an adverse effect on another. In summary, the visualisation of in situ particle detail provided by Test 5 is the most effective indicator of composite impact performance of those discussed, although it is costly in time and money.

4.2.3 Quantifying the Scope for Improvement through Formulation

In this section, various composite formulations comprising the GCC material that was previously mentioned (and further treatments thereof) were produced using a single set of strictly-defined processing conditions and their application performance (i.e. the results of Test 9) is presented. The materials were also subjected to Tests 1-8 and how these affected the results of Test 9 is studied in close detail. Additionally, the scope for performance improvement through modifications to the processing conditions (such as time, temperature and intensity) is also described.

A series of composites that included the same principal GCC, PP and anti-oxidant components as that described previously (Formulation A), were produced. Each contained at least one chemical variation to the basic recipe. A total of twelve were selected for comparison, and are herein referred to as Formulations A-L. Details of their respective compositions can be found in Table 4.3.

	Mineral	Surface Treatment	Dose † (% w/w)	Polymer	Additives (besides 0.10 % anti-oxidant)	Dose ‡ (% w/w)
A	FilmLink520	None	<i>n/a</i>	HE125MO	None	<i>n/a</i>
B	FilmLink520	None	<i>n/a</i>	HE125MO	Silicone fluid (inert)	1.0
C	FilmLink520	None	<i>n/a</i>	HE125MO	Silicone fluid (functionalised)	1.0
D	FilmLink520	NaPAA	0.5	HE125MO	None	<i>n/a</i>
E	FilmLink520	NaPAA	1.0	HE125MO	None	<i>n/a</i>
F	FilmLink520	NaPAA	2.0	HE125MO	None	<i>n/a</i>
G	FilmLink520	Stearic Acid	0.5	HE125MO	None	<i>n/a</i>
H	FilmLink520	Stearic Acid	1.0	HE125MO	None	<i>n/a</i>
I	FilmLink520	Stearic Acid	2.0	HE125MO	None	<i>n/a</i>
J	FilmLink520	PHSA	0.5	HE125MO	None	<i>n/a</i>
K	FilmLink520	PHSA	1.0	HE125MO	None	<i>n/a</i>
L	FilmLink520	PHSA	2.0	HE125MO	None	<i>n/a</i>

Table 4.3; A list of the names of the formulations that were used and what they contained. † Values in % w/w referring to the weight of the treatment relative to that of the mineral on which it was applied. ‡ Values in % w/w referring to the weight of the overall composite. NaPAA refers to sodium polyacrylate, PHSA refers to polyhydroxystearic acid.

As indicated, each subsequent formulation varies from the original; either applied to the mineral surface prior to mixing or added during the mixing process itself. Table 4.4 shows how the various formulations performed in each of the previously described tests, including impact resistance, Test 9. There is a large amount of data, so the key points must be summarised. This will now feature, descending the rows of data that appear in Table 4.4.

Tests 1 – 4 relate to particle-based tests. In Test 1 (particle size by aqueous laser light scattering), untreated surfaces and those treated with sodium polyacrylate (a water-soluble substance) performed to similar levels, with the latter providing slightly finer measured sizes. In either case, the particles appeared to have been well dispersed in the aqueous medium, giving size data that was believed to represent individual particles, as opposed to particulates. For stearic acid and PHSA surface treatments (water-insoluble substances) however, the measured particle sizes showed significant coarseness; the extent of which generally reflected the dose of these treatments, with the most severe case being found for Formulation I (GCC + 2 % stearic acid). These observations were attributed to the level of compatibility between the treating and suspending media that could favour or prevent particle dispersion, the size of particulates and therefore the manner in which the light becomes scattered. Test 2 (the Hegman Gauge test) showed very little ability to differentiate between various GCC samples. These top-cut values are very similar to the d_{98} values from dispersed materials in Test 1, implying that each of the particle grades were fully dispersed by the method protocol. Test 3 (moisture absorption) showed a correlation between surface hydrophilicity and material hygroscopicity; with surfaces that most favourably dispersed in Test 1 naturally absorbing the greatest amounts of residual moisture, and vice versa. In Test 4 (determining maximum packing from suspension rheology) untreated grades dispersed the least favourably in squalane (a liquid at room temperature with a dielectric constant similar to PP) according to the maximum level of packing efficiency they could obtain. Each of the treatments applied to the surface improved this level to some degree. That reached by the sodium polyacrylate treatment was the least noticeable,

with the hydrophobic treatments improving the value greatly; to a level that indicated high degrees of particle dispersion in this medium.

Tests 5 – 9 were performed on PP composites that comprised the particles of Formulations A-L. It was observed when sampling material for Test 5, the random sampling method to pre-defined sections that was adopted would not necessarily appear to be representative of the surrounding surface. While 'zooming out' to a lower magnification would encompass a greater area, it would simultaneously cause some of the high quality resolution of the resulting image to be lost, which was a key justification for using the technique originally. The preparation times and capital cost of such a scanning electron microscope rendered its use to be counter-productive in this context, when the information could be ascertained more representatively in much simpler ways. Test 5 (visualising fractured surfaces using SEM to derive particle sizes in situ) revealed the presence of very coarse particulates for Formulation F (GCC + 2 % sodium polyacrylate), although the inconsistency in finding these particles led to the mean value being susceptible to the greatest degree of variation for any Formulation. The hydrophobic treatments showed the most effectively dispersed particles, although the statistical deficiencies of the Test must be acknowledged; the size of the areas viewed and the numbers of particles accounted meant that the data could not be guaranteed to have been representative. The results of Test 4 were in some way reflected by those of Test 5 regarding dispersion, with the exception of the polyacrylate substance. This was thought to have been due to the insensitivity of Test 4 to small amounts of coarse particles and the statistical deficiencies of the analysis in Test 5. Otherwise, the interaction between the surfaces in squalane and in PP to provide dispersion appeared to be similar.

Test		Formulation											
		A	B	C	D	E	F	G	H	I	J	K	L
1	value	1.89	1.89	1.89	1.80	1.81	1.80	13.4	41.0	192	7.54	90.0	78.2
2	value	8	8	8	7	7	7	7	7	9	7	7	7
3	value	0.11	0.11	0.11	0.14	0.17	0.21	0.11	0.09	0.09	0.07	0.08	0.08
4	value	40.6	40.6	40.6	45.6	51.4	51.6	68.4	74.3	70.3	74.5	74.5	76.5
5	value	4.04	4.23	3.95	8.16	6.06	24.6	3.25	3.30	5.94	2.95	3.03	2.98
6	value	44.9	42.4	34.9	45.2	45.0	44.9	48.5	47.3	47.4	48.0	46.3	46.6
7	value	27.3	25.2	26.8	27.9	29.2	29.3	29.0	28.2	27.6	27.5	27.2	27.6
8	value	37.3	30.6	33.4	36.7	35.9	40.9	34.4	32.4	35.1	35.1	35.6	37.9
9	value	8.19	8.44	13.2	7.69	7.57	5.29	11.0	14.2	12.8	14.2	13.9	14.3
	% br.	20	10	0	10	20	40	10	0	0	0	0	0

Table 4.4; How Formulations A-L performed in Tests 1-9

Test 6 (total crystalline content from DSC) showed that the values could be increased or decreased according to the overall formulation from that of the untreated surface. Silicone fluid additives reduced this level, with the functionalised grade doing so most profoundly. PP copolymers (data not shown) typically had a crystallinity between 20 – 35 % due to the widespread disruption to the linear structure of the chains of which it consists and the final crystalline structure of the matrix formed on cooling. It was shown that the silicone fluid additive was capable of achieving a similar effect. The hydrophobic treatments, especially those at the smallest doses of 0.5 % induced the greatest levels of crystallinity of each of the Formulations tested. This could be a reflection of material being present that was not at the particle surface, but ‘free’; elsewhere in the matrix, and therefore affecting the structure on cooling. Test 7 (tensile strength) showed that many of the samples exhibited similar degrees of tensile strength. Since there is no chemical bonding between the particles and the polymer chains, then incorporating particles only replaces the cross-sectional area of polymer chains that are able to undergo uniaxial tension from removed locations (12.5 cm along the axis of strain away from the central cross-section). An inverse dependency was found between the values of Tests 8 and 9 (flexural strength and impact resistance respectively), which was elaborated on in previous chapters. Test 9 showed that the functionalised silicone fluid additive

improved the impact resistance of the resulting composite. The reduced proportion of crystalline content in co-polymers is typically reflected by an improved impact resistance, and a similar mechanism was attributed to the cause of this phenomenon. The poorest-performing particle surface in this test (Formulation F) was believed to have been due to a larger proportion of coarse particulates, as detected in situ of the composite in Test 5. However, the limited number of these coarse particles that could be detected with this method ruled out the possibility of exploring this relationship in greater detail.

Additional data (not shown – see Appendix) showed that mixing the original master-batches one additional time, in an attempt to improve the quality of dispersive mixing in the melt, did not result in any significant changes as measured by Test 9. Applying three or more of these processes however showed evidence of polymer degradation in its visual properties and its detectable odour during processing, as well as in Tests 6 and 9.

4.5 Summary

To aid the clarity of this chapter, which has encompassed a diverse range of topics, the majority of the results presented have already included discussion adjacent to them. Therefore, this section is predominantly a summary of the main points that have been raised.

A current commercial grade of GCC mineral filler has been incorporated into PP using conventional processes in order to establish the potential usefulness of various testing methods that were employed during the entire composition process, as markers for downstream performance and in their more general logistical aspects. The use of suspension rheology and particle size analysis have been identified as the most potentially useful of these tests, although the latter of these was deemed unjustifiable in allowing for quick and effective research of high volumes of different materials. Formulation H was regarded as the most cost-effective of those prepared, in relation to the performance that it provided (see Chapter 9 for further details of costing). While functionalised

additives and bespoke surface treatments have shown to offer some benefits to the impact property, they did not prove to be sufficiently more beneficial to justify their selection, compared to more cost-effective alternatives.

With this information, several important research paths were highlighted. Firstly, given that the pursuit of expensive novel mineral surface treatments has been largely rejected as inexpensive formulations have proven to perform effectively, it is possible that the manner in which these commodity materials are prepared on an industrial scale using conventional twin screw extrusion is consuming unnecessary costs in its processing energy. The feasibility of alternative techniques should therefore be studied more closely. Secondly, given the need for some form of *in situ* particle imaging and the difficulties encountered regarding representativeness when using high resolution methods such as electron microscopy, research should be conducted into how both speed and representativeness could be achieved by using alternative techniques. Thirdly and finally, although the GCC grade described in the above work is one that is currently commercially available and very widely used, the potential for incorporating cost-effective minerals processing technology into the conventional composite formulation method should also be researched. The remainder of this Thesis addresses each of these three identified research paths, with the aim of providing processes, analyses and materials that are intended to shape and guide conventional composite technology in the future.

CHAPTER FIVE

The Application of Cost-Effective Technology to Improve the Impact Resistance of PP/GCC Composites Using an Alternative Mixing Process

FIGURES AND TABLES

Figure 5.1; Demonstrating a visual test of filler dispersion within concentrates by lowering their concentration to form plaques using an injection moulding process, for two different samples that A) passed and B) failed	114
Figure 5.2; Optical microscopy on particles types that appeared A) dispersed and B) un-dispersed	119
Figure 5.3; Fractured surfaces of concentrate forms under SEM at 800 x magnification, for GCC + 1% stearic acid in polyethylene wax in filler concentrations of A) 88 % and B) 90 % (w/w)	120
Figure 5.4; Fractured surfaces of concentrate forms under SEM at 1600 x magnification, for GCC + 1% stearic acid in polyethylene wax in filler concentrations of A) 88 % and B) 90 % (w/w)	121
Figure 5.5; Fractured surfaces of concentrate forms under SEM at 3200 x magnification, for GCC + 1% stearic acid in polyethylene wax in filler concentrations of A) 88 % and B) 90 % (w/w)	121
Figure 5.6; Quantification of a mixing phenomenon encountered during the injection moulding of filled PP composites from GCC concentrates in Equilibration (Samples 1-8), Collection (Samples 9-13) and Purge (Samples 14-20).	124
Figure 5.7; Investigating mixing phenomena during the injection moulding of filled PP composites from materials pre-mixed using TSE, in equilibration, collection and purge. The axes are identical in scale to those in Figure 5.6	125
Figure 5.8; Product forms of an 88 % w/w GCC/PE wax concentrate. Diameter (mm) as follows; i) $3.5 \leq d < 9.5$, ii) $2.0 \leq d < 3.5$ and iii) $0.0 < d < 2.0$	126
Figure 5.9; Observing mixing during the injection moulding process through consistency in sample masses for three different sizes of (88 % w/w) product form diluted to 15 % w/w plaques. The error bars were obtained from three repeat measurements using the same batch materials.....	127
Figure 5.10; The sample masses of an 88 % w/w amorphous GCC/wax concentrate of diameter $2.0 \leq d$ (mm) < 3.5, when mixed with PP down to the % values (w/w) shown.....	128
Figure 5.11; A roughly-spherical product form	129
Figure 5.12; The sample masses of an 88 % w/w spherical GCC/wax concentrate of diameter $2.0 \leq d$ (mm) < 3.5, when mixed with PP down to the % values (w/w) shown	130
Figure 5.13; IFWIT results for the developed concentrate form to assess the differences in wax binder formulations.....	131
Table 5.1; Pass or fail (P/F) results following visual inspection of injection moulded specimens comprising GCC (FilmLink520) and PP (various types) made from TSE pellets and powders. †IM pellets were made from the resulting un-dispersed plaques from the previous sample, shown in the row above it.....	114
Table 5.2; Various instruments for producing highly concentrated dispersed mineral forms were considered relatively to each other on unspecified laboratory-scale equipment. †These attributes improved with automation. ‡ Production Rate relates to the maximum number of different batches producible per unit time.	115
Table 5.3; Particle properties of fine GCC grades, acquired by aqueous laser-light scattering. Steepness, $S = 100 \times d_{30}/d_{70}$	116
Table 5.4; Details of selected polymer waxes. Wax Type ‘E’ refers to ethylene co-polymer. Acid Value; DIN EN ISO 3682 ASTM D 1386, Density at 23 °C; DIN 53 479 ASTM D 1505, Softening Temperature; DIN 51 801/2 ASTM D 127.	117

Table 5.5; Maximum volumetric packing efficiencies (ϕ_{max}) of concentrate formulations, determined by 1) the repeated addition of particles to binder materials in their molten liquid forms and where available, 2) by suspension rheology	117
Table 5.6; Pass or fail (P/F) results following visual inspection of injection moulded specimens comprising 10 % (w/w) GCC and PP (HE125MO) made from wax-concentrate forms.....	119
Table 5.7; IFWIT data for visually-dispersed injection moulded composites (concentration = C_1) formed from concentrated material (concentration = C_0) and pure PP polymer, mixed in different proportions. Also shown (in the final row) is the result that was characteristic of all visually 'failed' types. IFWIT 'failed' where all tests (of at least ten) resulted in brittle fracture.....	122
Table 5.8; The effects of replacing 25 % w/w of PP wax in an 88 % w/w GCC/PP wax concentrate with various polyolefins on rheology in the melt, hardness and susceptibility to dusting when cooled and visual dispersion when diluted into 15 % w/w plaques.....	129
Table 5.9; The performance of various waxes as binders of GCC for impact-resistant applications. † 7.1 % w/w of wax replaced with Dow Corning silicone fluid. ‡ 7.1 % w/w of wax replaced with Shin-Etsu KPN 3504 modified silicone.....	131

5 THE APPLICATION OF COST-EFFECTIVE TECHNOLOGY TO IMPROVE THE IMPACT RESISTANCE OF PP/GCC COMPOSITES USING AN ALTERNATIVE MIXING PROCESS

5.1 Introduction

An alternative mixing process from the conventional twin-screw extrusion (TSE) method of mixing raw materials to form polymer composites may prove more advantageous to commercial formulation, compared to that conventional method. As highlighted in the previous chapter, one of these advantages could be a reduced level of energy consumption across the entire mixing process, in the case where raw materials will mix sufficiently favourably and require less-intensive mixing processes and/or fewer cycles of heating and cooling to form a product of similar quality to one which was made by (unnecessarily) intensive processes. It was found previously that ground calcium carbonate (GCC), when treated appropriately could mix with polypropylene (PP) in a manner sufficiently favourable to provide the composite material with toughness, to the extent that predominantly ductile behaviour would be observed, even under moderately high strain rates.

Reducing the mixing intensity alone would not be sufficient to warrant a total upheaval of the production methods. Further advantages would need to be offered by an alternative process, since such an adjustment can be made easily when performing TSE, by altering the conditions under which it is performed. TSE instruments in the polymer processing industry require certain characteristics of extrudate to make it possible to run at high throughputs (i.e. the extrudate must be sufficiently ductile when it emerges from the die, thereby allowing it to maintain a continuous strand as it stretches and is pulled through a cooling bath, during only a short residence in which it must become sufficiently brittle to be subsequently granulated without interruption). Therefore even the most concentrated masterbatches are confined to having a lower concentration than that which is physically possible to produce. For mineral particles with a median diameter of 1 – 100 μm , approximately 50 – 70 % (w/w) polymer composite masterbatches are typically produced in commercial TSE processes [1] which for particles with a true density of 2.6 – 2.7 $\text{g}\cdot\text{cm}^{-3}$ in a medium

with a density of $0.9 - 1.0 \text{ g.cm}^{-3}$ (as is typical for mineral/polymer composites) corresponds to 25 – 45 % (v/v). If such particles were mono-disperse spheres, it would be theoretically possible to prepare such mixtures at about 64 % (v/v), as allowed by random maximum packing characteristics, with the particles being genuinely dispersed (with ‘wetted’ surfaces i.e. physically separated from one another, albeit by a very thin layer of binder material). If an alternative mixing method from TSE could be used to prepare such highly concentrated forms then, provided that these materials could successfully re-disperse, several advantages could be gained in technical, logistical and commercial aspects. Technically, the mixing of materials of higher concentration inherently allows for a more intensive mixing process, in terms of the proportion of input energy which is transferred into shearing particles per unit material volume, as required to achieve dispersion [2]. Logistically, these materials provide advantages when being handled, transported and stored. The space they occupy is naturally more volumetrically-efficient per unit mass of the particles they contain, compared to materials with a lower concentration. This may even be true when compared to particles in powder form, depending on their bulk density. Particles in powder form are also highly susceptible to their storage conditions, allowing undesirable effects such as compaction and moisture absorption to occur, whereas particles in the form of high-solids concentrates may not be, depending on the material which is used to bind them. Commercially, from the perspective of a producer of particles which are ultimately intended for use as fillers, there is the possibility of direct sale of their product to independent producers of final applications, which in their highly-concentrated forms would require only a small additional content of binder material which they would source externally. This is as opposed to selling their product in the form of a powder or an aqueous suspension to an independent masterbatch formulator for example, who will then sell *their* product to producers of the final application. Additionally, assurances in particle characteristics (i.e. their quality) are significantly less susceptible to being invalidated when selling fine, and possibly hygroscopic, materials when they are in a more inert form, such as one that binds them in a concentrated, yet dispersed form. From a general perspective, a more efficient overall formulation process would be allowed by using re-dispersible concentrates, if one of the three conventional heating-and-cooling

cycles (as introduced in Chapter 2) could be removed. Also the reduction of the particle dust is regarded as advantageous to many aspects of the overall process [3].

The practical research required to investigate the formulation of highly concentrated materials for the purposes of their re-dispersion can be divided into two parts. The first part to test the feasibility of implementing the concept, including aspects of formulation (i.e. identifying any materials that are effective in this context and ways in which they may be combined) and analysis (i.e. quantifying the extent of 'success' with which formulation has been performed). The second part, on the condition of identifying a feasible concept, would be to optimise the formulation; researching how to overcome any limitations of the chosen technique and developing the most cost-effective materials and methods for large-scale production.

The most successfully dispersing particulate materials in a similar context as this have been identified in the previous chapter as GCC with a median particle diameter of 2 μm , coated with 1.0 % (w/w) stearic acid. However, additional particle requirements might be necessary. On the one hand, a broad size distribution could be more favourable in this case as it allows for a greater packing efficiency. On the other, particles below a certain size may become less likely to mix effectively and particles above a certain size will limit their performance in an impact-resistant application material, therefore limiting the lower and upper boundaries of the particle size distribution respectively [4].

The breadth of the particle size distribution is therefore limited to certain boundaries. Their concentration should be maximised, provided that their surface can still be wetted by the substance used to bind them. When considering this substance that binds particles together in a concentrated, but also a re-dispersible and matrix-compatible form, relatively low-viscosity materials have proven to be desirable in other fields; their low viscosity has been found to favour the magnitude of the concentrations attainable during their formation, as well as their subsequent distribution throughout the polymer matrix [5]. However, higher viscosities have also been shown to benefit the intensity of the shear during mixing [6]. Other physical properties of the formed concentrate may be less clear-

cut; it should be sufficiently tough, for example such that it does not easily reduce to dust during transport or conveyance, whereas it cannot be too hard such that its form cannot be shaped (if this is performed at room temperature). It must finally be chemically similar enough to the matrix such that adequate mixing is not prohibited by chemical incompatibility. Waxes are materials that can fit within each of the above criteria as a binding substance. These are polymeric materials which may be pliable or brittle at room temperature, but undergo a softening phase transition above 40 °C without degrading, during which their viscosity lowers significantly. Both natural and synthetic waxes are produced commercially to fit many applications including treatments for surface protection, additives in plastics (such as pigment binders and mould-release agents), inks, building materials and cosmetics [7].

When researching candidate materials that can be made into highly-concentrated dispersed mixtures, they must be analysed in a manner which is representative of their final application after they have been made for the most effective formulations to be recognised. As described in the previous chapter, representative upstream indicators of subsequent application performance are highly desirable, and should be researched, although their representativeness naturally diminishes the more upstream they are.

Using practical research to investigate viable formulations and analyses, constructs a foundation from which a product can be developed. Depending on the nature of the concentrate material, such development could take on many forms that are specific to those materials. Therefore speculation at this stage can only be general. However, it is clear that the key aspects of development should aim to maximise the degree of dispersive mixing in the concentrate form and the degree of subsequent distributive mixing in the composite form to benefit the final performance. A dispersible GCC filler grade has already been identified as having high potential to provide polymer toughness to PP and delivering this potential and building on it is therefore the fundamental objective of the development stage, in whichever way it is achieved.

5.2 Aims of this Chapter

The first aim of this chapter will be to determine the feasibility of preparing a concentrated mixture of GCC mineral in a binding substance and then subsequently successfully distributing the mineral throughout a PP matrix. Therefore, a further aim arises since some method of determining the extent of 'success' will be required and must therefore be developed. The second aim will be based on the outcome of the first. If the product cannot be made or if it can be made but provides no successful results, then the causes for these should be investigated and overcome where possible. With successful results, the main aim will become studying ways of improving the extent of this success, by looking further into the aspects of the product which have made it so favourable and developing them accordingly.

5.3 Hypothesis

It was hypothesised that a 2 μm GCC formulation, shown to cost-effectively benefit the toughness of PP in conventional composite mixing techniques in Chapter 4, could also be made to disperse favourably into PP matrices from a form whose mineral concentration approached that of its maximum packing fraction based on theoretical and rheological data. Furthermore, it was reasoned that such a product, if implemented effectively, could provide many advantages over the conventional processes present during large-scale composites formulation.

5.4 Results

5.4.1 Research

This first section features results that relate to the feasibility of the proposed concept, to various candidate materials, their relative quantities and the methods that could be used to mix them and finally to the analytical approach.

Before any materials were produced, the ability to successfully use a single injection moulding cycle to achieve various aims was assessed. The instrument is routinely used for converting (often filled)

polymers as pellets into moulded specimens, without altering the filler concentration. Table 5.1 shows that the moulding process was able to distribute dispersed-filler pellets (that were made from TSE) by using additional PP to produce final specimens with a filler concentration of 10 % (w/w).

Surface Treatment	Dose / %	Original Filler Form	Filler Form Conc. / %	Pellet PP Matrix	Final PP Matrix	Final Conc. / %	P/F
None	-	TSE Pellets	30	HE125MO	HE125MO	10	P
Stearic Acid	1.0	"	"	"	"	10	P
"	"	"	"	"	"	30	P
"	"	"	"	RB206MO	"	10	P
None	-	Powder	~99	-	"	10	F
Stearic Acid	1.0	"	"	-	"	"	F
"	"	IM Pellets †	10	HE125MO	"	"	F

Table 5.1; Pass or fail (P/F) results following visual inspection of injection moulded specimens comprising GCC (FilmLink520) and PP (various types) made from TSE pellets and powders. †IM pellets were made from the resulting un-dispersed plaques from the previous sample, shown in the row above it

Figure 5.1 shows the how easily the visual distinction between passing and failing materials (i.e. those dispersed and those un-dispersed) could be made.



Figure 5.1; Demonstrating a visual test of filler dispersion within concentrates by lowering their concentration to form plaques using an injection moulding process, for two different samples that A) passed and B) failed

Shown in Table 5.1 is the inability of the mixing process had to disperse powder materials, even those whose surfaces were treated in a manner that had rendered them 'favourable' to mixing with

PP in other applications and whose un-dispersed surfaces had already been wetted by the matrix polymer.

Therefore, the idea of moulding formed polymer composites from their very raw materials from just one heating-and-cooling cycle was not pursued further. The results showed that 60 % (w/w) previously-dispersed materials could be distributed throughout a PP matrix to a visual standard using an injection moulding process, and therefore no evidence was found that the same thing could not also be achieved for filler materials of a higher concentration, provided that the particles within them had been appropriately dispersed.

The requirements of the process that could be used to form the concentrated materials depend to some extent on the nature of the materials involved. For example, binder materials that are liquid at room temperature will not require heat from the process in order to become mixed. Four methods are described in Table 5.2 that can produce granulated products from particles in their powder form and additional material. However, in order to generate the necessary degree of dispersion, processes that can impart the highest shear intensity during mixing are desirable.

Method	Material Versatility	Shear Intensity	Production Rate ‡	Capacity	Extra Steps Required
Single-step Granulator	Medium	Low	Low	Medium	No
Ball Mill	Medium	High	Low	Medium	Yes
Twin-Roll Mill	High	High	Medium	High†	No†
Twin-Screw Batch Mixer	High	High	High	Low	Yes

Table 5.2; Various instruments for producing highly concentrated dispersed mineral forms were considered relatively to each other on unspecified laboratory-scale equipment. †These attributes improved with automation. ‡ Production Rate relates to the maximum number of different batches producible per unit time.

Ball milling is a potentially viable alternative on the smaller scales, as it is capable of providing high levels of shear intensity during mixing. However unlike some of these processes, there are few advantages that can be gained when scaling up, regarding overall process efficiency. The high versatility, shear intensity and production rate as described made the twin-screw batch mixing

process highly suitable to conduct effective and thorough research. The limited sample capacity and requirement for further steps (granule shaping or screening) with the process were disadvantageous at a laboratory scale, but neither would be relevant in large-scale processes. Amongst its advantages, the batch mixing instrument enabled a measurement of torque; the resistance that the material was able to impart to the rotating screws during their operation, and it also enabled on-line manual intervention such as the ability to add materials to the mix during operation. Both of these, together with real-time visual inspection, allowed for precise measurement of the maximum concentration that could be reached when mixing a given particle formulation into a given binding substance, which as discussed with the rheological experiments in Chapter 4, could reflect the quality of the particulate dispersion that has been achieved. For each of these reasons, this method was chosen as the most suitable.

Various GCC grades were tested, to understand the thresholds of particle characteristics that could prove problematic in the overall process. The ‘breadth’ of the particle size distribution and the coarsest particles it contained were of most relevance to the required function of the filler. Table 5.3 shows these particle properties for various grades, as used in the research stage.

Mineral Name	Supplier	d₅₀ / μm	d₉₈ / μm	S	Referred To As...
C140	Imerys UK	5.99	26.4	18.6	‘broad’
C110	Imerys UK	2.43	12.9	31.8	‘med-broad’
FilmLink520	Imerys UK	1.89	8.02	40.9	‘med-steep’
FilmLink400	Imerys UK	1.40	6.85	46.9	‘steep’

Table 5.3; Particle properties of fine GCC grades, acquired by aqueous laser-light scattering. Steepness, $S = 100 \times d_{30}/d_{70}$

For the selection of binder materials, low values of softening temperature and acid value were desirable. Table 5.4 shows these and other properties for three principal wax types. High acid values are known to be detrimental to mechanical properties of polyolefin admixtures, [8]. although the magnitude at which it becomes relevant to this particular case was not precisely known. Low values

in softening temperature and viscosity favour lower-energy processes, although higher melt viscosities can provide technical mixing advantages. The ultimate selection criterion was to be the manner in which these waxes could sustain GCC particles, which was not known at this stage.

Wax Name	Supplier	Wax Type	Acid Val / mg.g ⁻¹	Density / g.cm ⁻³	Softening Temp / °C	Viscosity at Soft. Temp / mPa.s
Luwax ES 91014	BASF	E	40	0.93	100 – 108	14
Licowax PE 130 P	Clariant	PE	17	0.97	127 – 132	300
Ceridust 6071	Clariant	PP	0	0.89	156 – 164	800

Table 5.4; Details of selected polymer waxes. Wax Type 'E' refers to ethylene co-polymer. Acid Value; DIN EN ISO 3682 ASTM D 1386, Density at 23 °C; DIN 53 479 ASTM D 1505, Softening Temperature; DIN 51 801/2 ASTM D 127. Data sourced from elsewhere [9].

Table 5.5 shows the maximum concentrations that could be achieved using the selected grades of GCC mineral and polymer wax types during in the twin-screw mixing batch process.

Mineral Distribution	Surface Treatment	Wax Type	Torque _{max} / Nm	P _{max} (1) /% w/w	φ _{max} (1) / v/v	φ _{max} (2) / v/v
'broad'	None	PE	15 ± 1	77.3	0.549	-
'med-broad'	"	"	18 ± 3	75.2	0.520	-
'med-steep'	"	"	24 ± 2	69.6	0.450	0.469
'steep'	"	"	29 ± 5	61.3	0.362	0.409
"	0.5 % PHSA	"	12 ± 1	87.7	0.718	0.745
"	1.0 % stearic acid	"	7 ± 1	89.8	0.759	0.743
"	"	PP	42 ± 4	88.4	0.715	"
"	"	E	26 ± 3	68.8	0.431	"

Table 5.5; Maximum volumetric packing efficiencies (φ_{max}) of concentrate formulations, determined by 1) the repeated addition of particles to binder materials in their molten liquid forms and where available, 2) by suspension rheology

It was seen that for the untreated surfaces, the maximum recorded torque during mixing and the maximum packing value occurred simultaneously and also with the breadth of the particle size distribution. This was attributed to the broader distributions having greater packing efficiencies and therefore lower viscosities at a given concentration. The proportion of fine particle sizes was also thought to increase viscosity at a given concentration, as found previously, and therefore the torque

that got imparted to the rotating screws. The use of treatments on the GCC surface dramatically reduced torque and increased the maximum concentrations, which was also attributed to the lower viscosity this measure provides; the overcoming of the need for mechanical dispersion by using chemical means. The concentration found using the ethylene copolymer wax was not greater than 70 % (w/w) for stearic acid treatment (as shown) or indeed any of the surface treatments applied to it (not shown). While disadvantageous compared to higher concentrations, the binder material was not disregarded at this stage.

It has therefore been possible to prepare highly-concentrated dispersed particle forms, whose concentration in some cases approached that of their theoretical maximum based on rheological data. In order to determine whether various forms had been successfully dispersed during this mixing process, they were injection moulded in the same manner as the TSE pellets that were shown in Table 5.1; 'diluted' from their initial concentration to 10 % (w/w). It has already been shown that this process was not capable of dispersing particles. It may therefore be used simply to determine whether dispersion in a form had been achieved.

Table 5.6 shows the results (the visual pass or fail) of concentrate-form dispersion that was found in a variety of different particle formulations, binder types and concentrations. In each case, the concentration that was selected was at least 1 % lower than the maximum achievable, as determined from the data shown in Table 5.5. This was a measure taken to account for experimental error in particle concentration when producing these materials, so that it would not exceed some threshold maximum value to ensure their dispersion thereby appearing un-dispersed and performing poorly in mechanical tests. It was predicted that this measure, or one similar to it might also be taken during large-scale processes. The results show that each of the selected particle grades were dispersed within their concentrate forms in the polyolefin waxes, although this was not the case for (the lower concentration) ethylene co-polymer wax. It was therefore ruled out as a candidate binder material at this stage. This test of visual dispersion would be unable to provide the level of information that

would be required at later stages of research and development to differentiate between the ‘successfully dispersing’ samples. Methods were needed that could provide higher resolution information regarding particle dispersion.

Mineral Distribution	Surface Treatment	Wax Type	Form Conc. / % w/w	Vis. P/F
‘broad’	None	PE	74.0	P
‘steep’	“	“	58.0	P
‘med-broad’	“	“	72.0	P
‘med-steep’	“	“	60.0	P
“	0.5 % PHSA	“	86.0	P
“	1.0 % stearic acid	“	88.0	P
“	“	PP	86.0	P
“	“	E	66.0	F

Table 5.6; Pass or fail (P/F) results following visual inspection of injection moulded specimens comprising 10 % (w/w) GCC and PP (HE125MO) made from wax-concentrate forms

The feasibility of determining the dispersion quality upstream in the process was considered. The images in Figure 5.2 were acquired by optical microscopy performed at 75 x magnification on particle formulations (to be subsequently incorporated into concentrated form) when mixed with squalane at 30 % w/w for 5 minutes at 500 rpm using an overhead rotational mixer (Heidolph, Germany).

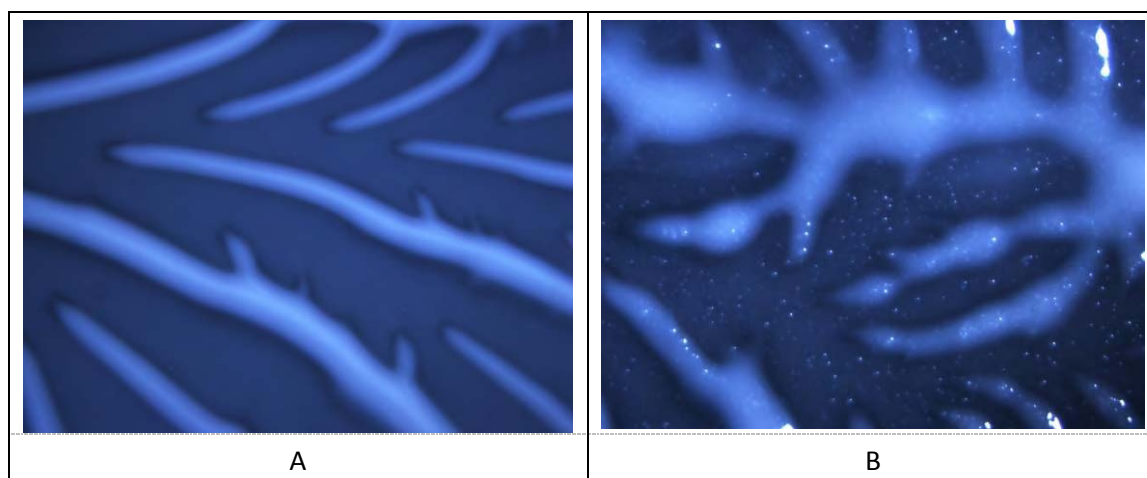


Figure 5.2; Optical microscopy on particles types that appeared A) dispersed and B) un-dispersed

The test revealed only the most significant differences in particle formulations, such as surface treatment type (as shown). It lacked the resolution to determine more subtle differences and was incapable of accounting for the effects of downstream processes on their behaviour.

Highly resolved visual evidence of dispersion quality of particles in their concentrated forms was sought. Optical microscopy was also performed on these materials but the resolution allowed by the technique was found to be lower than that which was required to successfully differentiate samples at an appropriate scale. Therefore, scanning-electron microscopy (SEM) was used. The images of Figure 5.3, Figure 5.4 and Figure 5.5 show the differences between subsequently dispersing and non-dispersing concentrate forms (as determined from the results in Table 5.6) at 800, 1600 and 3200x respectively. Even higher magnifications than these were adjudged to have been exposed to misrepresentation, accounting as they did for only very small areas and particle numbers.

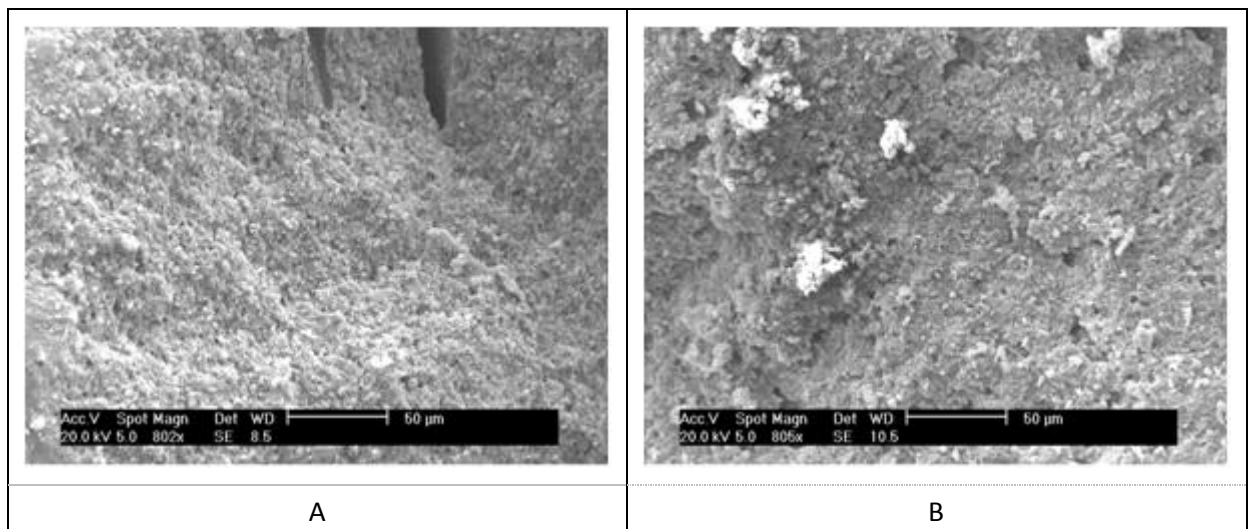


Figure 5.3; Fractured surfaces of concentrate forms under SEM at 800 x magnification, for GCC + 1% stearic acid in polyethylene wax in filler concentrations of A) 88 % and B) 90 % (w/w)

The images shown were representative of all the GCC/polyolefin wax material at concentrations just below and just above that of its identified maximum packing level; homogeneity of newly fractured surfaces for the lower of the two concentrations was consistently found, whereas those of higher concentration (that were not subsequently shown visually to have been dispersed) consistently showed evidence of inhomogeneities, which appeared to be clusters of un-dispersed GCC.

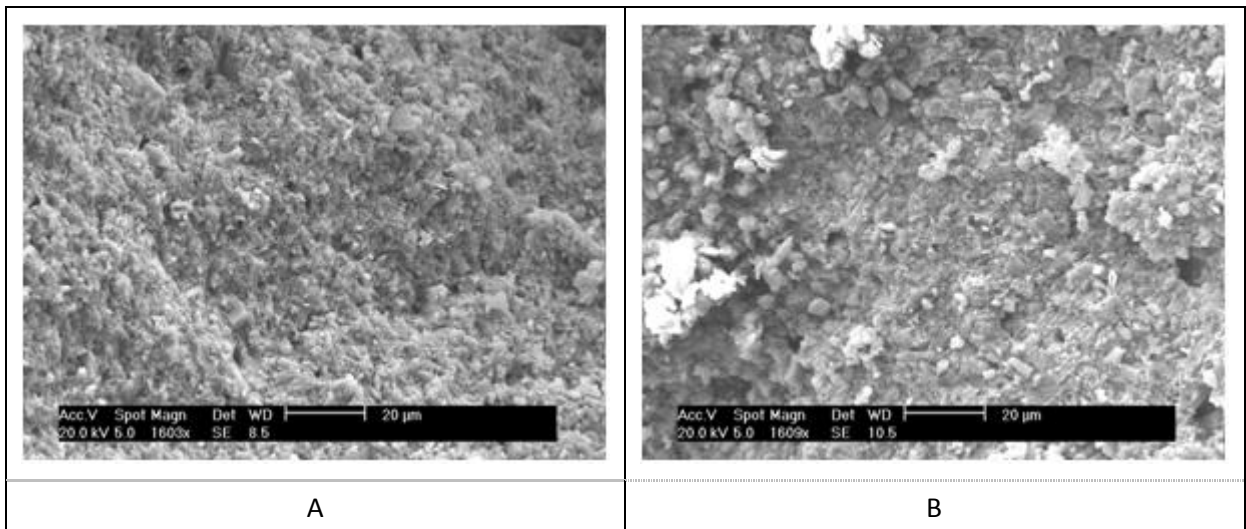


Figure 5.4; Fractured surfaces of concentrate forms under SEM at 1600 x magnification, for GCC + 1% stearic acid in polyethylene wax in filler concentrations of A) 88 % and B) 90 % (w/w)

Higher resolution images taken at 1600 and 3200 x magnification were able to demonstrate fine details of fundamental particles in the lower concentration materials and closer details of GCC clusters for the materials of a higher concentration.

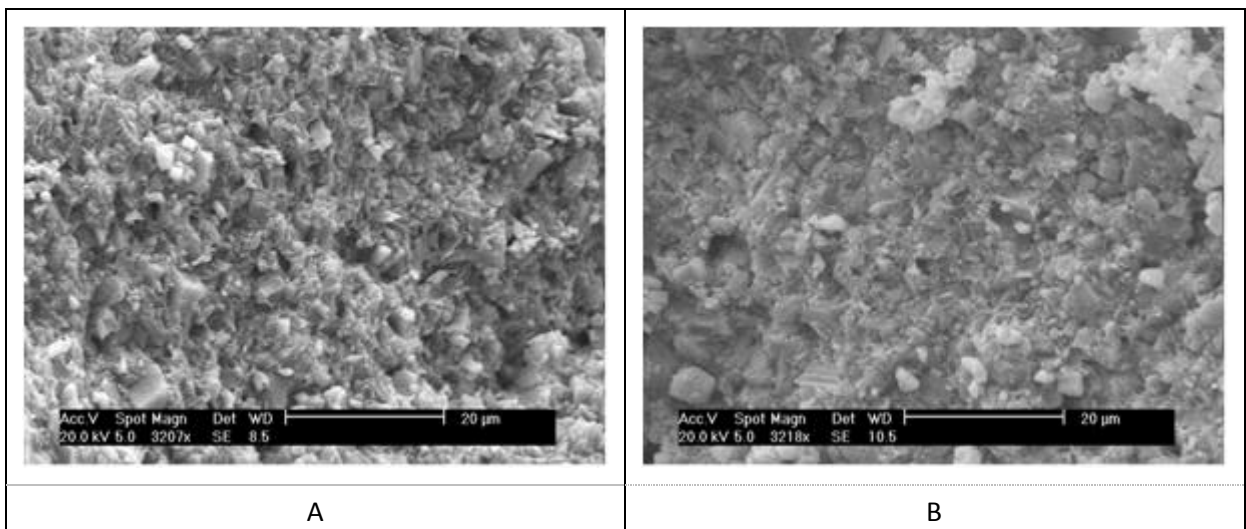


Figure 5.5; Fractured surfaces of concentrate forms under SEM at 3200 x magnification, for GCC + 1% stearic acid in polyethylene wax in filler concentrations of A) 88 % and B) 90 % (w/w)

When considering fillers designed to provide toughness to a polymer, a suitable measure of performance is the instrumented falling-weight impact test (IFWIT), as argued to be the case in previous chapters. One advantage of using this test is that provided the injection moulding process was performed (as would be the case here), the test could be performed quickly, allowing visual

inspection to take place before testing, so that any un-dispersed samples could be discarded. These would give, without exception, poor results on any test of particle dispersion, including IFWIT. Also, because it was the most downstream test available on this scale, it was most naturally representative of the intended application. The data it provided is shown in Table 5.7. The mixing quality (both dispersive and distributive aspects) were inferred from the impact resistance behaviour.

GCC Type	Surface Treatment	Wax Type	C ₀ / % (w/w)	C ₁ / % (w/w)	Vis. P/F	IFW P/F	Energy to Break / J	Brittle / %
med-steep	1% stearic acid	PE	88.0	5	P	F	1.11 ± 0.13	100
"	"	"	88.0	10	P	P	5.84 ± 0.63	70
"	"	"	88.0	15	P	P	6.49 ± 0.63	30
"	"	"	88.0	20	P	P	7.76 ± 0.78	20
"	"	"	88.0	25	P	P	7.52 ± 1.41	10
"	"	"	88.0	30	P	P	7.78 ± 1.14	0
broad	1% stearic acid	PP	88.0	15	P	F	1.32 ± 0.16	100
steep	"	"	66.0	15	P	P	4.46 ± 1.09	50
med-broad	"	"	88.0	15	P	F	1.18 ± 0.15	100
med-steep	"	"	88.0	15	P	P	6.02 ± 0.41	30
"	"	PE	88.0	15	P	P	6.49 ± 0.63	30
"	1% PHSA	PE	88.0	15	P	P	6.22 ± 1.45	30
"	None	PE	88.0	15	P	P	4.24 ± 0.74	80
-	-	-	-	-	F	F	1.23 ± 0.25	100

Table 5.7; IFWIT data for visually-dispersed injection moulded composites (concentration = C₁) formed from concentrated material (concentration = C₀) and pure PP polymer, mixed in different proportions. Also shown (in the final row) is the result that was characteristic of all visually 'failed' types. IFWIT 'failed' where all tests (of at least ten) resulted in brittle fracture

The medium-steep GCC particles, the 1 % stearic acid treatment and the PE grade of wax binder consistently provided greater toughening to 15 % w/w PP composites, as measured using IFWIT. Both the broad and med-broad particle grades consistently failed the impact test, despite being regarded as dispersed from visual methods. This was attributed to the detrimental effect of the coarse particles they contained (regardless of the state of their dispersion) to impact resistance, and the grades were therefore disregarded from future formulations. It was found that by increasing the matrix concentration to which the concentrated materials were diluted, generally greater values of

impact resistance and fewer instances of brittle fracture were observed. Neither of the extreme ends of the shown range (5 – 30 % w/w) were regarded as a suitable single value for future work, because of the inability to differentiate between different samples at these values. At the lower end, of 5 %, even samples produced by the TSE process would mostly result in brittle fracture and there was no reason to believe that plaques produced from the concentrate route would perform to a better standard. At the high end, a plateau of impact resistance values was observed, which would also hinder differentiation between similar types. At 15 % w/w, the sample shown in Table 5.7 had 30 % brittle fracturing, which was a sharp decline from the 70 % shown by 10 % w/w samples. It seemed that if there was a threshold of reinforcement to be identified with these data, then it was between these values. The higher of these two was selected for future formulations, since the total composition was the most favourable of those attempted up to that point; the goal of future work would be to improve further on its performance.

5.4.2 *Development*

A 'general method', consisting of materials, processes and analyses with which concentrated GCC filler materials in polyolefin waxes could be produced at concentrations > 70 % (w/w) and subsequently dispersed in PP to 15 % (w/w), has been identified. This second section features results that relate to the development of this method; making adjustments to the materials and methods within the boundaries of the general method to identify and address specific difficulties in production, including those which will become more relevant to larger scale processing.

Having observed that dispersive mixing could be consistently achieved under the appropriate conditions within the concentrate form, to the point where subsequently produced composite materials could resist impact under a high strain rate, the next logical step to improve on the formulation was regarded as maximising the degree of distributive mixing. An observation was made that on occasion injection moulded plaques would become noticeably heavier at the end of a moulding process and that when this occurred it appeared to be independent of the number of

moulding cycles required to reach the end of the process. This observation was quantified by recording the mass of each consecutively produced plaque, as shown in Figure 5.6.

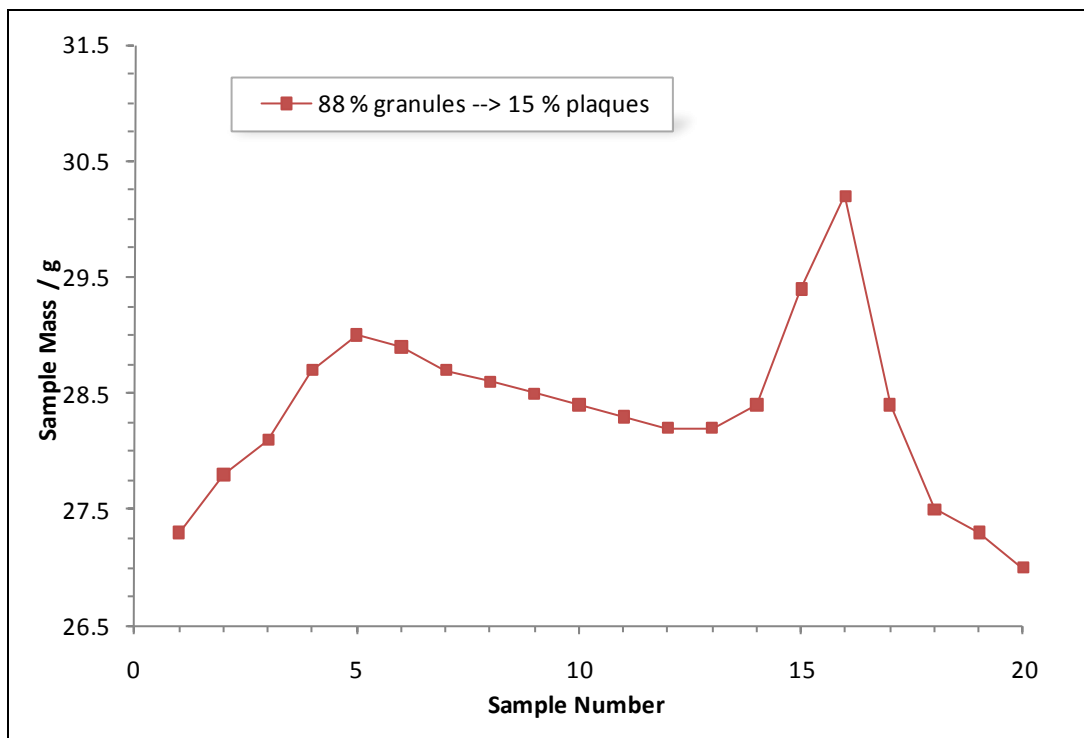


Figure 5.6; Quantification of a mixing phenomenon encountered during the injection moulding of filled PP composites from GCC concentrates in Equilibration (Samples 1-8), Collection (Samples 9-13) and Purge (Samples 14-20).

It was found that the precision in the masses of consecutively produced plaques was relatively poor during the collection stage, and that the recorded masses in some cases did increase significantly towards the end of their processing. It was hypothesised that the uniformity in sample mass was a direct effect of the degree of distributive mixing that had occurred. This was tested by performing the same measurements on plaques made from pre-mixed pelletized forms; as resulted from the TSE process. The results from this experiment are shown in Figure 5.7. It was observed that the degree of mixing within these moulded composites, as indicated by the consistency in the masses of collected samples was significantly higher than in those prepared from concentrated materials. This supported the recording of collected sample masses to assess mixing uniformity within the injection moulding process, and did not contradict the previous hypothesis. However, the observations of

increasing sample mass at the end of some concentrate-derived composites could not be fully explained by a simple difference in the extent of distributive mixing.

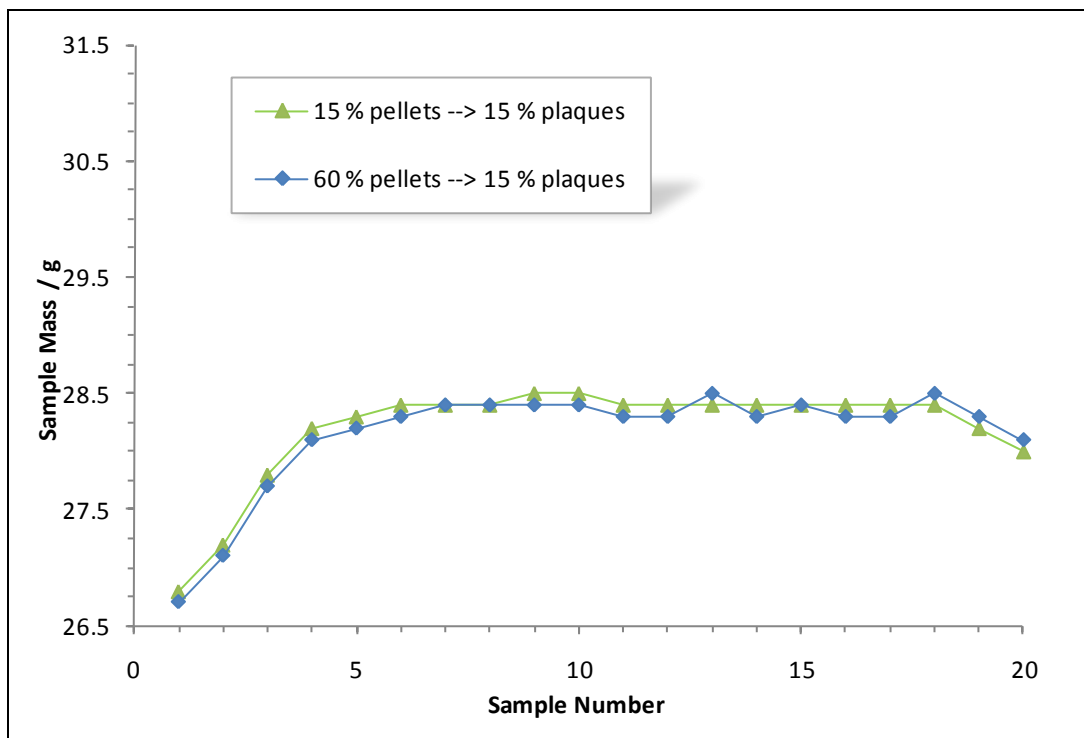


Figure 5.7; Investigating mixing phenomena during the injection moulding of filled PP composites from materials pre-mixed using TSE, in equilibration, collection and purge. The axes are identical in scale to those in Figure 5.6

It was believed that phase segregation during the conveying of materials was the sole cause of the increasing sample mass phenomenon, as well as playing some role in the overall extent of distributive mixing that the moulding process could impart. There were several differences between the GCC-containing granular forms introduced to the injection moulding process (other than the degree of mixing alone) that could be the cause. Three primary properties of the granules that could affect mixing were identified; their size, shape and surface finish. (The mixing proportions, concentrations of different phases and therefore the densities were also acknowledged, although these had been somewhat confined to fixed values by the general method). A secondary granule property was identified as granule strength. This could affect segregation in a practical environment. For example, the transportation of large quantities of material could cause weaker granules to

fracture, release dust or distort, thereby altering their size, shape and surface finish and their resulting segregation behaviour.

The granule size of two components was known to affect their segregation behaviour when agitated to induce mixing, with the coarser component being preferentially segregated towards the top (i.e. furthest from the centre of the Earth) and the finer component towards the bottom, so that the lowest centre of gravity would be eventually obtained [10]. Concentrate granules that are much larger or much smaller than polymer pellets (which are typically 3 – 4 mm in diameter) will favour segregation from them during conveyance and potentially limit their distributive mixing potential in an injection moulding process. Following the production of concentrated forms from a batch mixing unit, the resulting viscous semi-solid was sufficiently pliable to be pressed between two large parallel plates before cooling and setting. Custom sizes and shapes were then cut manually. Following the production of 500 g of concentrate consisting of 88 % w/w treated med-steep GCC in PE wax, the resulting material was screened into three fractions, divided by 2.0, 3.5 and 9.5 mm screens. The resulting materials are shown in Figure 5.8.



Figure 5.8; Product forms of an 88 % w/w GCC/PE wax concentrate. Diameter (mm) as follows; i) $3.5 \leq d < 9.5$, ii) $2.0 \leq d < 3.5$ and iii) $0.0 < d < 2.0$

It was hypothesised that different segregation behaviour would result from using these different forms due to the difference in the sizes of these materials and that this would be reflected in the masses of the plaques produced. In Figure 5.9, these results from three repeated measurements of each size form are displayed.

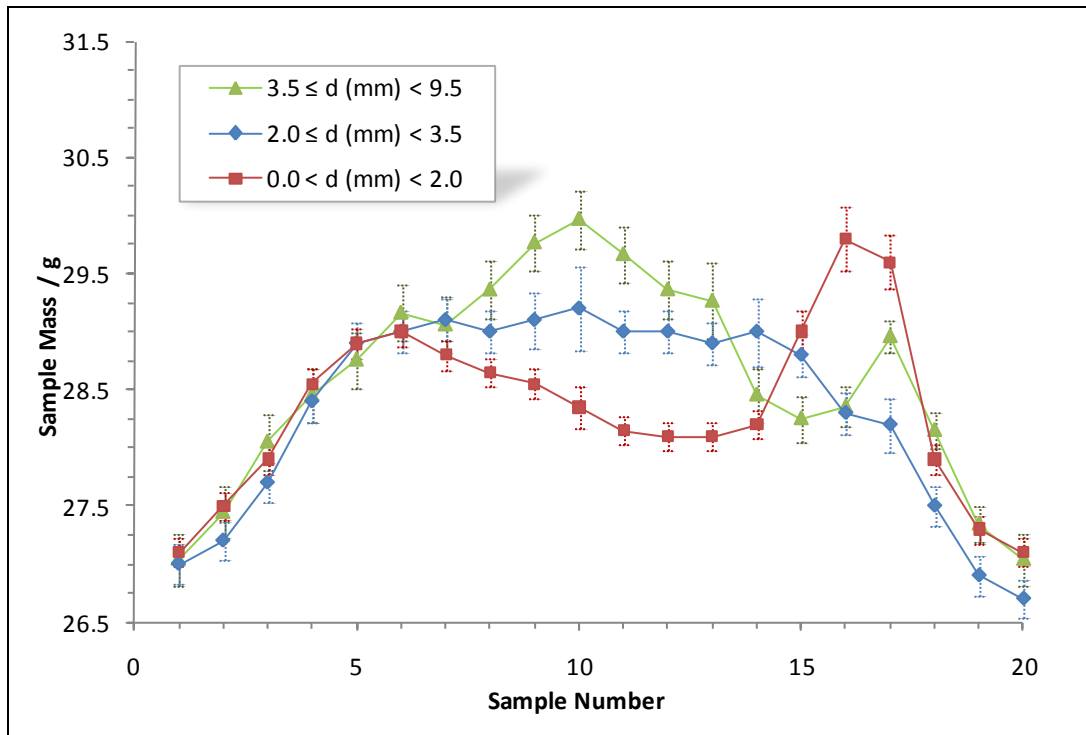


Figure 5.9; Observing mixing during the injection moulding process through consistency in sample masses for three different sizes of (88 % w/w) product form diluted to 15 % w/w plaques. The error bars were obtained from three repeat measurements using the same batch materials

The finest form of concentrate material resulted in the most significant proportion of segregated material reflected by the area under the peak found between samples 15-17. The central of the three sizes of form did not show a significant peak at this stage. However, it was consistently observed that the coarsest of the three forms did. It was believed that this was due their large size causing temporary blockages during the conveyance, relieved by their fracturing. The materials were brittle to the point that they could be easily broken up in the hand (which also resulted in dust and fine particles being produced as the result of the break). This fracture was therefore suspected to lead to the creation of fine particles which would result in a tangible peak of sample mass between samples 16-17 due to the fine material becoming segregated, albeit a smaller quantity than that of

the finest form. The medium of the three sizes was less susceptible to fracturing due to the dimensions of the conveying device and did not fracture to the same extent, did not create as many fine particles and therefore did not show a peak in the latter stages of the injection moulding process. Figure 5.10 shows the resulting masses when diluting the concentrate material to various plaque concentrations between 5 and 30 % w/w. It can be seen that for 20, 25 and 30 % plaques, the segregation phenomenon was again observed, but was not the case for less concentrated products. This was attributed to both a greater statistical likelihood of granule fracture and a greater quantity of resulting fine material, both caused by their greater proportion in the conveyed mixture.

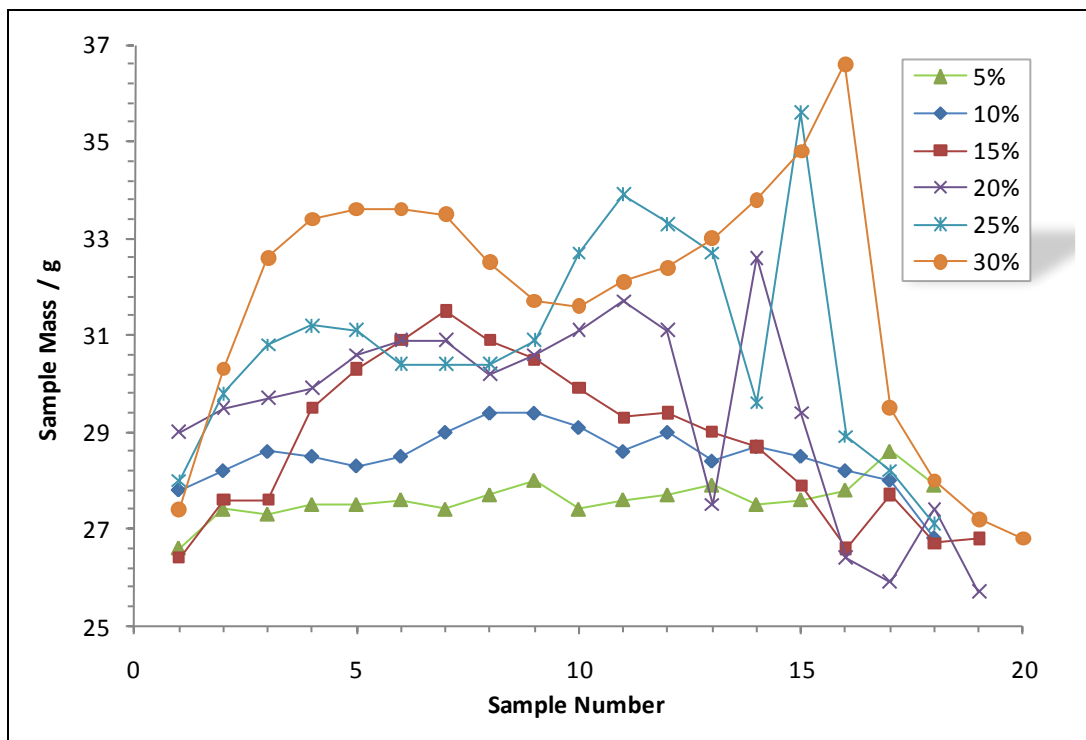


Figure 5.10; The sample masses of an 88 % w/w amorphous GCC/wax concentrate of diameter $2.0 \leq d \text{ (mm)} < 3.5$, when mixed with PP down to the % values (w/w) shown

Replacing a portion of wax in a concentrate formulation with higher-viscosity polymers was performed to improve the strength of the granules to reduce the extent of unwanted fine particles formed by their fracture. Various polymers were shown to be effective at reducing this extent, as seen in Table 5.8, whilst also rendering the granule surfaces to be more similar to those of polymer pellets with which they would be mixed. However, the hardest and toughest materials were naturally of the highest melt viscosities. Not only were dramatic increases in mixing torque detected,

but a correlation was found between increasing mixing torque and their visual appearance following the injection moulding process. These were attributed to inherent physical properties of the replacement materials, most significantly their melt viscosity.

PP Wax Replacement	Torque _{max} / Nm	Manually Friable?	Cut w/ Knife?	Dust?	Vis. P/F	Remarks on Visual Dispersion
PP Wax (none)	42 ± 2	Yes	Yes	Yes	P	Achieved
PP homopolymer	50 ± 3	No	Yes	Yes	F	Small particulates visible
PP copolymer	61 ± 3	No	Yes	No	F	Significant particulates
PP-g-MA	79 ± 5	No	No	No	F	Widespread clumping

Table 5.8; The effects of replacing 25 % w/w of PP wax in an 88 % w/w GCC/PP wax concentrate with various polyolefins on rheology in the melt, hardness and susceptibility to dusting when cooled and visual dispersion when diluted into 15 % w/w plaques

The difference in shape between two granular components was known to affect segregation behaviour during mixing [10]. Furthermore, it was believed that granules of similar shape (and size) to that of polymer pellets would be less susceptible to the fracturing that had been previously observed in forms with a minimally-controlled, amorphous shape. Figure 5.11 depicts a product form that was created following concentrate production by rotational abrasion of the form with PP polymer pellets.



Figure 5.11; A roughly-spherical product form

The performance of these pellets, in terms of the consistency in mass found in plaques that resulted from an injection moulding dilution process, was assessed using various final concentrations between 5 and 30 % w/w. The results are shown in Figure 5.12. It can be seen that the degree of mass consistency is much greater for this concentrate form, compared to the more amorphous form, despite these having equivalent granule strengths. From the results, it was shown that a spherical concentrate form was less susceptible to fracture during conveyance and that a generally greater degree of mass consistency was observed, also due to the greater similarity in shape between the two granular components.

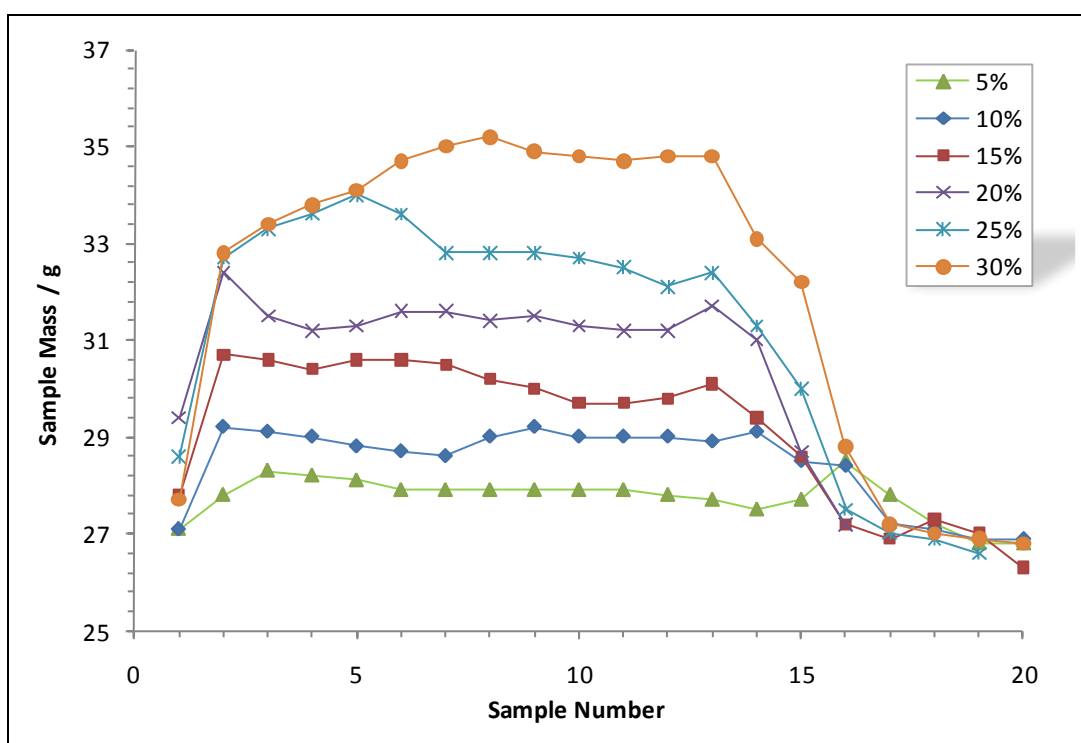


Figure 5.12; The sample masses of an 88 % w/w spherical GCC/wax concentrate of diameter $2.0 \leq d \text{ (mm)} < 3.5$, when mixed with PP down to the % values (w/w) shown

The product had been in development to a point where more subtle variations in the formula and the methods used to prepare it could be suitably investigated. The developed form was indeed used to test a series of different wax binder materials, the majority of which were polyolefin in character. The results from IFWIT measurements from 15 % w/w PP matrix materials derived from 86 % w/w spherical concentrates containing GCC coated with 1.0 % w/w stearic acid bound in various polyolefin waxes are shown in Figure 5.13.

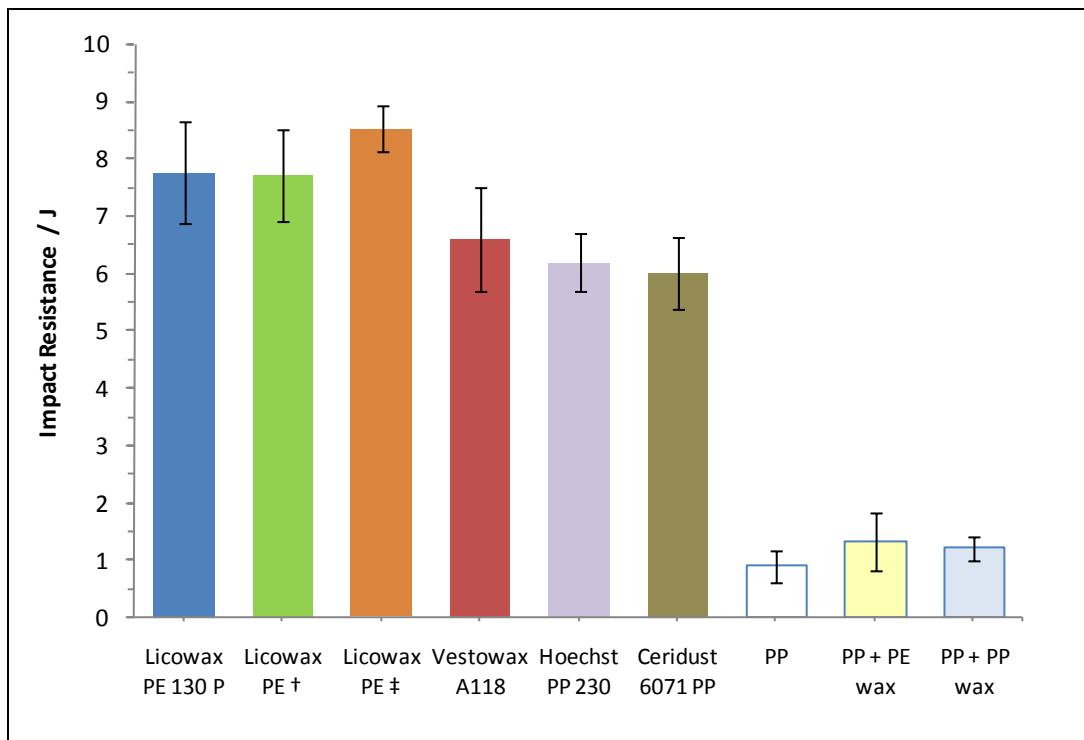


Figure 5.13; IFWIT results for the developed concentrate form to assess the differences in wax binder formulations

Further details of these results including the proportion of brittle fractures encountered and the nature of the selected waxes features in Table 5.9.

Wax Name	Wax Type	Supplier	Impact Resistance / J	Brittle / %
Licowax PE 130 P	PE	Clariant	7.76 ± 0.88	10
Licowax PE †	PE	Clariant	7.71 ± 0.80	20
Licowax PE ‡	PE	Clariant	8.52 ± 0.39	10
Vestowax A118	PE/paraffin	Evonik	6.60 ± 0.91	30
Hoechst PP 230	PP	BASF	6.19 ± 0.49	20
Ceridust 6071 PP	PP	Clariant	5.99 ± 0.63	30
Unfilled Types	Various	-	1.13 ± 0.61	100

Table 5.9; The performance of various waxes as binders of GCC for impact-resistant applications. † 7.1 % w/w of wax replaced with Dow Corning silicone fluid. ‡ 7.1 % w/w of wax replaced with Shin-Etsu KPN 3504 modified silicone.

The results show that each of the selected waxes could be used to successfully distribute GCC in a concentrated form in order to toughen PP when mixed with it during injection moulding. Of the

waxes used, Licowax PE ‡ (with a functionalised silicone fluid additive) arguably performed most favourably, however the cost-effectiveness of using functionalised additives remained to be seen.

5.5 Summary

The concept of producing materials containing high concentrations (> 70 % w/w) of dispersed GCC for the purposes of effective subsequent mineral distribution into a PP matrix during a simple melting and conveying moulding process was proven to be possible using cost-effective processes. Many aspects of formulation of such materials have been considered by using an injection moulding operation with a minimal degree of back-mixing and allowing the most favourably-mixing materials to be more easily identifiable. Measures were performed with a view to pre-empt any difficulties that might be encountered during scale-up including how the material might behave in transit and the degree of control over the mixing process. The minimum requirements of any formulation designed to achieve the same goals have been identified. Firstly this was to use a shear-intensive mixing process to mix particles with a d_{98} finer than 12.9 μm (8.02 μm was the coarsest value that still proved effective), coated in such a way as to make them amenable to cost-effective mixing in concentrations of > 85 % w/w with a low viscosity polyolefin wax, such that the particles are dispersed. Secondly, this was to create spherical forms of diameter roughly equivalent to those of the polymer matrix with which it will be mixed. Thirdly, this was to run an injection moulding process to 'dilute' the material concentration to 10 – 30 % w/w using the target PP matrix material such that it becomes sufficiently toughened to fracture under high rates of strain in a predominantly ductile manner. It has been reasoned that such a material should provide a wide range of advantages to the field of composites formulation and to purveyors of particles that require polymer mixing to become functional.

5.6 References

1. Murphy J. Additives for Plastics Handbook. Elsevier, 2nd ed. 2001
2. Ess JW. Characterization of Dispersive and Distributive Mixing in a Co-Rotating Twin-Screw Compounding Extruder. PhD Thesis, Brunel University, 1989
3. Wypych G. Handbook of Fillers. ChemTec Publishing, 2nd ed. 1999
4. Rothon RN. Particulate-Filled Polymer Composites. Rapra, 2nd ed. 2003
5. Private communication with Johnson Polymers (BASF), 2006
6. Mert M and Yilmazer U. Comparison of Polyamide 66-Organoclay Binary and Ternary Nanocomposites. Adv Polym Tech, 2009; 28(3): 155-164
7. Hess R, Bott R and Richter E. (Clariant) Waxes for Plastics Applications – An Overview. Fillers and Additives for Plastics Conference 2000.
8. <http://additives.clariant.com/pa/internet.nsf> (Accessed 27/5/2009)
9. http://www.specialchem4polymers.com/resources/articles/article.aspx?id=827&or=s528781_101_827&q=ceridust+6071+ (Accessed 13/9/2010)
10. Allen T. Powder Sampling and Particle Size Determination. Elsevier. 2003

CHAPTER SIX

An Automatable Visual
Analysis Technique for
Particulate Characteristics *in
situ* of Thin Polymer Films

FIGURES

Figure 6.1; An example of an original film image acquired by transmission optical microscopy	140
Figure 6.2; An original film before and after applying the optimised processing method	141
Figure 6.3; Particles in the binary image in Figure 6.2 represented as particle size distributions by proportions of A: number and B: volume	143
Figure 6.4; A particle size distribution based on area, acquired from a binary image	143
Figure 6.5; A: Particle resolution according to pixels counted per particle. L and U refer to lower and upper estimates of the lowest true resolution limit (30 and 100 pixels). Terms of the equation; y = diameter, x = pixels, π = constant, π and R = scale ratio (pixels per μm), which was 0.740. B: Particles classified by area, shown inset.....	144
Figure 6.6; Particle resolution according to pixels counted per particle, showing an example of the proportions of particles retained in terms of both volume and number.	145
Figure 6.7; Effects on falling-weight impact resistance by coarse particulate content derived by both statistical inferences on adding a coarse contaminant and direct measurement.....	147
Figure 6.8; SKIZ performed on an image at the previously-optimised brightness level. The image includes an overlay of the original particles	149
Figure 6.9; SKIZ performed on an image at a reduced brightness to improve zone clarity. The image includes an overlay of the particles present at that brightness level	149
Figure 6.10; A: Shows one dimension in which images were optimised. B: Sample data for zone size distribution that was acquired from an image processed at 65 % 'Brightness', as circled in A. (The image is shown in Figure 6.9).....	150
Figure 6.11; Images of the same area of film taken at exposures of 0.25 s and orientations of A: 0° and B: 25°	152
Figure 6.12; As Figure 6.11 B, but taken at 1.0 s exposure	152
Figure 6.13; Processed images from Figure 6.11; identified as A: clustered particulates and B: fundamental particles	153
Figure 6.14; A: Particle resolution for POM instrumentation compared to that shown in Figure 6.5, the slightly higher magnification ($\sim 75\times$ from $50\times$) and therefore R value now allows $6.5 - 12 \mu\text{m}$ resolution as previously defined. B: Particle size distributions at $R = 0.928$ for both particle and particulate phases, by cumulative area.	153

6 AN AUTOMATABLE VISUAL ANALYSIS TECHNIQUE FOR PARTICULATE CHARACTERISTICS IN SITU OF THIN POLYMER FILMS

6.1 Introduction

The size and spatial distribution of particulates within a polymer composite is known to affect several types of its bulk properties, [1-4]. including the ability of the material to resist impact [5]. In certain systems, it is established that a relatively large particle in an otherwise fine composite specimen (such as a single 30 μm particle occurring in a 2 μm dispersion) may act as a flaw; a site where stress will become concentrated under an impact event, acting as the point of crack initiation and greatly lowering the energy that the specimen is able to absorb prior to failure, therefore resulting in brittle fracture behaviour [6]. Theory regarding the effects of particles on the fracture mechanics of composites has been discussed in the thesis and is a subject of ongoing review [7].

There are several ways in which precise particle size distribution (PSD) data may be obtained prior to the incorporation of such particles into a matrix [8]. However, the mixing process they undergo is likely to affect their PSD. This may be due to the properties of the components, the extent of their compatibility or the manner and intensity in which they are combined. Therefore powder-acquired PSD data of the filler become irrelevant, unless elements of these data can be validated *in situ*. In the case of impact resistance, the scale and abundance of the coarsest particles is an especially relevant data element.

For all polymer composites, there are a number of techniques that are currently used directly and indirectly to ascertain *in situ* particle size attributes, such as focussed ion beam (FIB), scanning electron microscopy (SEM) and transmission electron microscopy (TEM) [9]. Each method can provide highly resolved (< 100 nm) particle visualisation, with TEM generally providing magnifications that are 1-2 orders of magnitude higher than SEM or FIB. However, each of these methods requires substantial sample preparation [10]. The combined attributes of preparation time and small fields-

of-view render these techniques statistically ineffective when wishing to acquire a representative PSD from images, especially for micron-scale filler particles. Thereby a need is created for a supplementary technique that can be used to identify meaningful quantities of larger particles. X-ray diffraction (XRD) is commonly performed on composites that comprise filler with a layered structure, such as clay minerals [11]. Usually, a sharp peak at a given angle of incidence, 2θ is used to confirm that the pristine mineral has laminar structure. The same angle range is studied in the composite; an absence of the identified peak implies that the layers of filler are delaminated in the composite structure. XRD does not provide particle visualisation and therefore it is rarely used without being accompanied by another, more robust sizing method. It is also limited to the analysis of filler materials that induce appropriate crystallographic responses, such as those described.

For some polymer composites, an alternative method of particle visualisation is possible, with the use of transmission optical microscopy on thin composite films [12]. The resolution that the technique provides ($< 10 \mu\text{m}$ resolution can be achieved for 50 - 75x magnification images) is inherently inferior to those provided using electron microscopy (capable of nano-scale resolution). However its low cost, simplicity and rapid visualisation of large areas and particles make it ideal in determining the scale and abundance of coarser filler material and fine filler material that is not successfully dispersed by the matrix. Acquired images are not naturally amenable to PSD analysis, without the use of software to perform a degree of image processing. While generic software packages may be able to perform automated processing and analysis, it is necessary to dictate exactly how this processing is performed so that the data can be understood and fully justified and tailored for specific purposes. An example where unmonitored analytical automation can lead to misrepresented data in this case might be where the 'particulate' data pertain in fact to non-particulate entities; such as bubbles, film-surface defects and irregularities, or any other extraneous visual contamination that has been imparted to the sample during its production, handling or preparation. While the provenance of these contaminants may be easy to attribute by eye,

unmonitored image processing is not necessarily able to do likewise, unless the visual characteristics of the unwanted entities are somehow understood by the software program.

A method was required to perform the task of image analysis to study various particle attributes, utilising simple and user-friendly commands in freely-available, public-domain software and a programmable numeric spreadsheet such as Microsoft Excel. The Results section of this Chapter describes the method development, implementation and its potential for automation.

6.1.1 Material Requirements

There are two general requirements that must be met of the composite to allow the presented technique to become feasible. The first of these is a physical requirement; the polymer matrix must be amenable to thin film production, thereby allowing film samples to be generated. If such amenability is poor, the filler may be incorporated into an alternative matrix. However, this is only advisable with careful matrix selection; there must be sufficient evidence that the replacement matrix induces the same effects on filler particles as the former, to ensure the validity of the assumptions that are made. The chemical and physical properties of the replacement matrix must induce the same degree of dispersion on the filler and also be amenable to film production. A relatively high melt viscosity (corresponding to a melt flow rate less than 6 g / 10 minutes at 230 °C, under a 2.16 kg load as a rule-of-thumb) of the polymer matrix is recommended for a continuous film-making procedure. The high melt viscosity is necessary in order for the material to retain some structure in its molten state thereby allowing it to be uniformly blown or cast into a thin film. The second of the general requirements is an optical requirement; the films must have sufficient clarity to enable optical microscopy by transmission. There is also a limitation on particle size (at the fine end of the distribution) due to particle resolution available to optical microscopy. This depends on the quality of the film, the magnification and the quality of the lens and for very fine particles will become limited in accordance with the wavelength of light. The filler loading also needs to be sufficiently low to enable the transmission of light through the film. The threshold value of loading

that provides this level of clarity depends on the propensity of the filler to pigment the composite film, the extent of crystallisation within the film and also the film thickness. Finally, implementations of assumptions required to predict non-spherical particles have proven successful elsewhere [13].

6.1.2 Types of Visual Analysis

Typical PSD characteristics that are often quoted with laser light scattering data (such as mean and median particle size and the distribution polydispersity) may be obtained from *in situ* visualisation. However, there are further particulate and film characteristics which are obtainable from the images that the technique provides, which are relevant to this thesis. These are; firstly, the scale and abundance of particularly coarse particles; secondly, the visual consistency of the film and thirdly, the size of particle aggregates (or any other forms of particle clusters) relative to the size of individual particle crystals, as measured *in situ*.

6.2 Aims of this Chapter

The four mentioned types of *in situ* property are to be explored for thin polypropylene films comprising low concentrations ($\leq 5\%$ w/w) of calcium carbonate filler, so that relevant properties relating to the size and dispersion of particles following polymer mixing could be representatively obtained. This is to be done by first preparing the materials, developing a method to capture and process the data and finally considering amendments to this method to make it more effective and more broadly applicable.

6.3 Hypothesis

It was hypothesised that by lowering the mineral concentration of GCC/PP composites from an application concentration to a diluted form, and then converting their form into thin cross-sections of film, representative particle and mixture properties could be obtained from visual characteristics of the film that would have otherwise been inaccessible, considerably time-consuming to acquire or unrepresentative of their actual state. Furthermore, it was hypothesised that the ability to separate different phases according to their optical properties would play a crucial role in determining the success of these techniques.

6.4 Sample Preparation

Various GCC powder samples were stored for a minimum period of 24 hours before being compounded into PP at 25 % w/w. The barrel temperatures from input to die were 170/175/175/180/185/200 °C, operating under a pressure of 6.9 ± 0.2 MPa with an average torque of 35 % at 440 rpm. A portion of the resulting masterbatch pellets were stored for 24 hours under vacuum at 50 °C before being injection moulded into 60 x 60 x 2 mm impact test specimens. The remaining masterbatch pellets were let down with additional PP of the same type to 5 and 2 wt. % independently using twin-screw extrusion, under similar conditions to the masterbatch preparation. Let-downs were cast as films (kneader extruder and roll mill - Collins, Germany) with the extrusion barrel temperatures steadily ranging from input to die between 200-240 °C, a melt temperature of 217 ± 1 °C, a barrel pressure of 6.2 ± 0.1 MPa and a current of 3.8 A.

6.5 Method Development and Results

6.5.1 Image Capture

Figure 6.1 shows a typical grey-scale film image acquired using a simple light microscope.



Figure 6.1; An example of an original film image acquired by transmission optical microscopy

The films were visualised using transmission optical microscopy (SMZ-U, Nikon JPN) and images at 50 and 75 x magnification were captured (DS-Fi1 digital sight, Nikon and NIS-Elements F software, Laboratory Imaging, CZ).

6.5.2 Image and Data Processing

Any digital processing technique that requires one phase to be separated from the rest can be re-drawn as a binary image; i.e. a pixel is labelled with either a 0 (white, representing the background) or a 1 (black, representing the phase of interest). An optimum brightness for acquiring the most accurate images was identified. The brightness range was limited by low particle counts at one extreme and sensitivity to non-particulate entities at the other. Details of how the optimisation was performed are featured in the Appendix.

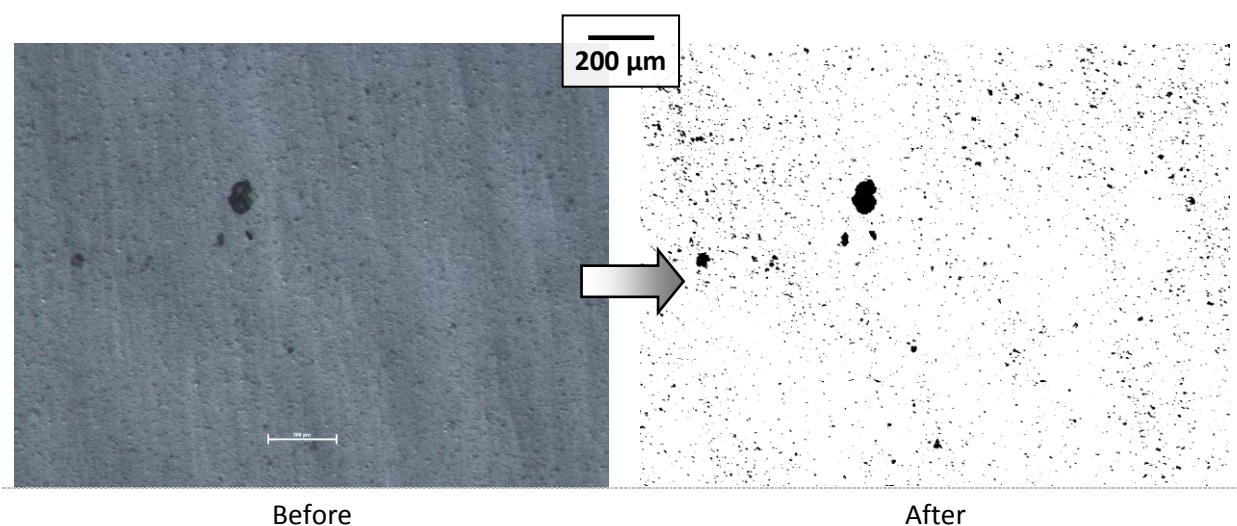


Figure 6.2; An original film before and after applying the optimised processing method

When converted to an appropriate binary form, a digital image becomes amenable to rapid computational processing, allowing for a range of particle properties to be derived; from simple percentage calculations, to particle recognition and size approximations, through to use of complex algorithms to quantify their distribution. Public domain image analysis software (ImageJ, National Institute of Health, US) was used to perform these operations, which are described in sections I-IV below.

(I) Particle Size Distribution

This is a measure of the relative concentration of particles within defined size groups across the detectable size range. For particles of the same material, the relative concentrations can be expressed by number, surface area, volume or some other type of proportion. Although volumetric measurements of two dimensional data must depend on algorithms that make some assumptions of particle shape to form the third dimension (which is not true for number distributions), they give the greatest degree of weighting to the coarsest particles, which is of most interest in this case. To explain this further, one might imagine the distribution of a beach ball (1 m in diameter) together with 999 grains of sand (each 2 mm in diameter). A number-based distribution would allocate an extreme minority (0.1 %) of the particles as having a diameter of 1 m, whereas a volume-based distribution would describe the same size as accounting for an extreme majority (99.9992 %). This is obviously an exaggerated example, but since both interpretations of proportion are accurate descriptions of the distribution in their own right, care must be taken in the application of such data to practical situations. In the case of identifying relative measures of the coarsest particles, volume-based analyses were selected.

With the images acquired and processed as per Figure 6.2, a list of particles with their pixel areas was obtained. These were converted from pixels² into μm^2 using a pre-calibrated scale-bar embedded in each image. By assuming particle circularity, these values were converted into their equivalent circular radii and diameters, in μm . Size ranges were defined into which each particle was placed by its diameter. By assuming particle sphericity, the mid-points of each size range could be converted into volumes in μm^3 and multiplied by the total number of particles within that range to derive a sub-total volume for each range. These were summed to form a total volume and each defined range was expressed as a volume percentage of this total. Graphs were then plotted using volume proportion plotted against the original diameter mid-points. Results for volume and number distributions are shown in Figure 6.3.

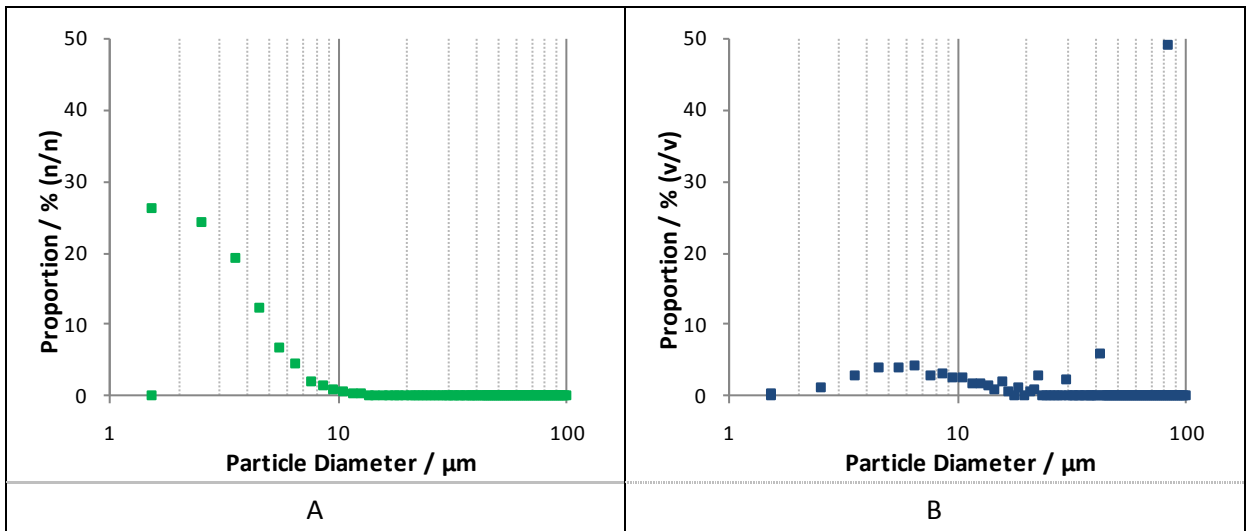


Figure 6.3; Particles in the binary image in Figure 6.2 represented as particle size distributions by proportions of A: number and B: volume

Number distributions derived in this way from two-dimensional images were inherently more accurate than volume distributions because they did not rely on assumptions to project a third dimension. However, they could not provide useful data for singular coarse particles, whereas volume distributions did so markedly. Area-based distributions were derived by summing the originally measured areas, offering both accuracy and applicability of the data to a practical situation. The data for this distribution is shown in Figure 6.4.

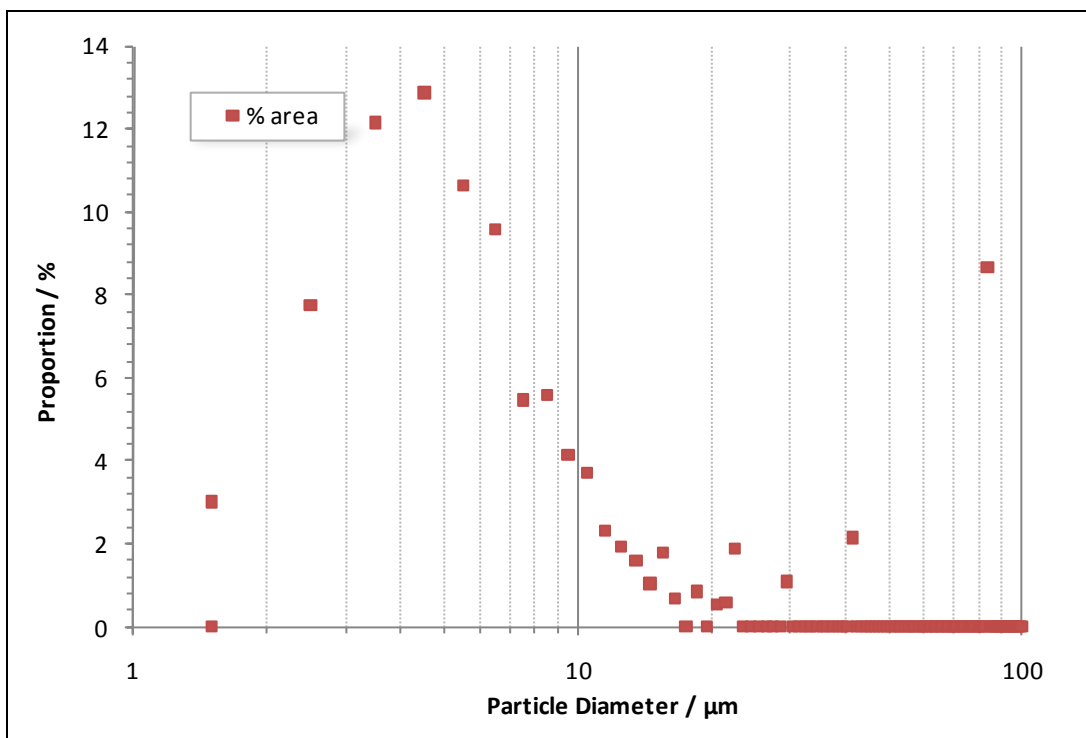


Figure 6.4; A particle size distribution based on area, acquired from a binary image

Area-based distributions were found to provide a noticeable peak for volume-dominating particles without compromising the clarity of the remaining data and being based on only a minimal degree of assumptions. In these examples, it can be seen that the largest particle (which was equated to a circular diameter of 83 – 84 μm) accounted for 0.02 % of the total particle number, 8.7 % of the total particle area and 49.1 % of the total projected particle volume. Area was regarded as the most useful measurement for the reasons described. However, performing these operations in a numerical spreadsheet allowed such rules for analysis to be easily altered, even retrospectively, if required.

Using image analysis to obtain PSD relies on a sufficient degree of particle resolution. In the example above, fine particle sizes are shown despite not all of the data being resolved. The number of pixels required for appropriate particle resolution was estimated to be between 30 and 100 pixels, which corresponded to a particle diameter of approximately 8 – 15 μm , as shown in Figure 6.5 A [14].

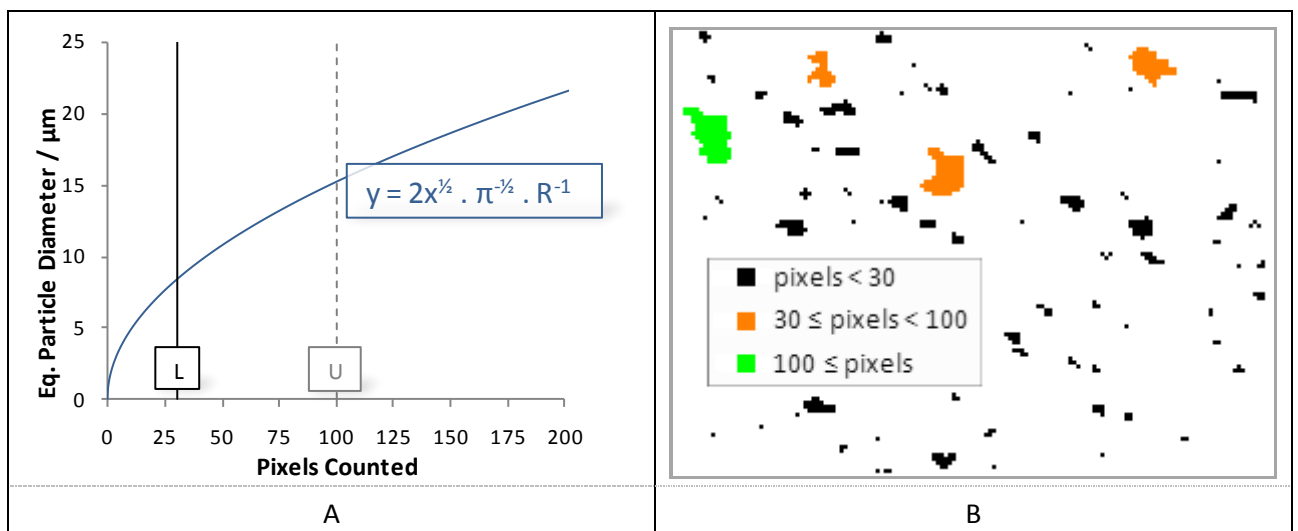


Figure 6.5; A: Particle resolution according to pixels counted per particle. L and U refer to lower and upper estimates of the lowest true resolution limit (30 and 100 pixels). Terms of the equation; y = diameter, x = pixels, π = constant, π and R = scale ratio (pixels per μm), which was 0.740. B: Particles classified by area, shown inset.

Maximum accuracy is only available when the entire size distribution falls within detectable range; it declines with the increasing proportion of non-detectable particles. Therefore in the context of this

thesis, this created a need for alternative methods of measurement because there was a known particle content that existed beyond the resolution boundaries of the technique (see parts II-IV).

Figure 6.6 demonstrates the proportion of particles (in number, area and projected-volume) that were omitted due to known resolution limitations, at both the lower and upper estimates of this value and includes the equivalent diameter of the particles, as previously calculated. The graph shows that by imposing the lower of the two estimates of resolution (30 pixels required), the proportion of original particles defined as detectable account for approximately 80.1, 34.1 and 3.8 % of the total projected volume, area and number respectively. Imposing the stricter estimate (100 pixels required) resulted in these reducing to 65.8, 15.2 and 0.4 % of the volume, area and number respectively. (Clearly the particles that were not detected could not contribute to these figures). Discontinuities in the data were identified in several areas. Firstly, one occurs between 0 – 1 pixels which was due to a pixel being by definition the smallest countable unit of a digital image. Secondly the weighting of the distributions can magnify the data discontinuity, which was observed especially at the coarse end of the volume-based distribution curve.

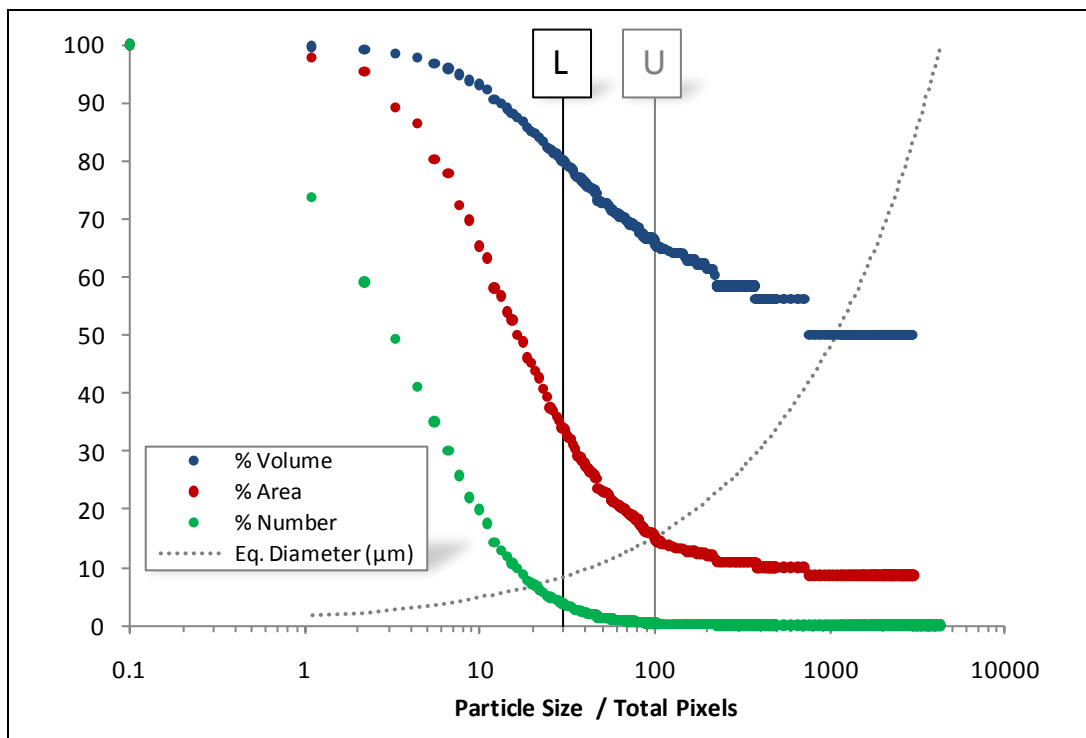


Figure 6.6; Particle resolution according to pixels counted per particle, showing an example of the proportions of particles retained in terms of both volume and number.

This discontinuity occurs because particles have a specific pixel size, which when exceeded (on the x-axis here) causes the particles of that size to be omitted. When those particles account for a significant proportion of the total proportion, steep steps were observed such as one occurring between 750 -800 pixels and another more significant one between 2900-3000 pixels. The same effect can be seen for the area distribution curve, albeit to a reduced extent. A final observation about using these films to acquire a particle size distribution is that the film thickness affected the results; an effect which can be seen in Figure 6.1. The thinnest cross-sections of film were able to transmit more light compared to thicker cross-sections of equal area, therefore appearing brighter in the original image. The way in which the images were optimised and made binary meant that fewer particles were detected in these areas, since their lighter hue rendered them more prone to visual omission when raising the brightness threshold. While this effect could be overcome (for example by suspending the film samples in a fixed depth of media whose refractive index matched that of the composite polymer), it must nevertheless be considered, especially for size measurements where a significant fraction of the distribution is close to the resolution limit of the instrument. Finally, it must be mentioned that the particular image processing method cannot detect any particles that have fully transmitted the incident light, thereby not becoming separated from the film phase.

(II) Coarse Particle Content

A technique was developed to account for situations where the limitations in resolution could significantly affect the accuracy of the data acquired at the finest end of the particle size range but where a measure of the coarser particles was nevertheless required. The occurrence of particles with a diameter $> \sim 20\text{-}30\ \mu\text{m}$ is highly significant to the field of fine filler treatments for the improvement of composite toughness. A useful quantification would be the frequency of such particles that were detected over a given area of film; which could in turn be projected into a volumetric concentration and compared with mechanical test data. Such a property is measurable from film images acquired by optical microscopy (and processed in a very similar way to that described above). The lack of resolution might mean that a tight collection of small particles could

be mistaken for a large particle. However, it was thought that such a collection would still act as a mechanical flaw within a mineral/polymer composite and the extent to which such entities are present is as relevant to the field as are coarse, yet solid entities.

Using image analysis software, a particle list was exported from a binary image (such as that shown on the right in Figure 6.2), with a minimum size below which data would not be reported. The size could be selected as appropriate. Applying the same approximations and formulae as above, the number of pixels for this minimum was set to both 172 and 385 to correspond to equivalent circular particle diameters of 20 and 30 μm respectively (at a scale of 0.74 pixels / μm). The size of these particles together with their frequency was collected over ten randomly-sampled sections of film per sample. The results for particles > 30 μm in film that contained 5 % w/w calcium carbonate were compared to impact resistances that were measured at 30 % w/w from various specimens that were derived from the same original source material. The relationship between these two observations is demonstrated graphically in Figure 6.7.

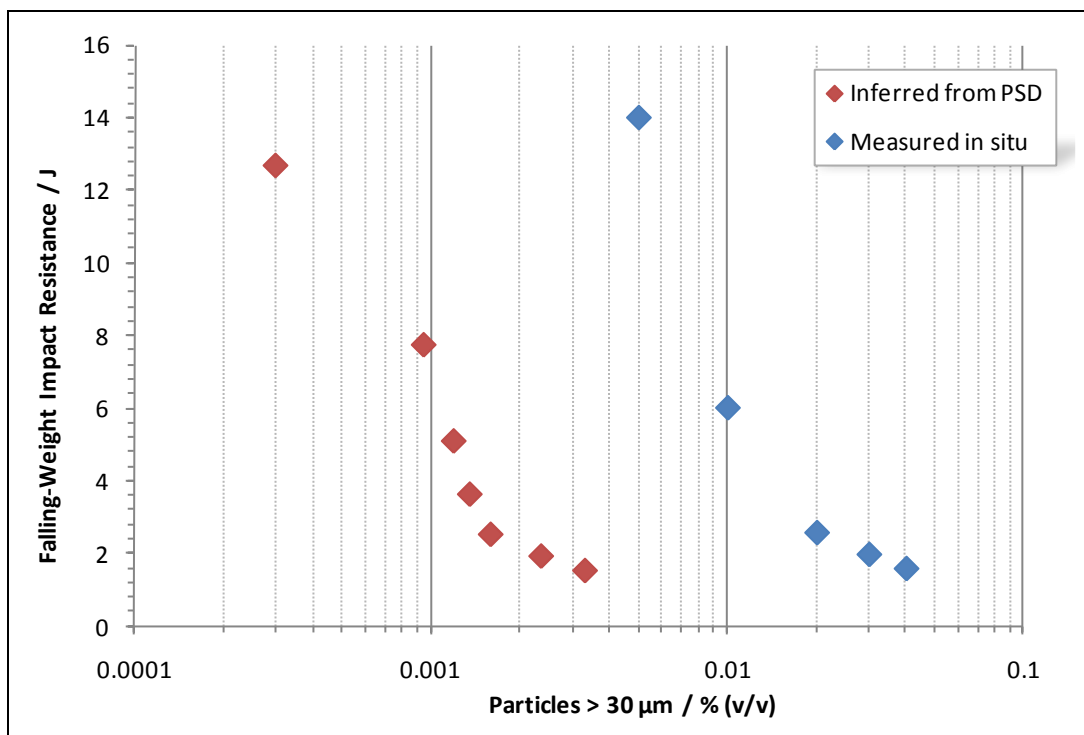


Figure 6.7; Effects on falling-weight impact resistance by coarse particulate content derived by both statistical inferences on adding a coarse contaminant and direct measurement

As well as *in situ* data, also shown in the figure is the volumetric concentration of particles $> 30 \mu\text{m}$ that were calculated to have been present following a deliberate replacement of small proportions of otherwise fine, dispersing calcium carbonate with a coarser grade of particles (measuring $0 - 200 \mu\text{m}$ in diameter). The results appear to show that despite the same general trend, coarse content as inferred from statistical methods underestimated the sensitivity to coarse particles that were subsequently identified *in situ*, by approximately one order of magnitude. This discrepancy was attributed to inaccurate statistical assumptions, including the alteration in particle size distribution that has been shown to occur during mixing.

(III) Film Homogeneity

There are certain applications to which visual uniformity of films is an important property. This could be any visual uniformity, such as having an even thickness or an even particulate dispersion. For situations where accurate and complete particle size distribution data cannot be achieved using optical microscopy (such as that described above) it may still be useful to quantify the general visual uniformity. Skeletonisation by influence zones (SKIZ) is a type of computational algorithm that is available to many image analysis software packages, including ImageJ. Operating on binary images it, in short, identifies “zones” in an image that are visually similar, generating the boundaries that define these separate zones.

Before performing the SKIZ process, ImageJ required the image to first be inverted (pixels assigned a ‘0’ became ‘1’ and vice versa, so that the background became black and the particles became white) so that the zones could be drawn as described. A binary film image (as in Figure 6.2; optimised for particle count and particle data accuracy) was inverted and skeletonised and the outcome (superimposed over the original binary particle image) can be seen in Figure 6.8. Although the image appeared to differentiate the regions of localised particle concentrations effectively, it was thought that the magnitude of zone area differences (‘zone clarity’) could be improved without losing any significant amount of the degree to which the original image was represented.

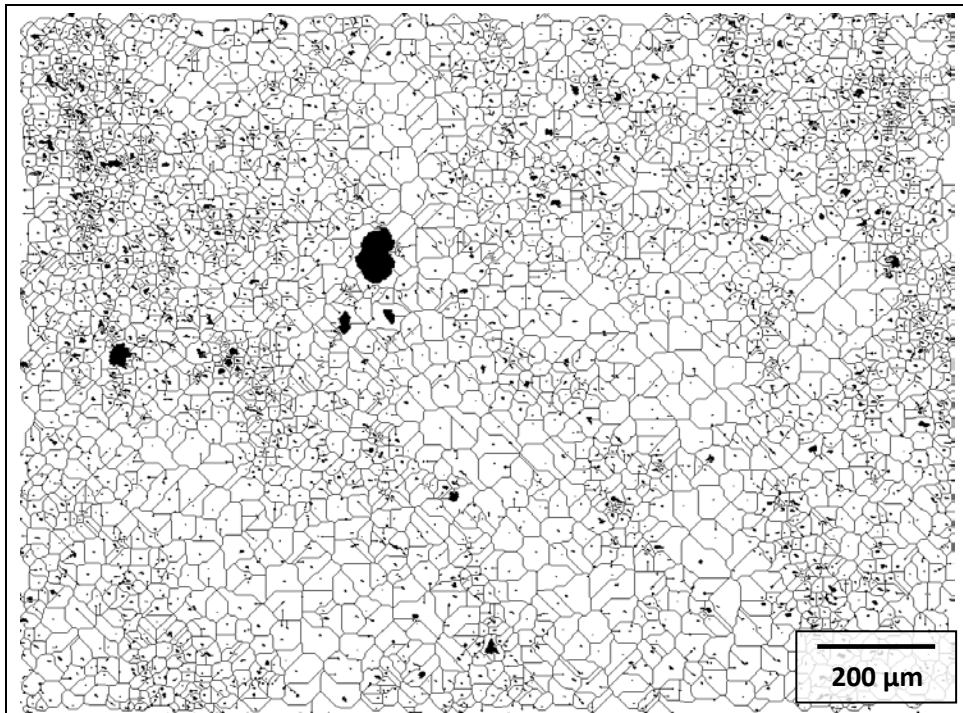


Figure 6.8; SKIZ performed on an image at the previously-optimised brightness level. The image includes an overlay of the original particles

Figure 6.9 shows the results of applying the same SKIZ process to an image with a brightness level that had been optimised for zone clarity, zone count, analysis time and relevance of its data.

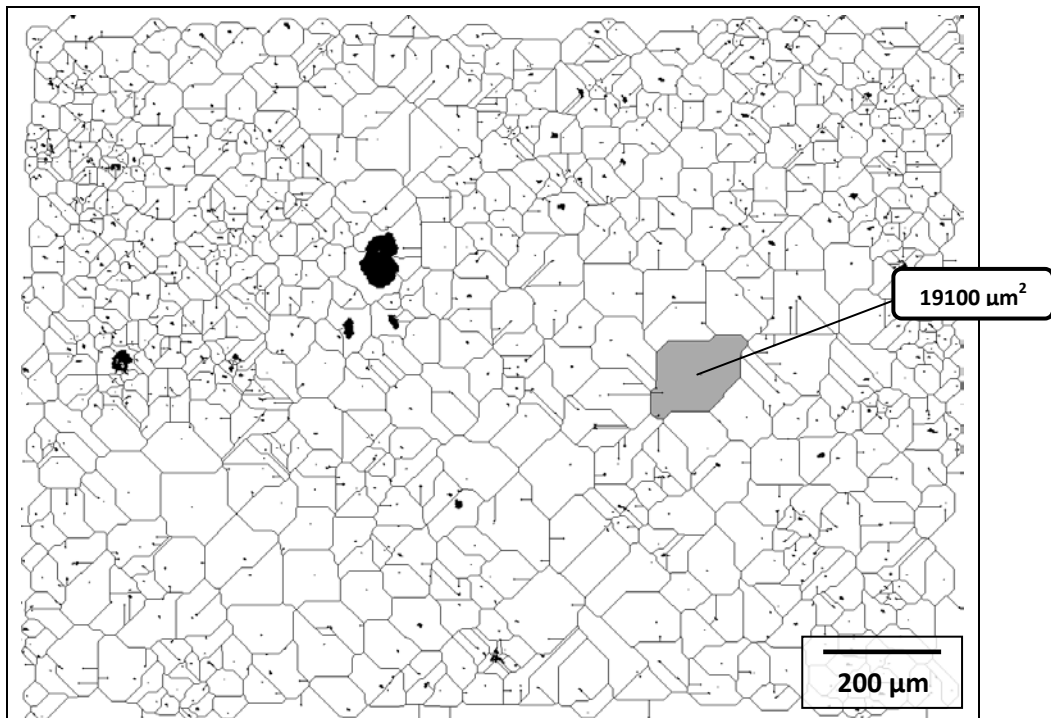


Figure 6.9; SKIZ performed on an image at a reduced brightness to improve zone clarity. The image includes an overlay of the particles present at that brightness level

There was no default code that came with ImageJ that could count the zone size distribution, so such a code was developed from new. In short, this would systematically transcend a row selecting every fifth pixel in that row and counting the zone area in which this pixel was placed. The zone area, along with the central position of that zone (in x-y coordinates on the image canvas) would be exported as one output line. At the end of the row, the same process would begin on the row ten pixels down (i.e. the y coordinate) from the first, off-set by five pixels across (i.e. on the x coordinate). This would continue until the entire canvas had been covered; just short of 25,000 measurements. These spacing dimensions were a compromise between computational demand (and therefore analysis time) and precision. The list of zones would then be subjected to various filtering processes to omit repetitions of the same zones, single-pixels entities (an unwanted by-product of the SKIZ algorithm) and the counting of the entire image as one 'zone', which could not otherwise be avoided. Further details of this method development, along with the image optimisation procedure can be found in the Appendix. A sample relationship upon which the optimisation was based feature in Figure 6.10, along with sample data.

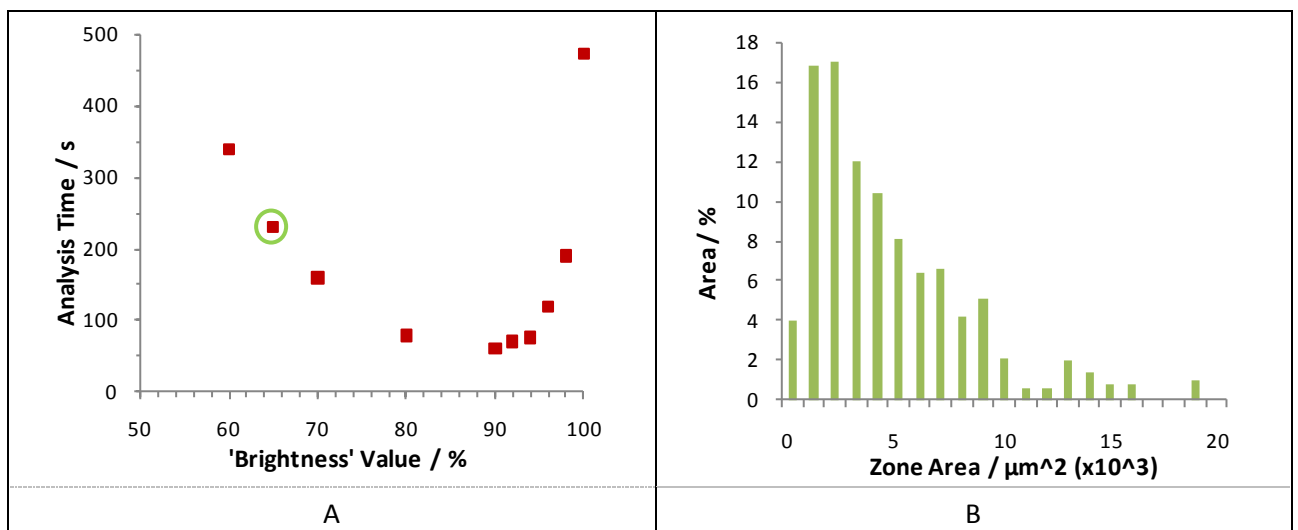


Figure 6.10; A: Shows one dimension in which images were optimised. B: Sample data for zone size distribution that was acquired from an image processed at 65 % 'Brightness', as circled in A. (The image is shown in Figure 6.9).

For cases where there is a high degree of control over the uniformity of the thickness of films comprising fine, well-dispersed particles, this technique becomes redundant. However, in situations where the surface chemistry of particles or other additives could affect the film consistency and/or

where large proportions of particles are too fine to be resolved then this type of measurement could prove useful. It remains the case that no attempts have as yet been made to separate light-transmitting filler particles from the transmitting film or from non-transmitting particle clusters.

(IV) Referential Cluster Size

Each of the methods that have so far been described in this Chapter has relied on the principle of visual phase separation simply by the degree of transmission of unfiltered light. This section aims to explore a supplementary separation process that has minimal effect on the overall costs and time required to perform the analysis. It was hypothesised that two translucent phases could be effectively separated for the purposes of visual analysis, as well as being separated from what were originally considered to be the sole particle phase, and that by doing so, useful information regarding thin composite films could be acquired.

Polarised optical microscopy (POM) can be used to study crystallinity within a polymeric structure, in cases where the proportion of crystallinity is particularly high, such as in polypropylene homopolymers [15]. The behaviour of light is a complex subject, beyond the scope of this thesis [16]. Therefore, only its outcomes (with some relevant simplified theory) are described here. A polarising filter ensures that the incident light is aligned according to the angle at which the filter is positioned. Translucent materials (including both polypropylene and calcite crystals) can affect the manner in which the light that passes through them behaves, as according to their refractive indices and other optical properties. Crystalline regions of polymer induce different optical effects to amorphous ones. Their respective molecular alignments consistently affect how they transmit light in both direction and wavelength. High degrees of molecular alignment in crystalline regions allows for distinct patterns of light to result, making it possible to identify these regions simply using a lens, a light source and a polarising filter. For materials with lower crystallinity such as mostly or completely amorphous ones, these optical effects become reduced or completely absent. For non-polarised incident light, the differences in crystallinity cannot be detected in this way.

A translucent material that does not rotate light or one that does so in a different manner to the material in which it is suspended can be visually separated from this phase with the appropriate use of polarised light. Figure 6.11 shows optical separation of two particulate phases in PP copolymer.

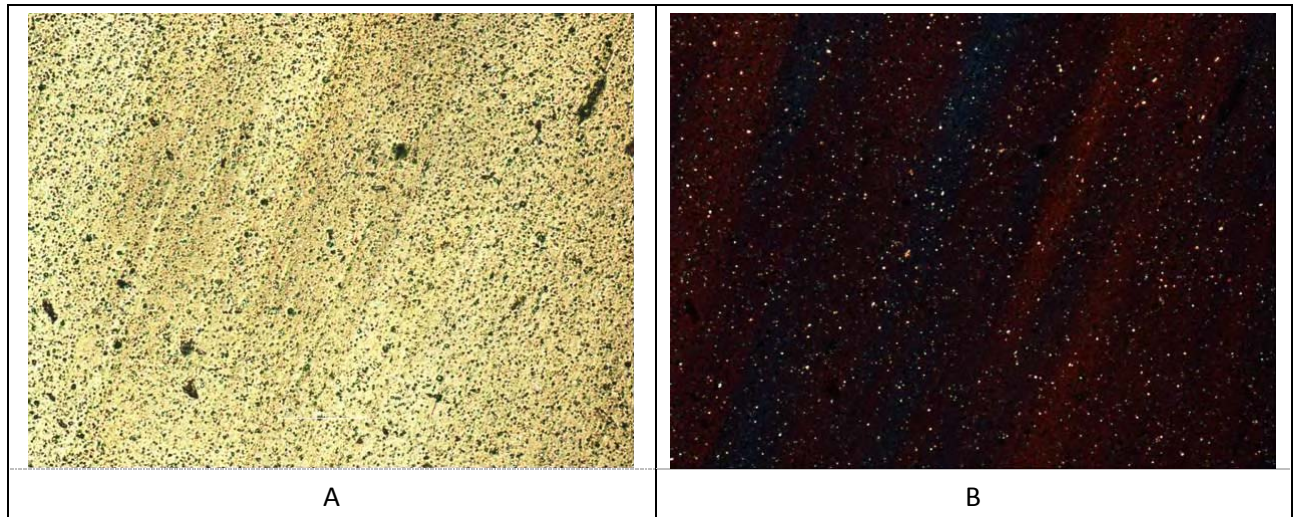


Figure 6.11; Images of the same area of film taken at exposures of 0.25 s and orientations of A: 0° and B: 25°

Figure 6.12 shows successful simultaneous multiple-phase separation by optical properties alone.

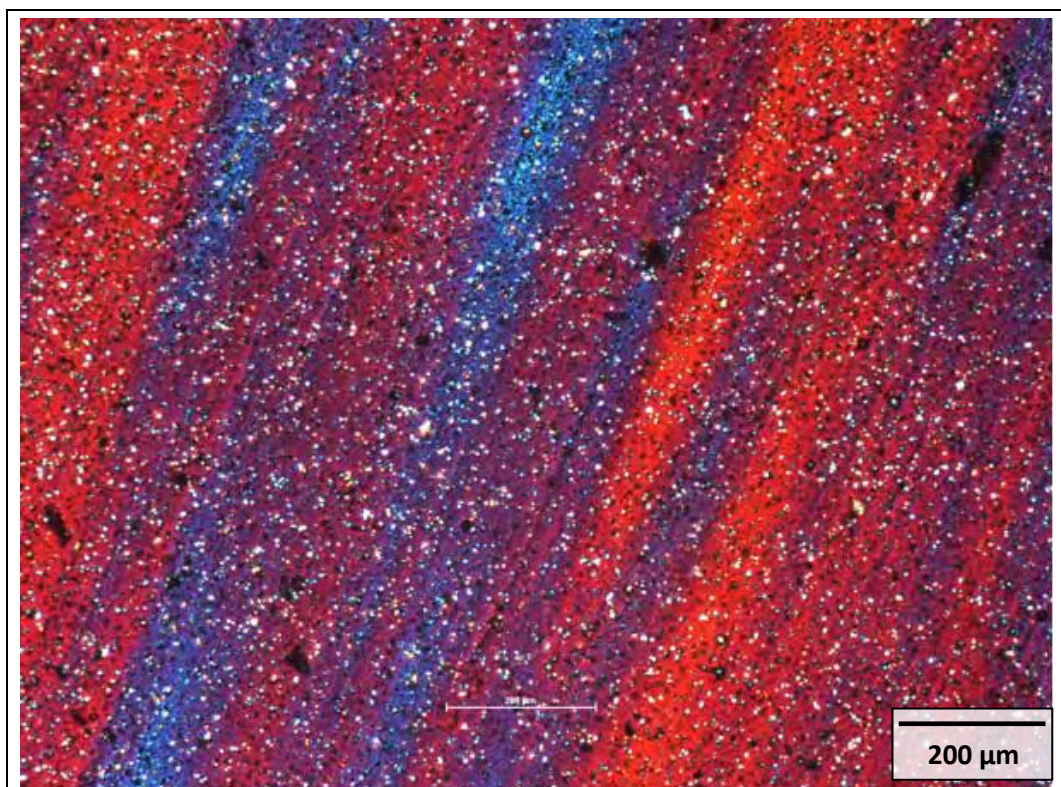


Figure 6.12;As Figure 6.11 B, but taken at 1.0 s exposure

The images show that some particles allowed the transmission of plane-polarised light to occur through them and some did not, and that in both cases this was independent of the light incident orientation (see Appendix for additional data). From these observations, these particles were assigned as being fundamental calcite crystal particles and aggregated cluster particulates respectively. The original images were processed (described previously) and shown in Figure 6.13

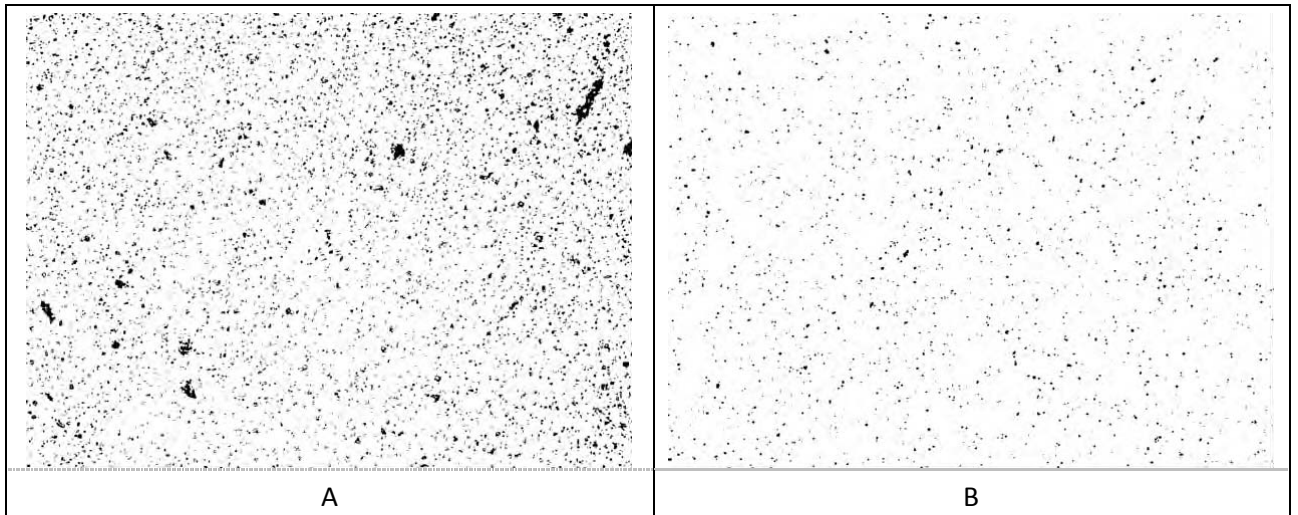


Figure 6.13; Processed images from Figure 6.11; identified as A: clustered particulates and B: fundamental particles

Size distribution data by area for both classes of particulate entity are shown in Figure 6.14 B.

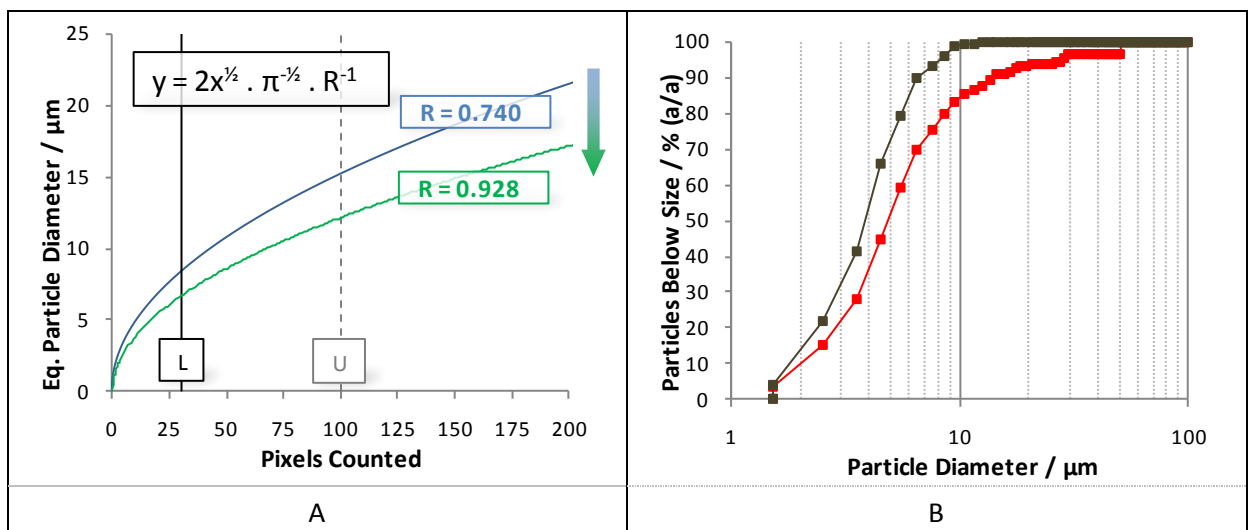


Figure 6.14; A: Particle resolution for POM instrumentation compared to that shown in Figure 6.5, the slightly higher magnification ($\sim 75\times$ from $50\times$) and therefore R value now allows $6.5 - 12 \mu\text{m}$ resolution as previously defined. B: Particle size distributions at $R = 0.928$ for both particle and particulate phases, by cumulative area.

From the size distributions of the two separate types of particle both taken *in situ* from the same image, a referential measurement can be derived. For example, the size below which 90 % of their total respective areas occur (i.e. a d_{90} measurement) could be compared as a factor. This would be a measure of the extent to which particles have formed clusters. In this case, the clustering factor determined in this way was calculated as 2.13 in this particular example. It is predicted that this measurement should provide visual film characteristics of composites with greater levels of repeatability and reproducibility due to its *in situ* and referential nature.

6.6 Summary

The following aims to contextualise each identified measurement within the thesis; analysing fine GCC in films at low concentrations to further understand the effect of processing on particles and the failure mechanisms during impact of the original higher-concentration polymer.

The fundamental particle sizes of the calcium carbonate grades used in the project are quite fine. In many cases, the majority of the particles are indeed finer than that which may be accurately detected by transmission optical microscopy. Therefore in this particular case, values of the overall PSD properties (for example mean and median size and the dispersity of the distribution) can only pertain to the fraction of particles that exceed the resolution limit (which was identified as being between 6.5 – 8 μm , depending on the apparatus), thus rendering these PSD values unintentionally selective and unrepresentative. Little can be interpreted from standard processed images regarding the level of dispersive mixing that the particles have undergone in the polymer. However, the scale and abundance of particulates of a threshold (minimum) size which is greater than that determined to be detectable resolution minimum can be fully representative. This intentional selectivity is particularly useful for the thesis; it is these very entities which have been proven to act as sites of stress concentration and therefore crack initiation of filled composites during an impact event.

The analysis of the size and distribution of skeletonised zones can reveal information about the distributive mixing of the particles within a film, regardless of the particle size and instrument resolution. Therefore it should prove useful for the thesis, in situations where fine particle structure cannot be fully resolved. It is however not independent from direct particles, and an identified 'zone' may in fact be a particle itself, especially when it is relatively large. The optical properties of the various phases that were demonstrated rendered them amenable to the referential size analysis technique using a polarised filter. Although the finer fraction of filler will remain undetected, the proportions of fundamental particles and collective clusters can nevertheless be interpreted to give information regarding the relative extent to which particle clustering has (or has not) occurred on mixing. There is potential to automate the entire analytical process for any of the techniques described, both in the collection of images and especially their computational analysis. Computational code to achieve parts of this was heavily used, with the most relevant parts being presented in the Appendix.

Completely automatable analytical techniques for use with polymers comprising low concentrations of filler have been presented. It is predicted that those presented in parts I-III could be adapted to many combinations of suitable materials, whereas part IV would be limited to translucent filler particles.

6.7 References

1. Lange FF. Interaction of a crack front with a second-phase dispersion. *Philos Mag* 1970; 22(179): 983-992
2. Song M, Wong CW, Jin J, Ansarifard A, Zhang ZY and Richardson M. Preparation and characterization of poly(styrene-co-butadiene) and polybutadiene rubber/clay nanocomposites. *Polym Int* 2005; 54(3): 560-568
3. Fu SY, Feng XQ, Lauke B and Mai YW. Effects of particle size, particle/matrix interface adhesion and particle loading on mechanical properties of particulate-polymer composites. *Composites Part B* 2008; 39(6): 933-961
4. Rahman IA, Vejayakumaran R, Sipaut CS, Ismail J and Chee CK. Size-dependent physicochemical and optical properties of silica nanoparticles. *Mater Chem Phys* 2009; 114(1): 328-332
5. Saminathan K, Selvakumar P and Bhatnagar N. Fracture studies of polypropylene/nanoclay composite. Part II: Failure mechanism under fracture loads. *Polym Test* 2008; 27(4): 453-458
6. Bartczak Z, Argon AS, Cohen RE, and Weinberg M. Toughness mechanism in semi-crystalline polymer blends. *Polym J* 1999; 40(9): 2331-2365
7. Kinloch AJ and Young RJ. *Fracture Behaviour of Polymers*. Applied Science Publishers. 1983
8. James P. *Principles, Methods and Application of Particle Size Analysis*. Cambridge University Press. 2007
9. Zhu YD, Allen GC, Adams JM, Gittins D, Herrero M, Benito P and Heard PJ. Dispersion characterization in layered double hydroxide/Nylon 66 nanocomposites using FIB imaging. *J Appl Polym Sci* 2008; 108(6): 4108-4113
10. Egerton RF. *Physical principles of electron microscopy: an introduction to TEM, SEM, and AEM*. Springer. 2005
11. Yang QQ, Guo ZX and Yu J. Comparison of polyamide 66/montmorillonite nanocomposites prepared from polyamide 6 and polyamide 66 based masterbatches. *Chin J Polym Sci* 2008; 26(6): 689-696
12. Sawyer LC, Grubb DT and Meyers GF. *Polymer Microscopy: Characterization and evaluation of materials*. Springer, 3rd ed. 2008
13. Igathinathane C, Pordesimo LO, Columbus EP, Batchelor WD and Methuku SR. Shape identification and particle size distribution from basic shape parameters using ImageJ. *Comput Electron Agric* 2008; 63(2): 168-182
14. Private communication with Malvern Instruments, 2009
15. Spencer M. *Fundamentals of Light Microscopy*. Cambridge University Press. 1982
16. Hecht E. *Optics (International Edition)*. Pearson Education, 4th ed. 2003

CHAPTER SEVEN

The Preparation and Testing of Finer Filler

FIGURES AND TABLES

Figure 7.1; The specific materials, processes and analyses used in this Chapter	159
Figure 7.2; The effect of energy consumption of the impeller motor on the median particle diameter (by LLS) of GCCs using two different sizes of grinding media, m1 and m2. Logarithmic axes were used to improve clarity of data, while maintaining a reasonable experimental range.....	162
Figure 7.3; The particle size distributions of spray-dried, chemical-free GCC samples in A; water and B; n-hexane. In each case, the dried samples were compared to their jet-milled derivatives.....	166
Figure 7.4; A graph to demonstrate the effect of shear rate on shear stress for a workable range of suspension concentrations, showing yield stresses by extrapolation. The example featured is 1.89 μm mineral suspended in squalane	167
Figure 7.5; The effect of varying mineral concentration on suspension viscosity at a shear rate of 277 s^{-1} . Featured are minerals (sizes by LSS), suspended with high shear at various concentrations in squalane. A residual fit for each curve was determined using the Krieger-Dougherty model.....	168
Figure 7.6; A graph to demonstrate an alternative experimental calculation of maximum volume fraction, performed at a shear rate of 277 s^{-1} . The data shown was also derived from mineral grades suspended with high shear in squalane liquid	169
Table 7.1; The effects of median particle size, d_{50} on the maximum suspension concentration that enabled sustained operation, C_{ms} , the apparent operating yield, Y_1 and the resulting powder moisture content, W (percentages by mass)	164
Table 7.2; The specific surface areas, determined by BET and top-cut values of dry powders dispersed in an alkyd resin, using a Hegman gauge. SG stands for sand-ground.....	165
Table 7.3; Particulate suspension rheological properties at 30 % w/w in squalane, determined from shear stress versus shear rate measurements.....	168
Table 7.4; Particle packing data, derived from rheology at 30 % w/w in squalane ($\rho = 810 \text{ kg}\cdot\text{m}^{-3}$) using (1), linear extrapolation methods, as demonstrated and (2) the Krieger-Dougherty equation. The values of ϕ_{max} and anisotropy were those which were found to provide the nearest model fit to the experimental data.	170
Table 7.5; The effect of mineral treatment (protocol derived from chapter 4) on falling-weight impact resistance measurements at 30 % w/w mineral concentration in PP homo-polymer and the unfilled resin. In grey: samples that were included here for comparison purposes only. *Brittle fractures only	171
Table 7.6; Falling-weight impact resistance measurements of treated mineral samples in PP co-polymer at 30 % w/w mineral concentration and the unfilled resin	172
Table 7.7; Various relevant visual particle properties of samples at 5 % w/w in thin films derived from PP co-polymer. Particle properties (left-to-right) are; median and mean particle diameters, mono-dispersity, coarse particulate count, film inhomogeneity and aggregation factor.....	173

7 THE PREPARATION AND TESTING OF FINER FILLER

7.1 Introduction

Armed with a practical understanding of effective surface chemistries and formulation methods that enhance a material’s ability to resist impact, a theoretical understanding of factors that are purported to improve this property and with a rapid, reliable measurement to assess key visual composite properties *in situ*; the expectations in performance of current mineral/polymer composites formed using a commercially viable process could be rigorously tested.

As indicated by literature sources, it should be possible to improve the ability of a two-phase material to resist impact simply by maximising the fineness of the dispersion of the discrete phase in that of the continuous. The practical limitations in producing fine reinforcing particles and then ensuring that they disperse finely in subsequent processes must however be understood and addressed if this type of product is to become successfully produced on the global scale.

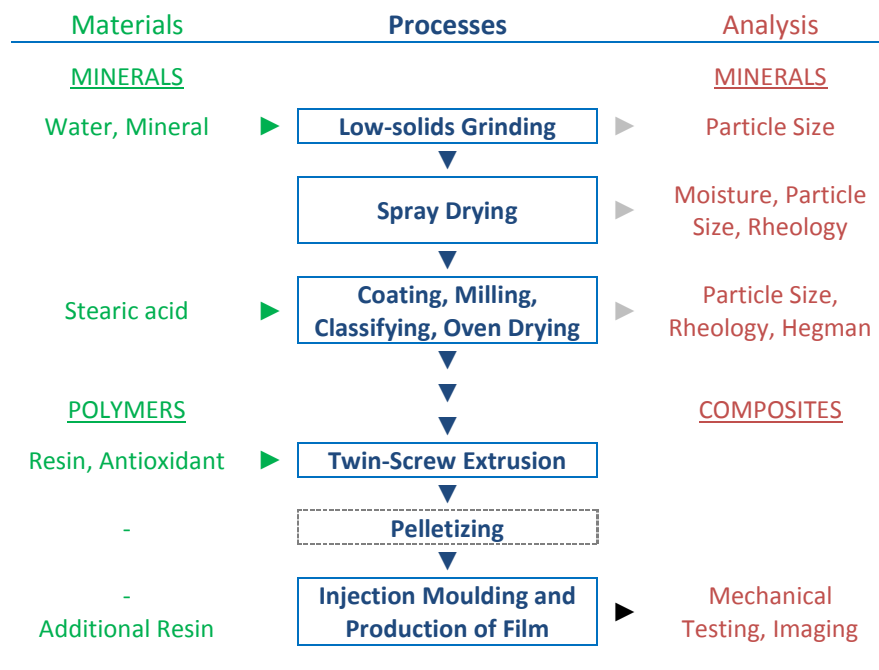


Figure 7.1; The specific materials, processes and analyses used in this Chapter

As highlighted in Figure 3.3, there are typically individual mineral and polymer processes that make up the formulation process for the production of fine minerals and their incorporation into a

polymer. For the purposes of researching finer grades of mineral, certain conventions of traditional processes must be disregarded, although the equipment used may remain the same. For example, while aqueous comminution will conventionally take place with dispersant (to maximise the suspension concentration for a given viscosity and therefore to improve grinding efficiency), it is necessary to omit this processing aid when it is suspected that the dispersant itself could cause down-stream processing difficulties, detrimental to the final application or for research purposes; when interference with subsequently-applied treatments would make the individual effects of these treatments difficult to elucidate. This was indeed deemed to be the case and therefore during the comminution process, viscosity was to be lowered using water only.

Despite its convenience, the exclusive use of aqueous-based particle size measurements taken during comminution to try to deduce one representative value of median particle size is flawed, in two types of circumstance. Firstly, when a drying process is subsequently required; this process may affect the particle size distribution by favouring aggregation during or following the drying process, which becomes more energetically favourable with finer particle sizes. Secondly, the measurement will not be representative when the intended application is non-aqueous; the ability of water to reduce weakly-aggregated particulates down to their fundamental particles is due to the right combination of dielectric and rheological properties, which many other liquids do not possess. Polypropylene (PP) could be argued to possess neither. A representative *in situ* measurement technique, such as that described in the previous chapter, will account for any variations to particle size and shape that may have been imposed.

The other features of the typical formulation process may be followed fairly conventionally. Classifying the material following drying is recommended to exclude significantly larger aggregated material formed on drying. It must be remembered however that no classifier is perfectly fraction-specific while giving 100 % yield of that desired fraction, and even if it was, the effects of post-classification handling, storage and processing on the particle size distribution must still be considered.

Following the results found in previous chapters of this thesis, the stearic acid modification of surface chemistry and other formulation aspects that were effective at improving the impact properties of 1.89 μm ground calcium carbonate (GCC) were considered and applied in this chapter (10 and 30 % w/w composites made using twin-screw extrusion, TSE). It was predicted that the finer particles would be more difficult to disperse. Therefore a rigid processing protocol was followed throughout the preparation of each ground mineral and subsequent to acquiring precipitated material. This included both surface chemistry and formulation technique. TSE was favoured as a formulation method over a high solids concentrate route for example, since as it has been established, TSE can provide a greater amount of particle shearing force during this process.

Therefore the results and following discussion in this chapter will exemplify and attempt to address the practical challenges that were encountered when trying to improve composite impact resistance by maximising the fineness of dispersion of GCC in PP, by using small-scale representations of a conventional large-scale industrial process, with optional additional materials and analyses used where appropriate.

7.2 Aims of this Chapter

The aims of this chapter are as follows: To prepare and acquire samples of finer-than-current calcium carbonate and to characterise their particle morphologies. To measure the effect on impact resistance that these have when incorporated into PP and to interpret these effects. To use *in situ* visualisation of particles in composite films to acquire representative particle size data post-composition. To identify the key particle features that affect composite quality and to pinpoint the processes in which these features are most susceptible to being compromised. Therefore, the aim is to understand the effects of using finer filler on impact resistance and to recommend paths of future research based on this understanding.

7.3 Hypothesis

The significance of the results will partly depend on their outcome through appropriately controlled experiments. It is hypothesised firstly, that genuinely finer calcium carbonate mineral incorporated into PP will cause its impact resistance to increase, and the relationship shall proceed down to finer dispersed particle sizes than are currently commercially available. Secondly, it is hypothesised that the costs associated with producing finer filler material and ensuring that this stays fine during the entire formulation process will increase, due to underlying physical phenomena and their leading to undesirable secondary effects. A significant engineering challenge is to identify the cost-effectiveness of filler; the costs associated with its production and subsequent processing compared to its ultimate property benefits. Thirdly, it is hypothesised that a broad range of analyses will be required to achieve a practical understanding of the role of flaw sizes in the fracture mechanism.

7.4 Results

7.4.1 Preparation

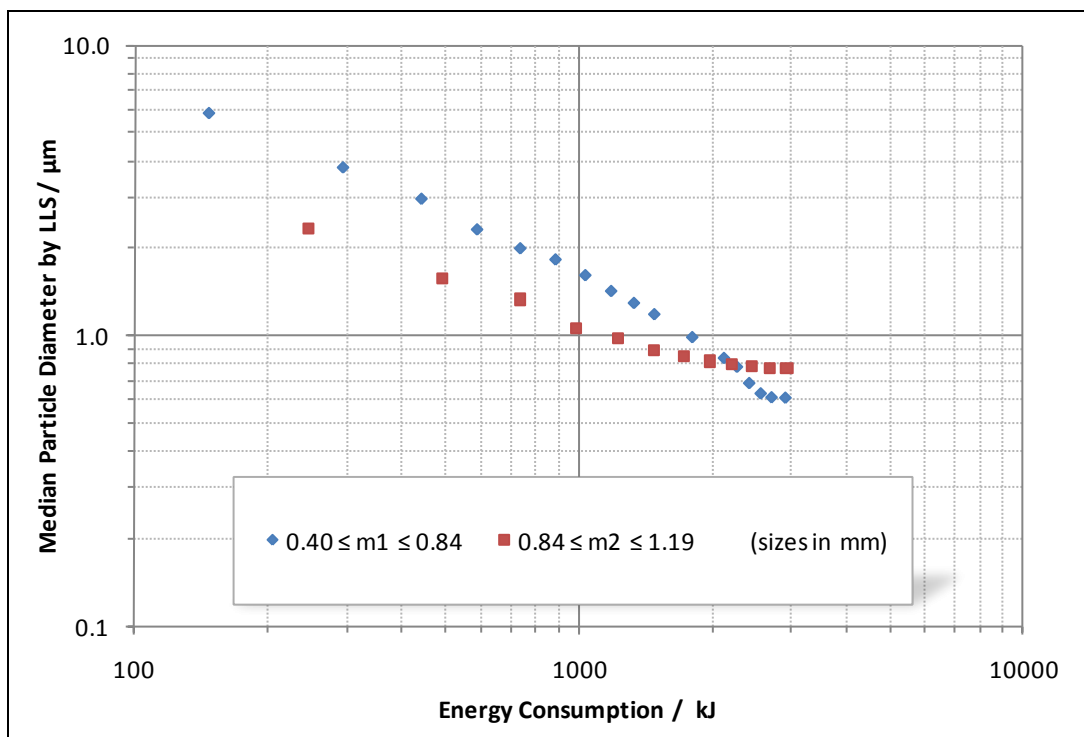


Figure 7.2; The effect of energy consumption of the impeller motor on the median particle diameter (by LLS) of GCCs using two different sizes of grinding media, m1 and m2. Logarithmic axes were used to improve clarity of data, while maintaining a reasonable experimental range

Results and observations from aqueous preparation stages (comminution and de-watering; used where applicable) will now be displayed and described, beginning with comminution. Figure 7.2 shows that increasing the total energy consumption of the grinding process caused the median particle diameter according to aqueous laser light scattering (LLS) to decrease exponentially, using both particle sizes of grinding media. Very fine particle sizes required large amounts of energy to produce and the grinding energy became increasingly less effective with decreasing particle size. It was not possible to accurately determine whether the median particle sizes would tend towards a certain value with increasing energy; these levels are far beyond the extremes of commercial and environmental justifiability in a scaled-up process. In the temporal confines of this experiment, the finest median particle sizes produced under these conditions were consistently of a size in the range of 0.5 – 0.6 μm . For finer grinding media, it was found that finer particle sizes could ultimately be achieved, despite a smaller change in size per unit energy during the initial 300 kWh of energy consumption. This observation is implied in Figure 7.2 since both media began with mineral with a median particle size of 13.84 μm , but the coarser grinding media, m2 produce finer mineral during the consumption of the first 900-1000 kJ of grinding energy.

It was possible with stirred media milling to produce minerals of finer particle size than some of those which are currently commercially produced for the purposes of impact resistance, according to LLS measurements taken from the milled suspension. The media milling process appeared to be able to reduce the particle size of a mineral to a fixed value that was independent of the total energy used, but dependent on the morphology of the grinding media. Finer media allowed the production of finer ultimate sizes compared to using coarser media, but the initial size reduction per unit energy was less. This is reflected in industrial processes where several media specifications may be used that are above all, progressively finer. As the grinding progressed, the suspension viscosity increased and the suspension therefore required additional energy to agitate. Therefore the assumption that the measured energy consumption was a reflection of the energy of grinding collisions became increasingly inaccurate. The use of water to lower the suspension viscosity mitigated this agitation energy effect, but was deemed to reduce the statistical likelihood of successful grinding events

occurring. Although the use of dispersant would have allowed for a significant increase of suspension concentration without increasing the viscosity, the approach was not used in this case, as it was adjudged that this would affect subsequent chemical treatments made down-stream in the overall process.

Following aqueous comminution, a suspension de-watering process was required. Results pertaining to a spray-drying process (as described in Chapter 3) will now be presented.

Sample Source	d_{50} / μm	C_{ms} / %	$Q / \text{m}^3 \cdot \text{s}^{-1}$ ($\times 10^{-6}$)	$M_{cc} / \text{kg} \cdot \text{s}^{-1}$ ($\times 10^{-3}$)	$M_{\text{water}} / \text{kg} \cdot \text{s}^{-1}$ ($\times 10^{-3}$)	W / %	Y_1 / %
FilmLink520	1.89	61.3	0.728	0.727	0.459	0.09	89 ± 1.4
FilmLink400	1.40	58.4	0.698	0.644	0.459	0.12	92 ± 1.8
FilmLink1	0.71	26.2	0.607	0.395	0.460	1.30	88 ± 7.0
FilmLink520	0.69	26.7	0.607	0.389	0.462	0.92	83 ± 5.5

Table 7.1; The effects of median particle size, d_{50} on the maximum suspension concentration that enabled sustained operation, C_{ms} , the apparent operating yield, Y_1 and the resulting powder moisture content, W (percentages by mass)

The data in Table 7.1 show that the maximum concentration that enabled sustained operation, C_{ms} was affected by the median particle size of the suspended solids, with finer sizes producing more viscous suspensions at comparable concentrations. In order to achieve comparable required rates of water removal, M_{water} the volumetric flow rates of introduction, Q were adjusted in accordance with C_{ms} . Higher values of C_{ms} allowed for more mineral input, quantified in steady operation by the mass of mineral introduced per unit time. The dryness of powders produced was in rough accordance with the suspension concentration, with concentrated suspensions becoming the most successfully dried. The ground samples with a lower C_{ms} value appeared to dry at similar mean operating yields, Y_1 but the yield inconsistency (represented by the standard deviation across ten lots of 30-minute collection periods) increased with decreasing C_{ms} .

Viscous effects played an important role in the maximum throughput and effectiveness of the spray-drying process. The natural outcome of preparing finer minerals in aqueous suspension is for the suspension viscosity at a given concentration to increase and therefore limit the drying potential.

7.4.2 Testing

The dried minerals were then jet-milled. It was observed that the handling of the powders became more difficult by doing so, which was increasingly prevalent with finer particle sizes. Each spray dried mineral became less able to flow following milling. Once dried and classified, the calcium carbonate materials were tested as powders, along with those prepared by other means and those acquired externally. This section contains the results and observations of these tests.

Sample Name	BET s.s.a. / m ² .g ⁻¹	Hegman Top-Cut / μm			
		1	2	3	Mean
FilmLink520	2.0	7	9	7	8
FilmLink400	2.2	7	7	7	7
FilmLink1 (SG)	11.1	95	85	95	92
PCC	25.0	115	115	110	113

Table 7.2; The specific surface areas, determined by BET and top-cut values of dry powders dispersed in an alkyd resin, using a Hegman gauge. SG stands for sand-ground

Table 7.2 shows data acquired by Hegman gauge tests (see Chapter 3). The coarsest particulates were found in the finer of the purported median particle size mineral preparations (as determined by aqueous LLS). This was despite a measureable increase in the specific surface area, as determined by BET adsorption [1].

Suspensions containing the finer ground particles were found to be the least effectively spray-dried as they demonstrated the coarsest particle sizes, according to the Hegman gauge test. Finer mineral that was acquired by means other than grinding and drying (i.e. precipitation) also exhibited a coarse top-cut by this test. Neither of the methods used to produce finer mineral (< 1 μm) enabled re-dispersion of particle sizes to sizes in accordance with those acquired by LLS, whereas the values

were in close accordance when testing coarser mineral ($> 1 \mu\text{m}$). This may support the argument that the failure to maintain a fine particle size throughout processing, despite being purportedly fine, was an intrinsic aspect of fine particles and not solely due to lack of quality of the processes.

Alternatively, both processes may have lacked the required quality to have ensured that no coarse particulates were present or subsequently became present.

Particle sizes were then measured in water and the less-polar but still low viscosity liquid, n-hexane. The respective refractive indices of these liquids were taken into consideration by the algorithm that interpreted their size distribution from the laser diffraction patterns. All data were recorded from a single instrument. All the necessary powder measurements were taken in water, before the liquid was changed to n-hexane, with fresh powder being introduced to the new liquid. After changing the liquid, the instrument was allowed to equilibrate (see Appendix for specific details). Fresh powder was introduced for each liquid.

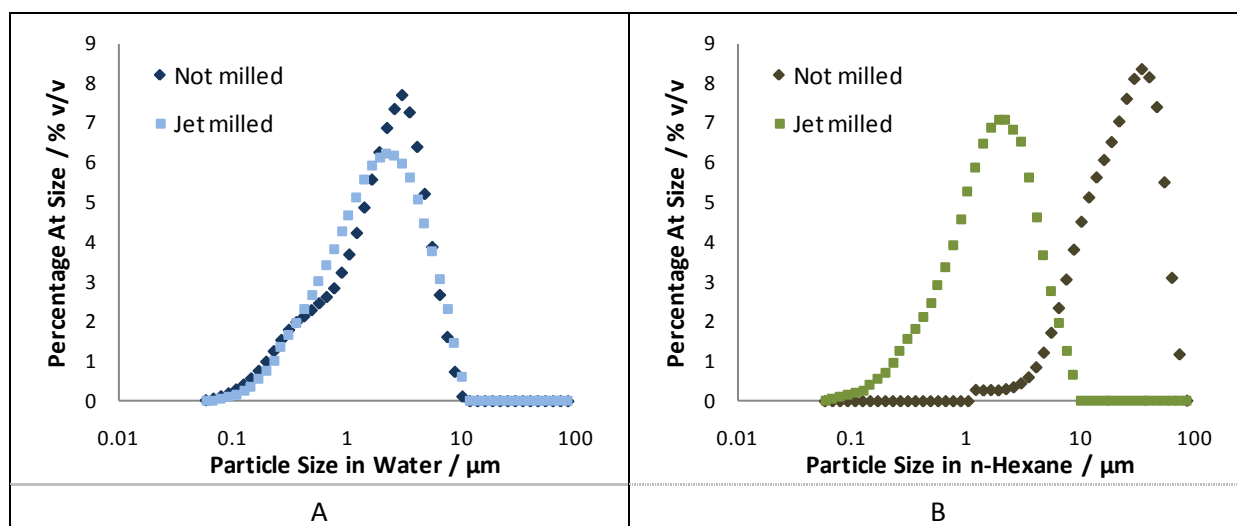


Figure 7.3; The particle size distributions of spray-dried, chemical-free GCC samples in A; water and B; n-hexane. In each case, the dried samples were compared to their jet-milled derivatives

From Figure 7.3 A, it can be seen that the aqueous particle size data of a spray-dried GCC was quite similar to its jet-milled derivative. However, Figure 7.3 B reveals that the spray-dried samples had a median particle diameter of more than one order of magnitude higher in the non-polar tests,

compared to the aqueous-based tests. Jet-milling appears to cause the distribution to revert to a magnitude much closer to that of the aqueous tests.

In order to learn more about the particle behaviour, the flow of suspensions that contained them were studied using cone-and-plate rheometry.

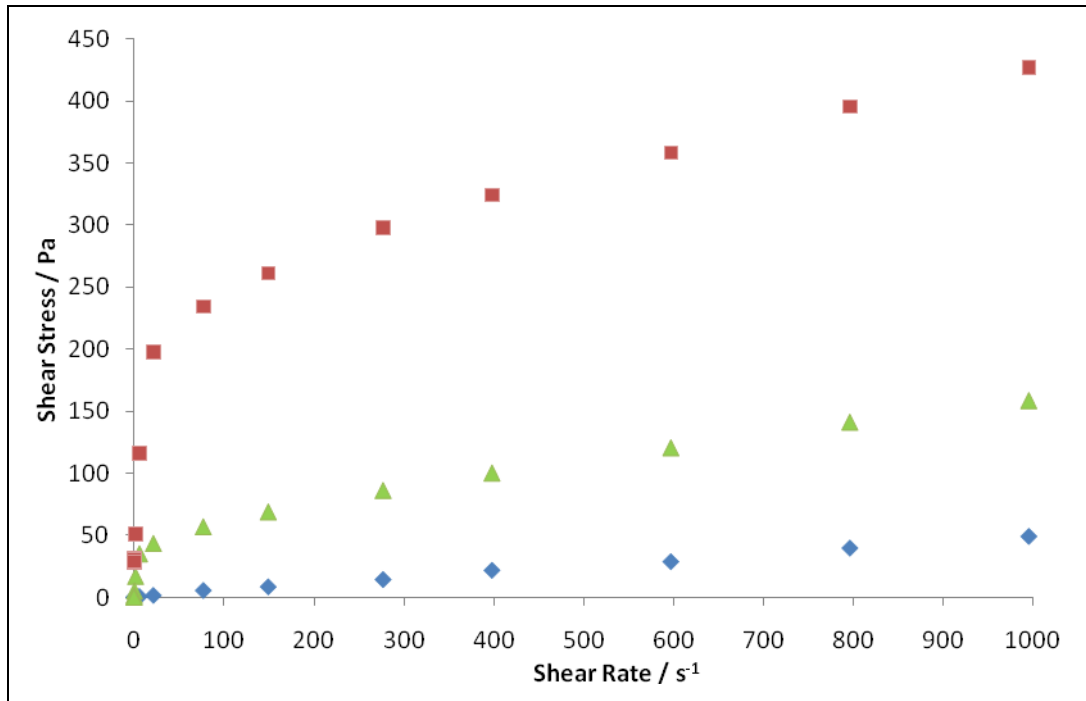


Figure 7.4; A graph to demonstrate the effect of shear rate on shear stress for a workable range of suspension concentrations, showing pseudoplastic behaviour. The example featured is 1.89 μm mineral suspended in squalane

Figure 7.4 demonstrates a typical stress response that results from increasing the shear rate in increasing concentrations of calcium carbonate mineral in liquid suspensions. In this case, mineral at very low concentration in a given liquid did not exhibit a perceptible characteristic of shear-thinning, but it became visible and increasingly pronounced after increasing the mineral concentration. In such cases, the stress-responses at shear rates greater than a certain shear rate were virtually linear. The remaining response curves from the other combinations of mineral sizes, types of liquid and suspension concentrations may be found in the Appendix. The key results are summarised in Table 7.3.

Table 7.3 shows that of the tested GCC minerals suspended in squalane, the 1.89 μm sample had the lowest viscosity at a shear rate of 277 s^{-1} at 30 % w/w, which was the greatest shear value at which data from each mineral/liquid combination could be recorded. These viscosity data were in good agreement with the shear behaviour, as demonstrated in Figure 7.4.

d_{50} LLS / μm	η at 277 s^{-1} / $\text{Pa}\cdot\text{s} (\times 10^{-3})$
1.89	77.5
1.40	84.8
0.71	156
0.40	312

Table 7.3; Particulate suspension rheological properties at 30 % w/w in squalane, determined from shear stress versus shear rate measurements

Along with shear behaviour, the packing of samples was studied using cone-and-plate rheometry.

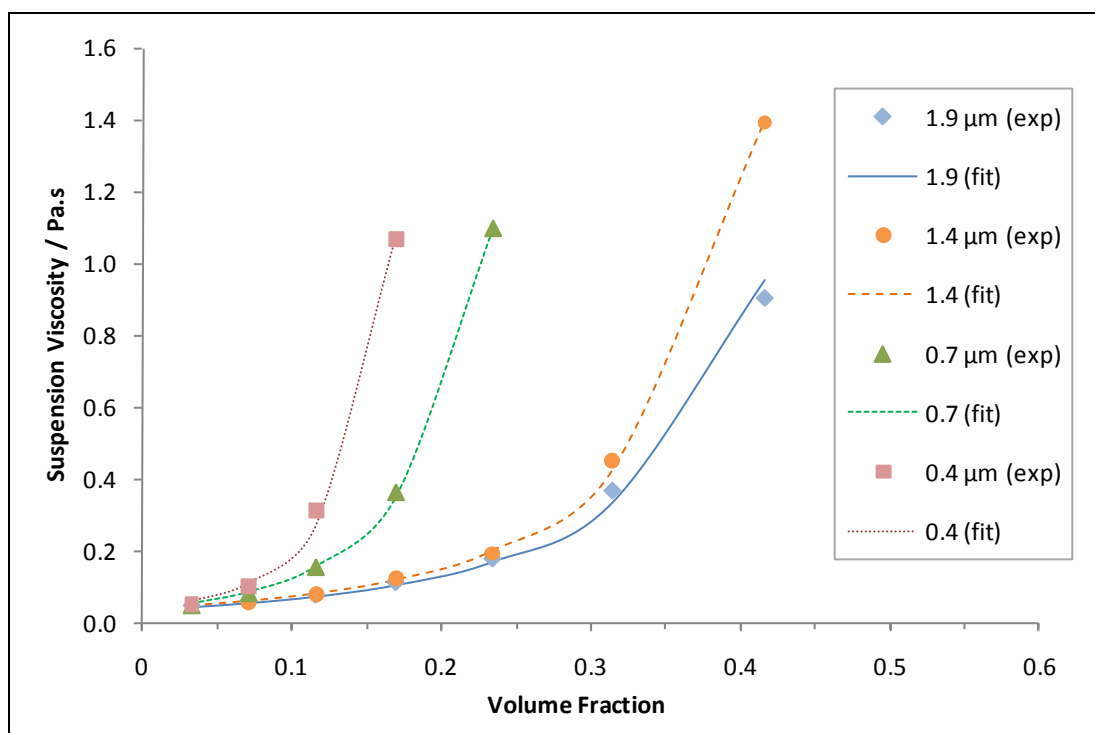


Figure 7.5; The effect of varying mineral concentration on suspension viscosity at a shear rate of 277 s^{-1} . Featured are minerals (sizes by LSS), suspended with high shear at various concentrations in squalane. A residual fit for each curve was determined using the Krieger-Dougherty model

Figure 7.5 shows the effect of suspension concentration on relative viscosity for calcium carbonate samples in squalane; a low-viscosity PP homologue. For each mineral size, the viscosity increases

exponentially with increasing concentration. Their behaviour in each case was modelled as per the Krieger-Dougherty equation, [2] with reasonable accuracy. Table 7.4 features further details of each model.

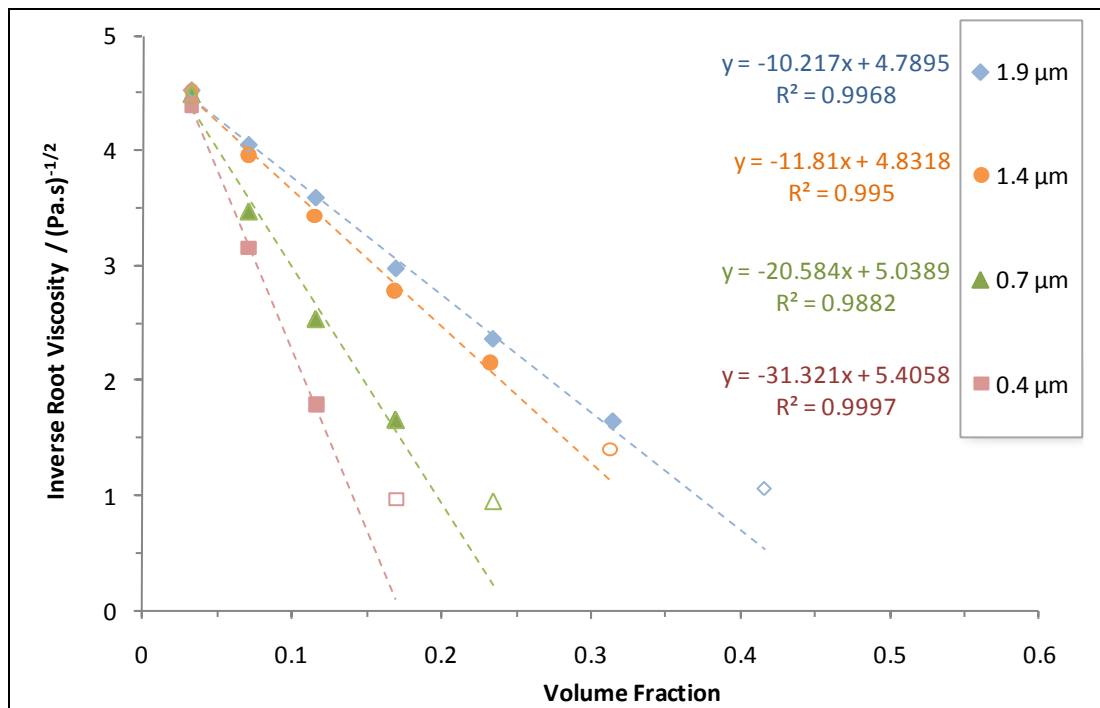


Figure 7.6; A graph to demonstrate an alternative experimental calculation of maximum volume fraction, performed at a shear rate of 277 s^{-1} . The data shown was also derived from mineral grades suspended with high shear in squalane liquid

To determine the maximum volume packing fraction using an alternative method [3], the inverse root of viscosity was plotted as a function of volume fraction as shown in Figure 7.6. Each curve appears to vary linearly for the majority proportion of the measured range, which represented that which was physically achievable with the mixing and testing apparatus. As shown, deviations from linearity were encountered at the high volume fraction extreme of each line. Inverse root viscosity values of less than $1.5 (\text{Pa.s})^{-1/2}$ were therefore omitted from the linear data extrapolation. Inherent difficulties in obtaining full data using this technique are highlighted, due to practical limitations of exploring high viscosity regions. The key results are summarised in Table 7.4, along with those previously determined as per Krieger-Dougherty. The interested reader is directed to the Appendix, where the origins of these data values are explained in greater detail.

d₅₀ LLS / μm	φ_{max} (1)		φ_{max} (2)		Aniso- tropy (2)
	(v/v)	(% w/w)	(v/v)	(% w/w)	
1.89	0.469	74.7	0.790	92.6	5.48
1.40	0.409	69.9	0.747	90.8	5.95
0.71	0.245	52.0	0.546	80.1	11.1
0.40	0.173	41.1	0.302	59.1	13.5

Table 7.4; Particle packing data, derived from rheology at 30 % w/w in squalane ($\rho = 810 \text{ kg.m}^{-3}$) using (1), linear extrapolation methods [3], as demonstrated and (2) the Krieger-Dougherty equation. The values of ϕ_{max} and anisotropy were those which were found to provide the nearest model fit to the experimental data.

The maximum volume packing fractions, ϕ_{max} in Table 7.4 were calculated using two methods; (1) the method shown in Figure 7.5 and (2) using the Krieger-Dougherty model, by varying the values of anisotropy and ϕ_{max} . Values of ϕ_{max} as calculated by method (1) were consistently lower than the equivalent values derived using method (2) and were closer in value to the maximum packing proportions that were achieved experimentally.

The data in Table 7.3 shows the pseudo-plastic behaviour of the suspensions. Table 7.4 shows that the maximum packing fraction of a mineral suspended in a medium (as determined from rheometry) correlated with the relative suspension viscosity at a given shear rate and the purported particle size of the sample. These viscous effects may be understood better by contemplating the proportion of suspending liquid that has interacted with the mineral. Since interaction may only occur at the particle surface, samples with higher specific surface areas will demand greater levels of liquid interaction, therefore leaving a smaller proportion of liquid in which to transport the particles. The phenomenon of increasing viscosity was also demonstrated when the particle concentration was increased, which was attributed to the same underlying cause. The consistent difference between the calculated maximum packing fractions was attributed to insufficient shear energy being transferred by the phase mixing process in sample preparation. While the result derived by the Krieger-Dougherty equation represented a theoretical maximum, that by the alternative method was a more accurate reflection of what could be experimentally achieved. However, there is a natural

difficulty in using this technique accurately, due to the limited data available especially at high concentrations.

The anisotropy values determined from the Krieger-Dougherty model show that the finest mineral samples by aqueous LLS had the least spherical particulate shapes. Since single calcite crystals have an aspect ratio of 2 – 3 [4], with no particle-particle interactions, these would be expected to produce a low anisotropy value, similar to that of a sphere (which is 2.5). With increasing particle aggregation, a particulate has more potential to deviate from isotropy, thus producing higher anisotropy values. This supports the argument that finer minerals (by aqueous LLS) have become aggregated.

Minerals were then incorporated into PP using TSE. The remainder of this section features the results of tests and observations of the resulting mineral/polymer composite specimens and their thin-film derivatives.

Purported Size / μm	Details	Mineral Conc. / % (w/w)	Energy to Break (Ductile) / J	Ductile Breaks / %
-	-	0	$1.10 \pm 0.35^*$	0
1.89	As received	30	7.73 ± 1.60	90
1.89	Treated	30	18.4 ± 1.38	100
1.40	As received	30	6.22 ± 1.56	60
1.40	Treated	30	14.3 ± 1.55	80
0.71	As received	30	$1.24 \pm 0.48^*$	0
0.71	Treated	30	3.18 ± 1.22	80
0.40 (PCC)	As received	30	3.39 ± 1.93	30

Table 7.5; The effect of mineral treatment (protocol derived from chapter 4) on falling-weight impact resistance measurements at 30 % w/w mineral concentration in PP homo-polymer and the unfilled resin. In grey: samples that were included here for comparison purposes only. *Brittle fractures only

Table 7.5 shows all materials used at 30 % w/w improved impact resistance, compared to unfilled homo-polymer. The aqueous median pre-formulation particle size did not correlate strongly with the energy absorbed (as may be expected). The established treatment was shown to be effective at increasing the amount of energy absorbed during impact up to the point of ductile fracture and at increasing the proportion of such ductile fractures for the minerals on which it was performed.

Purported Size / μm	Details	Mineral Conc. / % (w/w)	Energy to Break (Ductile) / J	Ductile Breaks / %
-	-	0	10.2 ± 4.8	80
1.89	Treated	30	12.7 ± 1.4	100
1.40	Treated	30	7.73 ± 1.6	90
0.71	Treated	30	5.08 ± 2.0	100
0.40 (PCC)	As received	30	3.61 ± 1.3	90

Table 7.6; Falling-weight impact resistance measurements of treated mineral samples in PP co-polymer at 30 % w/w mineral concentration and the unfilled resin

The results in Table 7.5 and Table 7.6 show that the pristine PP co-polymer (RB206MO) exhibited a greater proportion of higher-energy ductile fractures than the pristine homo-polymer (HE125MO) under given testing conditions. Following the incorporation of minerals at 30 % w/w however, the homo-polymer demonstrably had greater potential to become toughened, whereas this effect was less noticeable in the co-polymer due to its more ductile nature. The mineral with a purported median particle size of 1.89 μm produced the greatest extent of toughening in both systems.

The findings from mechanical testing showed that the purported particle sizes from LLS did not correlate with impact resistance, despite evidence that decreasing particle size caused improvements to impact resistance at a coarser size range in this work and from literature sources elsewhere [5-7]. This was attributed to the purported size being an inaccurate measurement, taken from an unrepresentative medium. This can also be supported by the results of top-cut from the Hegman gauge test, which showed a stronger correlation with impact resistance. The pristine co-polymer

displayed more ductile behaviour than homo-polymer under the testing conditions, although the latter was more amenable to an improved impact resistance on addition of mineral. This was attributed to differences in crystallinity. Discussion of crystalline phenomena is beyond the scope of the chapter; the co-polymer was included in these results because it was used subsequently for the purposes of particle analysis in films.

Masterbatches consisting of the minerals at 30 % w/w in the co-polymer resin were let down to a mineral concentration of 5 % w/w using only additional co-polymer under TSE. Thin films were produced and the material was analysed using optical microscopy.

d_{50} by LLS / μm	d_{50} <i>in situ</i> / μm	\bar{d} / μm	M (-)	> 30 μm / mm^{-3}	FIH (-)	AF (-)
1.89	5.42	4.79	49.8	1.7	1.5	2.9
1.40	6.47	6.01	48.5	3.5	1.7	4.6
0.71	9.85	8.38	33.7	21	10	14
0.40 (PCC)	15.6	9.16	29.3	26	12	39

Table 7.7; Various relevant visual particle properties of samples at 5 % w/w in thin films derived from PP co-polymer. Particle properties (left-to-right) are; median and mean particle diameters, mono-dispersity, coarse particulate count, film inhomogeneity and aggregation factor

Each result in Table 7.7 is in reasonable agreement with the others. The origin of each film property was introduced in the previous chapter. The finest particle size distributions *in situ* consistently correlate with; the least poly-disperse, the fewest counts of coarse particles, the most homogeneous spatial distributions and the least-aggregating. The coarsest *in situ* sizes also correlate with the finest sizes purported by the pre-formulation LLS method.

Different types of particle size data acquired *in situ* from films were in reasonable agreement with one another. They were not completely independent measurements. The most relevant measurements to impact resistance studies were originally identified as the coarse particulate (> 30

μm) content and spatial homogeneity. Samples found to have a high coarse particulate content *in situ* absorbed the least energy under falling-weight impact. Coarse particulates have been established as sites of stress concentration and fracture initiation. The way in which the spatial homogeneity was calculated meant that it was prone to becoming affected by the presence of coarse particulates. While useful in its own right, for the purposes of achieving greater impact resistance through (attempting to) decrease the particle size *in situ*, the spatial homogeneity property was considered less important.

7.5 Summary

The propensity of fine minerals to aggregate has been demonstrated. Regardless of the specific causation, it has been shown that unfavourable conditions can magnify the aggregation effect in calcium carbonate mineral. An example is the properties of the liquid in which it is suspended. The finest sizes of a given untreated sample were consistently acquired from aqueous suspensions. LLS data in n-hexane was not found to have facilitated de-aggregation, whereas in water it was. This is a highly significant nuance, since testing and application liquids are often different by convention.

It was not determined whether $1.89\ \mu\text{m}$ mineral represented a genuine optimum of particle size or whether the creation of finer sizes and associated processes, such as spray-drying using available technology, incurred some deleterious phenomenon of impact resistance, such as the production of a coarser particle size distribution.

There appears to be a strong case that coarse particulates were present in composites comprising purportedly finer mineral and also present in the powder prior to its incorporation into the polymer resin. Non-aqueous PSD measurements detected coarse particulates of a similar size following the spray-drying process ($\sim 70\ \mu\text{m}$). Coarse particulates were also detected during Hegman gauge testing. These support the theory that entities that have a detrimental effect on impact resistance were

present prior to them being introduced into the polymer, and not simply formed during the TSE process.

The production of finer particles caused down-stream processing difficulties to be encountered, including; limiting the effectiveness of drying and classifying the mineral, increasing the propensity of it to strongly aggregate and causing difficulties regarding its handling. Therefore the cost-effectiveness of preparing such mineral as commercial filler was compromised for the purposes of improving impact resistance in mass-produced polymer composites.

7.6 References

1. Brunauer S, Emmett PH and Teller E. Adsorption of Gases in Multi-Molecular Layers. *J Amer Chem Soc*, 1938; 60: 309-319
2. Krieger IM and Dougherty TJ. A Mechanism for Non-Newtonian Flow in Suspension of Rigid Spheres. *T Soc Rheol*, 1959; 3: 137-152
3. Beazley KM. Viscosity-Concentration Relations in Deflocculated Kaolin Suspensions. *J Coll Int Sci* 1972; 41(1): 105
4. Johnston J, Merwin HE and Williamson ED. The Several Forms of Calcium Carbonate. *Am J Sci* 1916; 41(246): 473-512
5. Dubnikova IL et al. Preparation and Characteristics of Composites Based on PP and Ultradispersed Calcium Carbonate. *Polym Sci Ser A*, 2008; 50(12): 1214-1225
6. Berezina SM et al. Effect of Rigid Particle Size on the Toughness of Filled PP. *J App Polym Sci*, 2004; 94(5): 1917-1926
7. Pukansky B and Moczo J. Morphology and Properties of Particulate Filled Polymers. *Macromol Symp*, 2004; 214: 115-134

CHAPTER EIGHT

Discussion

8 DISCUSSION

Specific observations have been made during the course of the experimental work, which were discussed on a chapter-by-chapter basis. However, a developed discussion is now presented; to consider the previously-discussed points as a continuum in relation to each other and in the context of preceding industrial understanding and academic literature. By doing this, the Thesis as a whole can be philosophised upon and more clearly conveyed, including its potential to alter current and future processes and how, if at all, various areas could be developed in the future.

The first use of mineral/polymer composites and their development to the present day was described. Their place in modern times was highlighted and the benefits of further scientific and commercial developments were considered, with a focus on the specific case of polypropylene filled with fine calcium carbonate particles to improve its impact resistance with minimal negative effects on other relevant properties. The Thesis then set out to characterise such a typical commercial formulation of a material that comprised filler with a median particle diameter of 2 μm and to investigate in a practical way the various possibilities of modifying that formulation. It was found that chemical functionality was required to significantly improve the performance of untreated filler. This could be through certain surface treatments to alter the compatibility of phases, such as stearic acid or similar or could be through the addition of free chemical (that is not previously bound to the filler) to alter crystalline properties, such as with a functionalised silicone additive. The potential to improve the general cost-effectiveness of a mineral/polymer composite by modifying the non-particulate ingredients and processing methods that contribute to its formulation was determined. Upstream markers to rapidly indicate subsequent composite performance were sought. The most successful particle-based measurements were identified as the Hegman gauge analysis and suspension rheology. In isolation the two tests were insufficient, but combining them simultaneously allowed both sensitivity to small quantities of coarse particles and the ability to assess particle compatibility with a range of different media in a quick and repeatable manner that created minimal waste. Media versatility was found to be a vital part of a successful marker. What appeared to be a

favourably-dispersing series of particles in one substance may not behave at all similarly in another. Observations from an aqueous-based dispersion measurement on surfaces treated with sodium polyacrylate for example would appear to show filler that had dispersed. The behaviour in polypropylene mixing was subsequently found to be less favourable than stearic acid coated particles; despite their seemingly poor aqueous performance. These observations lead to the recognition of media representativeness to being paramount to the applicability of an upstream marker.

Mixing particles into a polymer matrix could not be regarded as a fixed or predictable entity. This fact compromises the predicting power that pre-mixing tests have over final composite performance. Composite formation factors such as the mixing conditions, particle/matrix compatibility and polymer crystallisation effects were each cited as aspects which could profoundly alter the expectations of composite performance based only on particle measurements. However, despite direct composite-based measurements being inherently representative as they are applied post-mixing, no single routine analysis was found that could visualise particles appropriately; accounting for large particle numbers at sufficient resolution. While scanning electron microscopy was technically capable (in fact far surpassing technical requirements), its associated costs and time rendered it poor as an upstream performance marker. At this stage, composite formation would take place with the highest available degree of mixing intensity so that the validity of particle-based measurements could be upheld on the assumption that the mixing process was maximised in each case. Particle/polymer compatibility could still be considered from rheological analyses. However, differential scanning calorimetry was still required to provide crystallisation data. By using particle-based measurements, it was found that (despite the marginally-improved performance benefits that some functionalised reagents and surface treatments were able to provide) their relatively-high associated costs could not be justified by what were to become disproportionate benefits. The potential for this state of affairs to change in the future was predicted as being unlikely.

Research into non-particulate reagents represented only one branch of the overall tree of formulation. Research into other branches using the same principal materials (including mixing method and mineral sizes and surfaces) proved more promising in their potential cost-effectiveness. A method of formulating composites that comprised favourably-dispersing filler was developed, with a final suggested protocol that could amount to an alternative to the current commercial processing method. It was argued to be tantamount to reducing energy costs in processing and transportation. It involved the formation of a concentrated, yet dispersed mineral/wax product form at loadings that approached those allowed by their theoretical maximum based on their shape. The process involved a single cycle of heating and cooling of a wax (a polymer comprising relatively short molecular chains that have lower comparative melt viscosities as a result) during which mineral would be incorporated and mixed. At concentrations below a single, fixed value (depending on the system but typically 84-88 % w/w filler) the form was found to re-disperse in polymer matrices at concentrations relevant to current applications in a manner that could prove commercially competitive in terms of their impact resistance. The values of these maximum concentrations were linked to the maximum allowable concentrations that could still be fully wetted-out in the binding medium. The final composite materials were produced by a simple injection moulding process that was found to impart only minimal back-mixing; which was only possible for a favourably dispersing binder phase comprising dispersed filler particles. Composites made in this way from concentrated forms whose loadings were marginally above and below the theoretically-allowed maximum showed distinct 'pass' and 'fail' dispersion characteristics that were visually detectable, supporting the wetting-out theory of re-dispersion. It was shown that the method could not only reduce overall energy costs, but could also improve technical aspects such as having drastically-improved particle control post-production (for example to prevent deviations from the expected particle size distribution) and could indeed offer some other significant strategic advantages to a minerals processing company.

The data that contributed most significantly to the particle size findings were those acquired by the *in situ* particulate visualisation method that was developed for the purposes of this Thesis. Having

shown previously the significance of preparing representative media in which to disperse particles, films were made from the same original batch as that which would undergo mechanical testing. The technique did indeed show experimental integrity in this way since it was; applied following composite mixing and thereby accounted for any changes incurred during this process; capable of providing a measurement on material that derived from the exact same batch as that which would undergo mechanical tests, and finally; (in the case of calcite filler) able to compare data with a simultaneously-acquired measurement of fundamental filler particles. The principal technique determined particle sizes based on their two-dimensional areas within the film, although this led to the omission of significant areas of film due to limitations of resolution. This limited resolution issue could be overcome with current materials, since the analytes most relevant to the study were comfortably within the resolution limits. However, it was speculated that implementation of finer materials in the future would require a more powerful microscope that was not optics-based. Derivative techniques that were subsequently developed allowed the accounting of greater areas of film, to the point where any composite film could be analysed, provided that sufficient light could be transmitted through it.

Finally, it was conclusively demonstrated that the trend seen in the increasing impact resistance of a composite material by decreasing the median size of the filler dispersed within it became ineffectual in the extreme case, due to poor particle implementation that allowed the formation of particle clusters, which thereby created misleading data. It was regarded that this avenue of research had a much more favourable future outlook compared to the use of expensive non-particulate reagents, since it was determined that improvements in mixing technology and particle classification apparatus would be likely to occur in the future, making extreme particle size reduction a more cost-effective option. It was regarded that the 'particle size reduction' avenue of research had a much more favourable future outlook to the benefit of cost-effectiveness of mineral/polymer composites compared to functionalised additives, since it was determined that improvements in mixing technology and particle classification apparatus would be highly likely to occur in the future, thereby

lowering their cost and potentially improving their performance in terms of specific impact resistance benefit (the advantages this was hypothesised to bring in Chapter 1).

The work presented in this Thesis will hopefully prove valuable from the smaller scale of research through to development and right through to final mass-production to suit global material needs. In terms of future development, each aspect of research was considered to retain its validity.

Furthermore, with the predicted further rises in the dependence of the global population on polymer composites to meet daily material needs, including those comprising polypropylene and calcium carbonate, and with the finite capacity of the Earth to provide the raw materials required the strongly-favoured approach to use cost-effective materials, methods, research and utilisation while attempting to reduce unnecessary processes and reduce unnecessary waste that has been at the heart of the Thesis will prove to be increasingly relevant.

CHAPTER NINE

Conclusions

9 CONCLUSIONS

A typical commercial polypropylene composite formulation of an impact-resisting material comprising calcium carbonate filler with a median particle diameter of 2 μm was characterised, and the potential to improve its general cost-effectiveness by modifying the non-particulate ingredients and processing methods that contribute to its formulation was determined. Through the effective use of successfully-validated upstream markers to rapidly indicate subsequent composite performance, it was found that (despite the marginally-improved performance benefits that some functionalised reagents and surface treatments were able to provide) their relatively-high associated costs could not be justified by what were disproportionate benefits.

Material	Relative Cost per tonne	% in 30 wt% Composite	Relative Cost in composite
<i>Principal Materials</i>			
GCC	1.00	30	30
Polypropylene	4.75	70	330
<i>Optional Additives</i>			
PP-g-MA	14.65	1.0	14
Stearic Acid	1.65	0.3	0.5
40% Sodium Polyacrylate	6.25	0.1	0.6
PHSA	14.4	0.2	2.9
Functionalised silicone fluid	20.20	0.3	6.1

Table 9.1; Relative cost data for the formulation materials of GCC / PP composites. GCC is ground calcium carbonate and PHSA is poly(hydroxystearic acid). ‘% in Composite’ refers to the approximate mass fraction of final material that is present in a 30 % w/w formulation

Table 9.1 summarises the relative costs of the various materials and additives that were considered for inclusion into a composite. The negligible difference in composite performance that was gained with use of functionalised additives did not justify their cost, which ranged between 3 – 28 times as expensive.

The potential for this state of affairs to change in the future was predicted as being unlikely. However, the research into such reagents represented only one branch of the overall tree of formulation. Research into other branches of formulation using the same principal materials (including mixing method and mineral size and surface) proved more promising in their potential cost-effectiveness.

A method of formulating composites that comprised favourably-dispersing filler was developed, with a final suggested protocol that could amount to an alternative to the current commercial processing method. It was argued to be inherently tantamount to reducing energy costs in processing and transportation. It involved the formation of a concentrated, yet dispersed mineral/wax product form at loadings that approached those allowed by their theoretical maximum based on their shape. The form was found to re-disperse in polymer matrices at concentrations relevant to current applications in a manner that could prove commercially competitive in terms of their impact resistance. It was shown that this method could not only reduce overall energy costs, but could also improve technical aspects such as drastically improved particle control post-production and could indeed offer some other significant strategic advantages to a minerals processing company.

Formulation Method	Preparing Material for Moulding			Moulding		
	<i>Time</i>	<i>Power</i>	<i>Energy</i>	<i>Time</i>	<i>Power</i>	<i>Energy</i>
“Conventional TSE”	3.5	1.0	3.5	1.0	0.2	0.2
“High-solids Concentrate”	1.0	1.2	1.2	1.3	0.2	0.3

Table 9.2; Relative data for the energy consumption of two composite formulation methods. Values were based on the processing of ten separate preparations, each producing sufficient final polymer composite to produce ten specimens for impact test measurements.

Table 9.2 shows relative data for the energy consumption of the two fundamental approaches to polymer composite formulation, as presented in the Thesis. The marginal additional duration required to successfully mould specimens from high-solids concentrates compared to conventional twin-screw extrusion pellets was greatly outweighed by the additional duration required to prepare these pellets, even taking into account the lower intensity under which the process was performed.

The energy savings amounted to between 2 – 3 times for the new proposed route. This figure does not take into account other benefits of high-solids concentrates route, such as those found in transportation and storage.

The data that contributed most significantly to the particle size findings were those acquired by the *in situ* particulate visualisation method that was developed for the purposes of this Thesis. The technique was shown to contain experimental integrity, since it was; applied following composite mixing and thereby accounted for any changes incurred during this process; capable of providing a measurement on material that derived from the exact same batch as that which would undergo mechanical tests, and finally; (in the case of calcite filler) able to compare data with a simultaneously-acquired measurement of fundamental filler particles. The limited resolution of the technique was not regarded as a problem with current materials, since the analytes most relevant to the study were comfortably within the resolution limits. However, it was speculated that implementation of finer materials in the future would require a more powerful microscope that was not optics-based.

It was conclusively demonstrated that the trend seen in the increasing impact resistance of a composite material by decreasing the median size of the filler dispersed within it became ineffectual in the extreme case, due to poor particle implementation that allowed the formation of particle clusters, which thereby created misleading data. It was regarded that this avenue of research had a much more favourable future outlook compared to the use of expensive non-particulate reagents, since it was determined that improvements in mixing technology and particle classification apparatus would be likely to occur in the future, making extreme particle size reduction a more cost-effective option.

Finally, it is hoped that the work in this Thesis can contribute greatly to current and future polymers composites technology, by way of offering scientific knowledge and commercial efficiency into what

a material can do for society, compared to all the costs associated with its development and manufacture.

APPENDIX

Chapter	Description
Three	Programming code and screenshots in three parts; laser-light scattering, instrumented falling-weight impact resistance and image processing
Three, Six	Details of instrument equilibration for particle size determined by light-scattering, as measured using Malvern Mastersizer S
Three	The effect of motor speed on volumetric fluid flow for a peristaltic pump, using a range of mineral concentrations and resulting viscosities
Three, Seven	Raw data acquired from rotational rheology measurements of suspensions using Bohlin Advanced Rheometer
Three	Raw data acquired from rotational rheology measurements of molten PP/GCC composites using TA Instruments Ares Rheometer
Four	Mechanical testing data for consecutively-compounded materials that showed no significant improvements to properties through dispersion
Six	Details of image optimisation to achieve maximum particle resolution and maximum particle counts
Six	Method development and image-optimisation relevant to the visual analysis of films using skeletonisation by influence zones
Six	Image acquired by polarised optical microscopy that show light-transmitting behaviour for certain entities was independent of the angle of incidence
Seven	Explanations of the origins of rheological data values, including maximum theoretical packed volume fraction and anisotropy

Details of the above are located on the included CD.